Chapter 2
Bone Physiology and Biology

Jürg Andreas Gasser and Michaela Kneissel

Abstract This chapter is divided into three subsections: The bone biology part will provide some insight into the matrix composition as well as the origin and basic function attributed to the cellular components, the osteoblasts osteocytes and osteoclasts. In the second section, the interplay between these matrix components and the cells will be discussed in the context of skeletal growth, skeletal adaptation (modeling), and skeletal maintenance (bone remodeling). Finally, the third section will address similarities and differences in bone biology between human, nonhuman primate, rat, and mouse, the most commonly used species in the study of bone metabolic disorders. Other large animals like dogs, sheep, mini-pigs, or rabbits which are being successfully used to study orthopedic conditions (implant ingrowth, fracture healing, and bone augmentation) have not been addressed in this chapter.

Keywords Osteoblast • Osteoclast • Osteocyte • Bone formation • Bone resorption • Remodeling • Modeling • Cytokines • Growth factors • Markers • Intramembranous • Endochondral • Mice • Rats • NHP • Humans

2.1 Bone Biology

Bone is a special form of connective tissue, which unlike most other tissues is physiologically mineralized. On the organ level, bone is made up of the cartilaginous joints, the calcified cartilage of the growth plate (during skeletal growth only), the marrow space, and the mineralized cortical and trabecular bone structures (Weiner and Wagner 1998; Seeman 2008; Burr and Akkus 2014) (Fig. 2.1).

J.A. Gasser (✉) • M. Kneissel
Novartis Institutes for BioMedical Research, Department of Musculoskeletal Diseases, 4002 Basel, Switzerland
e-mail: juerg.gasser@novartis.com

S.Y. Smith et al. (eds.), *Bone Toxicology*, Molecular and Integrative Toxicology,
DOI 10.1007/978-3-319-56192-9_2

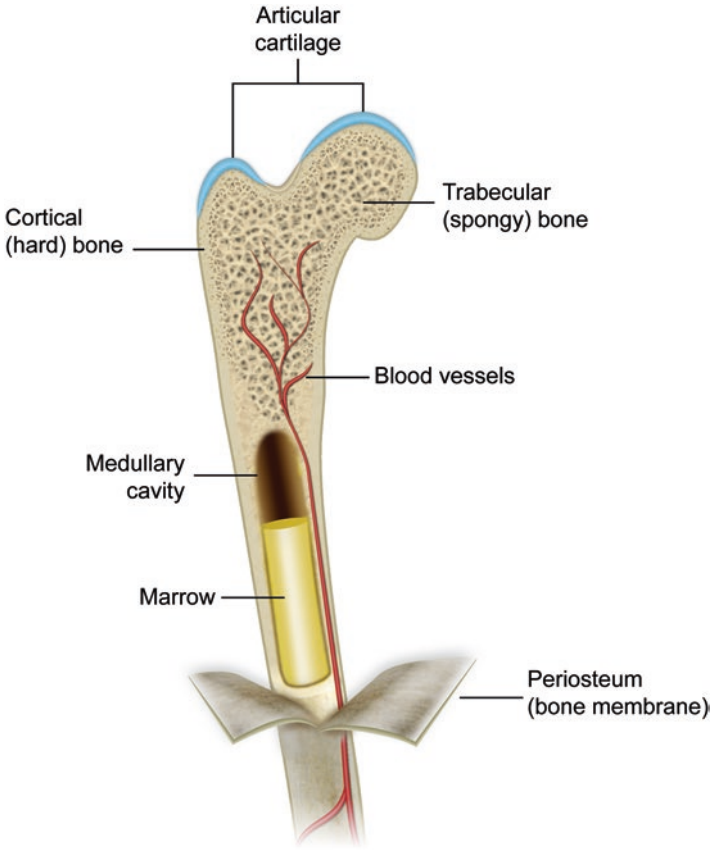

Fig. 2.1 Bone envelopes: On the macroscopic level, long bones are composed of the cartilaginous joints, porous cancellous bone, the more compact, denser cortical bone, and the marrow cavity. The subperiosteal surface in long bones is covered by a thin fibrocellular highly vascularized and innervated membrane, the periosteum

On the tissue level, bone consists of the mineralized and non-mineralized matrix (osteoid) and the three principal cellular components, the bone-forming osteoblasts, some of which become entrapped into the mineralizing bone matrix they lay down to become osteocytes, and the bone-resorbing osteoclasts. The origin of these cell types as well as the communication between them and their involvement in vital processes such as skeletal growth, bone adaptation (modeling), and bone maintenance (remodeling) will be discussed in more detail below.

Bone is a multifunctional tissue which serves as mechanical support and protection, is an essential part of hematopoiesis and mineral metabolism, and has a role as an endocrine organ. Bone is able to resist deformation from impact loading, but at the same time, it is also able to absorb or dissipate energy by changing shape without cracking (Currey 2002). The elastic properties of bone allow it to absorb energy

by deforming reversibly when loaded (elastic deformation) (Lanyon and Baggott 1976; Turner 2006). If the load exceeds bones' ability for elastic deformation, plastic deformation occurs, accompanied by permanent shape change and accumulation of microcracks, which helps to release energy (Currey 2002). Microdamage is a defense mechanism against a more serious event, namely, a complete fracture. Repetitive loading at physiologic levels may lead to fatigue damage, which requires a damage detection mechanism (osteocyte) and a repair function (remodeling) capable of preventing its accumulation thereby preventing failure in fatigue (Burr et al. 1998). To allow movement, bone also has to be light, and this lightness is achieved by constructing a version of the mineralized material consisting of trabecular plates and rods and bone marrow cavities, which are sites of hematopoiesis (Seeman 2008).

On the organ level, based on their anatomical location, bones can be divided into four distinct envelopes, namely, subperiosteal, endocortical, cancellous, and intracortical. This division reflects that these envelopes are morphologically distinct (Fig. 2.1). They play different roles in bone biology in health and disease and differ in their response to changes in the mechanical environment.

The subperiosteal surface in long bones is covered by a thin fibrocellular membrane, the periosteum, which is well vascularized and innervated by both sympathetic and sensory fibers. It is composed of an outer fibrous layer containing fibroblast-like cells and a deep cambium layer populated with highly osteogenic cells including mesenchymal stem cells. The osteogenic cells in the cambium layer drive the periosteal expansion during growth, the adaptive response to mechanical stimulation, and the process of fracture repair. Under normal circumstances the cells will produce highly organized lamellar bone, while under pathologic situations and in the initial phases of bone repair, disorganized woven bone may be produced. The mesenchymal cells contained in the cambium contribute to fracture repair, where they can differentiate into chondrocytes to form cartilage.

The endocortical (or endosteal) surface that surrounds the marrow cavity is not lined by a membrane but by a fenestrated layer of osteoprogenitor cells. These so-called lining cells are associated with capillaries near the bone surface and sinusoids in the bone marrow and may act as a "membrane." Lining cells are important for the regulation of the rapid calcium exchange and fluxes of hydrophilic ions between bone and the extracellular fluid.

Cancellous bone surfaces are morphologically and functionally similar to the endocortical surface. They are also covered by a fenestrated layer of lining cells which control ion fluxes (particularly calcium) and respond to mechanical and biological signals to induce bone formation or resorption.

Finally, the intracortical envelope is comprised of the surfaces of the Haversian canals, which are covered by a fenestrated layer of resting osteoprogenitor cells. The neurovascular bundle contained in the canal serves to regulate nutrient exchange between the blood vessels and the extracellular fluid, from where they pass through the canalicular system to be absorbed interstitially. The extracellular fluid is not only important for nutrient and calcium exchange, but it also appears to participate substantially in the transmission of signals between osteocytes embedded in the

mineralized matrix and from osteocytes to the cells on the bone surfaces and/or osteoprogenitor cells in the bone marrow.

Calcified tissue presents a considerable barrier for the diffusion of oxygen and nutrients and the removal of cellular waste products. For this reason, cells contained in a mineralized tissue must be localized within a distance of roughly 250 μm of their blood supply. This may be the reason why larger mammals like humans, dogs, primates, and rabbits, with a thicker cortical structure, require osteons. It may also explain why the average diameter of trabeculae in larger mammals is around 200 μm. Interestingly, longitudinal tunneling of substantially thickened trabeculae was observed in primates after bone building treatment with PTH(1–34) (Jerome et al. 2001). Vascular channels were always present in trabeculae thicker than 450 μm and were thought to improve metabolic exchange of deep-seated osteocytes by reducing the distance between cells and filtering surfaces in the thicker trabeculae (Lozupone and Favia 1990). Vascular structures in osteons show typical characteristics of capillaries that are 15 μm in diameter and are often paired. Essentially they are fenestrated, lack smooth muscle cells, are lined by an incomplete layer of endothelial cells, and surrounded by a continuous 40–60 nm thick basement membrane. The basement membrane acts to limit ion transport across the capillary.

Long bones are supplied by a nutrient artery entering the marrow cavity, which then fans out to run aligned with the longitudinal axis of the bone (Marenzana and Arnett 2013; McCarthy 2006; Brandi and Collin-Osdoby 2006). Blood flow in the medullary cavity is regulated by adrenergic and cholinergic sympathetic nerve fibers that either reduce or increase blood flow as required. Branches direct blood from the longitudinally oriented blood vessels to the endosteum, where it enters the intracortical capillary network flowing outward toward the periosteum. Roughly two-thirds of the cortical blood supply enters through the endocortical surface while the remainder is supplied from the highly vascularized subperiosteal side.

Cortical bone comprises most of the bone mass and mechanical function, while the less dense trabecular bone, among other functions, serves to redirect stresses originating in the proximity of the joints from movements to the stronger cortical shell. Throughout skeletal growth and in adult life, bones have to adapt to changes in the mechanical environment to prevent them from fracturing.

A protective function of bone is provided especially for organs situated in vital areas such as the thorax and head, where injuries could be fatal. Developmentally, protective bones like the calvarium and rib, which belong to the axial skeleton, are formed at least in part by a process called intramembranous ossification. This is different from the endochondral ossification (Fig. 2.12) seen in the long bones of the appendicular skeleton. Areas rich in cancellous bone like the iliac crest, vertebrae, and proximal femur continue to contribute significantly to hematopoiesis throughout life, while in adult life, in the marrow cavity of the long bones, red marrow is increasingly replaced with yellow fat. Yellow marrow appears to serve as energy store, and it might contribute to lipid metabolism and the regulation of triglycerides. Both cortical and trabecular bone are sites of long-term storage for calcium which is required for muscle contractions, blood clotting, the transmission of nerve impulses, and many enzymatic reactions. Calcium can be mobilized through two

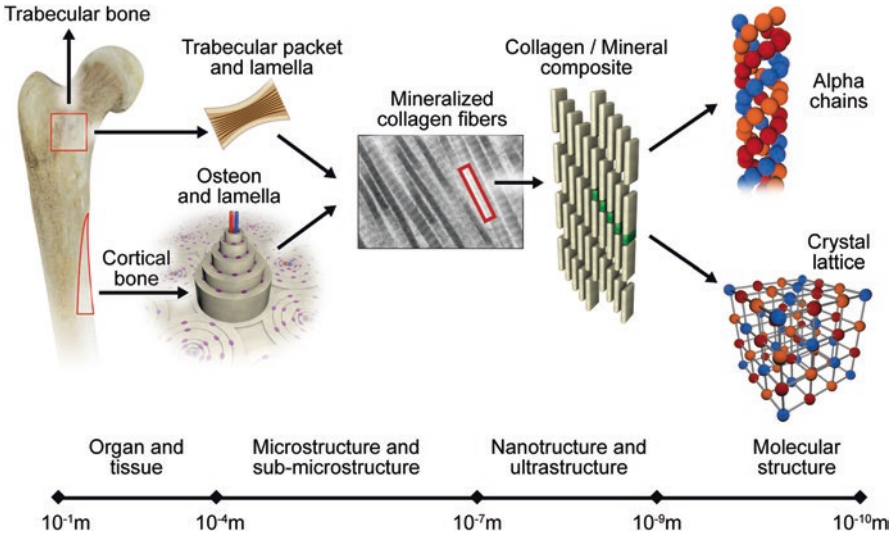

Fig. 2.2 Hierarchical organization of bone: At the organ level, bone is seen as a composite with dense cortical bone forming an outside shell and cancellous (trabecular) bone within the marrow cavity. At the microscopic level, cortical bone is composed of many Haversian systems (osteons). Osteons are composed of a central canal carrying a blood vessel, nerves, and lymphatics surrounded by layers of concentric lamellae. Although trabecular bone is also lamellar, its structure comprises of a combination of lamellae that run largely parallel to the trabecular surface and the remnants of older, remodeled bone that can appear osteon-like in some areas. At the ultra- and nanostructural levels, bone is a composite of collagen fibers with plates of mineral interspersed within the collagen fibrils as well as between the collagen fibers. The collagen fibrils are composed of molecules which form a triple helix out of two α_1 and a single α_2 chain

major processes. The extensive surface area which is formed by the canalicular system and the osteocyte lacunae allows for a rapid mobilization and redeposition of calcium to meet immediate demands, while the release of calcium generated by the more time-demanding process of bone remodeling can address changes in calcium demand over time scales spanning from several days to weeks.

To achieve its multiple diverse functions, bone is organized in a hierarchical manner (Burr and Akkus 2014) (Fig. 2.2). On a nanoscale level, the collagen and mineral form a composite material, with mineral providing stiffness and structure while type I collagen provides resilience and ductility. Collagen also serves as a template structure for the deposition of the mineral. At the microstructural or microscopic level, the individual collagen fibers and the mineral are organized primarily as defined by local functional requirements. Depending on the specific mechanical and biological needs, bone can be dense (cortical bone) or a meshwork (cancellous/trabecular bone). As eluded to previously, cortical bone is composed of many secondary Haversian systems or osteons (Fig. 2.3), which consist of a central canal carrying a blood vessel, nerves and lymphatics, and are surrounded by multiple layers of concentric lamellae. In contrast, while trabecular bone is also lamellar in

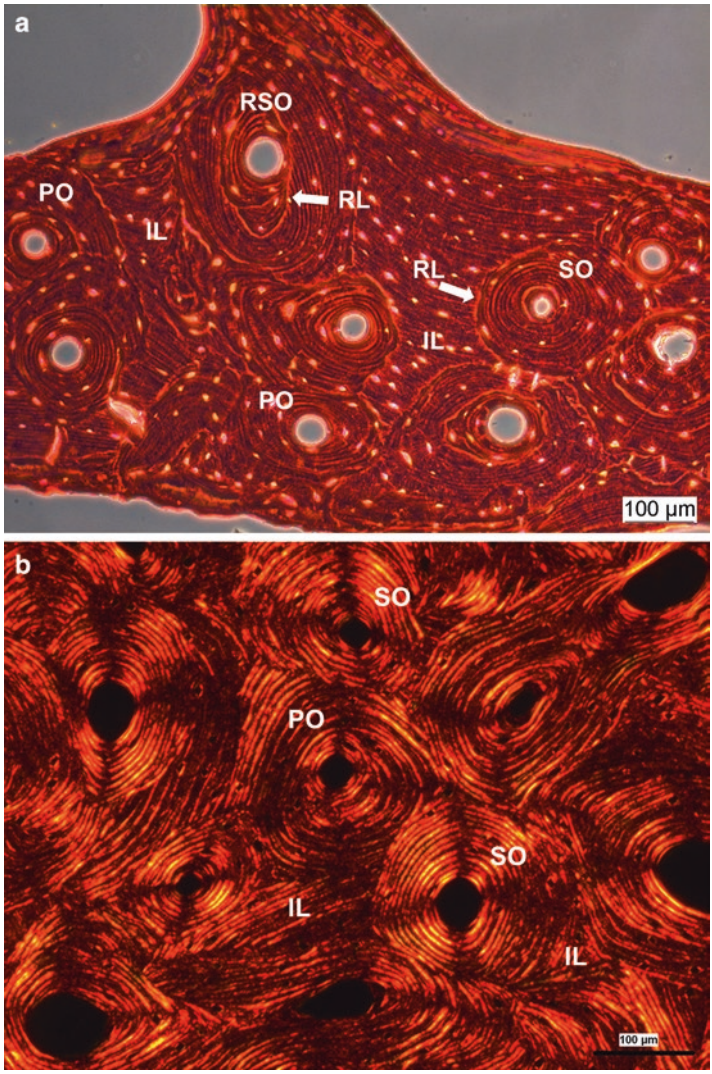

Fig. 2.3 Primary/secondary osteons. (**a**) decalcified human rib showing primary osteons (PO), intact secondary osteons (SO), and remodeled secondary osteons (RSO). Secondary osteons form longitudinally oriented fibers embedded in a matrix of interstitial lamellae (IL), but are separated from the matrix by a cement line (reversal line, ↑RL), a remnant formed during the creation of the secondary osteon at the location where osteoclastic bone resorption stops and bone formation begins (transverse section, 6 µm section, picrosirius staining, circularly polarized light). (**b**) decalcified human rib showing primary osteons (PO) and secondary osteons (SO). Variations in collagen orientation can be viewed using linearly polarized light in human cortical bone. Fibers that are oriented transversely to the direction of light appear bright, whereas those oriented along the path of the light are dark. In a cross section of cortical bone, dark osteons are composed of longitudinally oriented fibers (transverse section, 6 µm section, picrosirius staining, linearly polarized light)

structure, some of these lamellae run approximately in parallel to the trabecular surface, while some of the older remnants of remodeled bone have an almost osteon-like appearance. Finally at the macroscopic level, bone is composed of a dense cortical shell that is wrapped around the cancellous (trabecular) bone which is localized within the marrow cavity. Trabecular bone is made up mostly of primary lamellae, but in areas where bone has been extensively remodeled, hemiosteons which essentially look like half osteons may be present. Woven bone on the other hand represents a highly disorganized repair tissue where randomly arranged collagen I fibers are rapidly mineralized, thus lacking the typical lamellar pattern. It may form in non-pathological situations as a consequence of unusually high loads experienced by bones and in the region of the growth plate during endochondral ossification, or under pathological situations in response to inflammation or bone injury. Following a fracture, woven bone helps forming the callus that bridges the fracture gap providing initial stability during the early healing process. Eventually woven bone is always remodeled and replaced by normal lamellar bone, which provides better mechanical stability.

Primary bone is defined as new bone formed in a space where previously no bone existed, or formed on an existing surface of bone or mineralized cartilage (Burr and Akkus 2014). Thus, primary bone requires only bone formation, whereas secondary bone is defined as bone which is produced by the resorption of previously deposited bone followed by the formation of new bone in its place, a process called remodeling.

Primary lamellar bone is formed on the periosteal surface and is characterized by a series of parallel laminar sheets with few vascular canals. This dense, strong subperiosteal compartment serves primarily a mechanical function. Primary lamellar bone is also deposited on trabecular bone surfaces in the marrow cavity, where it serves a metabolic function in support of calcium metabolism. Plexiform, or fibrolamellar bone is a special variant of primary bone which is found in rapidly growing animals (cows and sheep) and has been reported in humans but limited to the time of major growth spurts. In plexiform bone, primary lamellar bone is deposited on a de novo-formed nonlamellar core substrate within the periosteal membrane (intramembranous ossification). The special arrangement allows increasing bone strength rapidly, as small amounts of bone deposited on the outer surface will contribute significantly to overall bone strength.

Primary osteons are formed by concentric deposition of osteonal lamellae around large vascular canals (Burr and Akkus, 2014) (Fig. 2.3). They consist of less than ten lamellae and measure around 50–100 μm in diameter. In contrast, secondary osteons which form the Haversian system are larger (100–250 μm in diameter) consisting of 20–25 lamellae, and they have a clearly visible cement line at their outer boundary. The cement line (reversal line) is a remnant of the reversal phase of bone remodeling, the process whereby secondary osteons are formed, and it indicates the point where osteoclastic bone resorption stops and bone formation begins. The central Haversian canal carries a neurovascular bundle. Haversian systems run at an average 11–17° angle with respect to the long axis of bone, closely following the dominant loading direction of the bone. Haversian vessels branch extensively and are connected to

transversely oriented blood vessels called Volkmann canals, which extend from the marrow vasculature to the periosteal membrane. Cement- or reversal lines serve a very important mechanical function in fatigue and fracture processes. Their ability to absorb energy inhibits crack propagation through the bone matrix, and they provide viscous damping in compact bone. High local shear stresses result in the deformation of the viscous cement line which will diminish the stress and hinder transmission of the energy to the growing crack. The remodeling of cortical bone will inevitably leave behind traces of non-remodeled primary or secondary osteons. These remnants of older bone are referred to as interstitial bone. Since the average tissue age of interstitial bone is older, it is more highly mineralized and more susceptible to microcrack accumulation.

Cortical bone forms the primary component of the diaphysis in the appendicular skeleton. In healthy bone with "normal" bone turnover, Haversian and Volkmann canals create a porosity of around 3–5%. Compact bone is also found in the metaphysis of long bones, surrounding the trabecular bone of vertebral bodies, in the iliac crest, ribs, and the skull, where it provides mechanical support and protection.

Cancellous bone is composed of plate- and rod-like structures of around 200 μm thickness (humans) and smaller dimensions in laboratory animals (Fig. 2.4). Cancellous bone is found in the vertebral bodies of the axial skeleton, the ribs, the iliac crest, and the metaphysis of the long bones in the appendicular skeleton. Due to its position, blood supply to trabecular bone is provided by the blood vessels embedded in the marrow cavity, rendering the need for an osteonal structure in general obsolete. Trabecular bone derives its contribution to mechanical strength

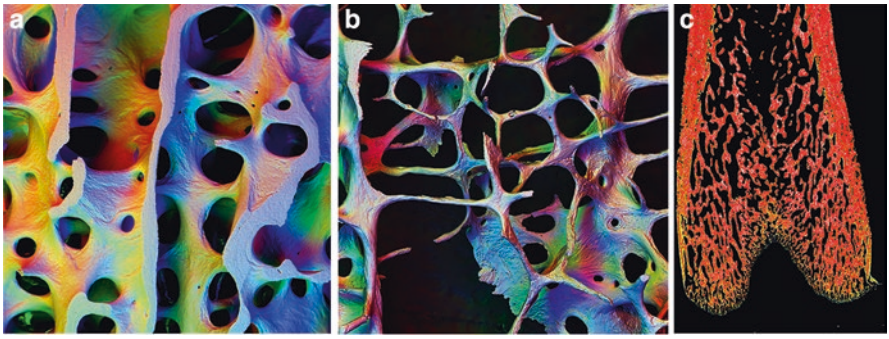

Fig. 2.4 Cancellous bone – rods and plates. (**a**) and (**b**) 20-kV BSE images of macerated, carbon coated, 3-mm-thick section of a human L4 vertebral body. Architecturally, cancellous bone is composed of plates and rods running at various angles to reflect the orientation of the major stresses within the bone. (**a**) shows normal healthy bone, whereas (**b**) shows classical signs of osteoporosis including trabecular thinning, loss of connectivity, and conversion of plate-like into rod-like structures in human bone (Both images courtesy of Prof. Alan Boyde, Queen Mary University of London, UK). (**c**) Trabeculae act as struts to support the outer cortical structure and to funnel the stresses experienced by them to the stronger, more massive cortical bone surrounding them. This important mechanical function is nicely apparent when looking at a longitudinal section through the distal femur metaphysis of a rat (**c**)

essentially from its architecture. Given its location in the metaphysis of long bones, it provides an efficient way of transmitting loads generated in the joints to the adjacent cortical bone. Because it is highly interconnected, vertical struts can be stabilized efficiently and prevented from buckling by the horizontal struts in the structure. Trabecular architecture and especially connectivity is thus an important determinant for the mechanical stability of cancellous bone, and this can be measured effectively by microCT analysis. Studies have shown that a decrease in trabecular number has a much greater negative impact on bone strength than the loss of an equal amount of bone through trabecular thinning (Van den Linden et al. 2001; Hernandez et al. 2006). In healthy human bone, most trabecular structures tend to be shaped in the load-bearing direction as plates rather than rods. Plates provide greater strength against bending in the load-bearing direction of long bones than rods. In conditions of bone loss, plate-like structures will be affected assuming a more elliptical rod-like shape and connectivity decreases. In the axial skeleton, this process seems to occur preferentially outside the primary loading axis, and the remaining struts remain aligned with the loading direction, which enable the structure to preserve some of its strength.

In addition to the mechanical function of metaphyseal cancellous bone for the transmission of loads from the joint to compact bone, a special compartment of trabecular bone is localized beneath the cartilage of the articular surface in the epiphysis, which may function as a cushion by attenuating forces generated by movement. Immediately beneath the joint, the subchondral plate, a layer of condensed cancellous bone is visible. Although the precise role of the subchondral plate and cancellous bone adjacent to the articular cartilage is still debated, it is generally assumed that it may be implicated in the development of osteoarthritis (Goldring and Goldring 2010).

2.1.1 Bone Composition

Bone is a composite material whose extracellular matrix consists of mineral (65%), water (10%), lipids (1%), and organic material (25%), the latter being composed predominantly of type I collagen (90%), noncollagenous proteins (10%). These components have both mechanical and metabolic functions, and the composition and architectural features vary with age (Boskey and Coleman 2010), gender, species, and the site which is studied (Donnelly et al. 2012), and it can be affected by disease and treatment (Boskey 2013; Mandair and Morris 2015).

The mechanical properties and thus the ability of bone to resist fracture are defined by the amount, proper arrangement, and characteristics of each of these components (quantity and quality) (Seeman 2008). In this context, the term “quality” usually refers to factors including composition (weight percent of each component), mineralization (organization of the mineral and its crystallite size), collagen content and collagen crosslinks, morphology (Jepsen 2011), microarchitecture (Patsch et al. 2011), and the presence of microcracks. The physical and chemical properties of

the mineral phase have been determined by various methods including chemical analysis, X-ray diffraction, transmission and atomic force microscopy, small angle scattering, and nuclear magnetic resonance (Boskey 2006a). Water can be bound to the mineral-collagen composite, or it can flow freely through canalicular and vascular channels in bone. Unbound water can be redistributed in response to skeletal loading, and it likely contributes to the signals detected by cells such as the osteocytes informing them of the local loading condition.

2.1.2 The Mineral

The largest proportion is occupied by the mineral phase consisting predominately of a nanocrystalline, highly substituted, poorly crystalline analog of the hydroxylapatite [$Ca_{10}(PO_4)_6(OH)_2$], as demonstrated by X-ray diffraction over 60 years ago (Weiner and Wagner 1998; Boskey 2007). In primary mineralization, a process that in humans occurs within the first 3 weeks after osteoid deposition by the osteoblast, mineral is deposited rapidly as an amorphous calcium phosphate along with large amounts of calcium carbonate. During this process about 60–70% of the total mineralization is achieved. As bone matures during the subsequent process of secondary mineralization, crystals grow in size to an eventual size of 40 × 3 × 7.5 nm, become more plate like and crystalline, and orient themselves parallel to one another and to the collagen fibrils. During the final bone maturation which in humans may take more than a year, the calcium carbonate content is reduced, but it continues to serve an important role in the maintenance of acid-base homeostasis. During episodes of acid load, systemic bicarbonate (HCO_3^-) is consumed to buffer the blood pH. The HCO_3^- deficiency is offset by carbonate and phosphate ions present in the bone matrix. In chronic acidosis, this mechanism helps to maintain blood pH, but it also results in bone loss.

The amount of mineral in bone can be quantified by a variety of techniques including gravimetric analyses (determination of ash weight), analysis of calcium and phosphate contents, and spectroscopic and densitometric analyses. Human bone, nonhuman primates, rats, and mice contain ~60–70% mineral/dry weight, depending upon site, species, and stage of development.

Variations in the distribution of mineral and its properties in bone can be illustrated by a variety of imaging techniques, including bone mineralization density distribution (BMDD), Raman (Kazanci et al. 2006; Morris and Mandair 2011; Mandair and Morris 2015), and infrared spectroscopic imaging (Boskey 2006b). Quantitative backscattered electron imaging is used for mapping the calcium concentrations and for the determination of BMDD (frequency distribution of calcium concentrations within the bone sample). Summarized by Boskey (2013), several studies have reported deviations from normal calcium distribution in diseases like osteomalacia, osteoporosis (peak shifted to the left of normal), classical and new forms of osteogenesis imperfecta, and following treatment with bisphosphonates (peak shifted to the right of normal).

2.1.3 The Organic Phase

The organic phase of bone consists primarily of type I collagen (~90%), noncollagenous proteins (NCPs, ~5%), or lipids (~2%). The proteins in the extracellular matrix of bone are often classified into two main groups, structural proteins (collagen and fibronectin) and proteins with specialized functions. The latter are involved in the regulation of collagen fibril diameter; serve as signaling molecules, growth factors, or enzymes; or have other functions.

Structural proteins: The most abundant protein in the bone matrix is type I collagen, a unique triple helical molecule consisting of two identical amino-acid α1-chains and one structurally similar but genetically different α2-chain (Rossert and de Crombrugghe 2002). Each chain is about 1,000 amino acids in length. Collagen fibrils are constructed from collagen molecules which are 300 nm long and 1.5 nm thick. Five of these molecules are stacked in a quarter-staggered array to form a microfibril structure, such that there are 67 nm hole zones between the ends of the molecules and spaces between the laterally contiguous molecules known as pores. The holes and pores serve as spaces which enable the deposition of plates of bone mineral during primary and secondary mineralization. Functionally, collagen serves as a template for mineral deposition, provides elasticity to the tissue, stabilizes the extracellular matrix, and binds other macromolecules. Collagen molecules consist of repeating glycine-X-Y residues which are often hydroxylated and glycosylated, giving rise to some of collagen's unique crosslinking ability. In bone, two types of crosslinks have been demonstrated which increase with age and are altered by disease or treatments. They are either formed enzymatically or by glycation (non-enzymatically mediated collagen cross-linking). Since the number of cross-links is an indicator of collagen maturity, it is not surprising that drugs which reduce bone remodeling (rate of bone renewal) have been shown to increase the number of cross-links. Pyridinoline and deoxypyridinoline are two mature cross-links formed by enzymatic collagen cross-linking near the end of the collagen molecule, the C and N-termini. The content of these mature cross-links increases up to the age of 10–15 years, to remain stable thereafter, possibly declining with age. An increased pyridinoline/deoxypyridinoline ratio appears to enhance compressive strength and stiffness. In contrast, the non-enzymatically formed advanced glycosylation end-products (AGEs), such as pentosidine, furosine, vesperlysine, imidazolone, and Nε-carboxymethyllysine, which are elevated in uncontrolled diabetics and in oxidative stress and are formed randomly, increase the brittleness of bone. Distribution of total cross-links in the bone matrix can be visualized in Fourier transform infrared microscopic imaging (FTIRI) (Boskey 2006b; Mandair and Morris 2015), and pentosidine is often used as a marker since it is the only AGE that can be quantified accurately. AGEs accumulating in the extracellular matrix can influence the proliferation and differentiation of bone-forming cells by interacting with a specific receptor called RAGE. Binding of AGEs to RAGE activates NF-κB in osteoblasts and stimulates cytokine production. AGEs also appear to regulate osteoclastogenesis and osteoclast activity. The presence of AGEs may reduce the solubility of collagen and of the mineralized matrix, thereby slowing down bone resorption.

Observations by microscopical or by X-ray diffraction analysis suggest that collagen fibers are preferentially oriented according to the predominant stress in the bone (Burr and Akkus 2014). Longitudinally oriented fibers are found in portions of bone that are under tension, whereas transversely oriented fibers are more abundant in regions which are usually exposed to compressive loads. It has been shown experimentally that altering the loading direction will change the fiber orientation in newly formed bone. This has been debated however as being an artifact due to characteristics of optics and light transmission. As an alternative, it has been suggested that collagen is organized in a twisted plywood configuration that is continuously rotated through 180° cycles (Weiner and Wagner 1998). Whether the collagen is twisted or not and how it becomes oriented is still under debate.

Noncollagenous proteins (NCPs) contribute 10–15% of the total bone protein content and approximately 2% of the total bone weight. They have important roles in the organization of the extracellular matrix, coordinate mineral-matrix and cell-matrix interactions, and regulate the process of bone mineralization. For a more in-depth review of the various NCPs and their role, the reader is referred to the review written by Boskey and Robey (2013). In brief, NCPs can be subdivided in several groups, namely, the serum-derived proteins, proteoglycans, and glycosylated proteins. In addition, at least 12 glycoproteins which appear to be involved in the cell attachment mediated by transient or stable focal adhesions to extracellular macromolecules are found among the NCPs. Finally, four gamma-carboxy-glutamic acid-containing proteins which appear to be involved in the regulation of cartilage, bone, or vascular calcification, namely, matrix gla protein (MGP), bone gla protein (BGP or osteocalcin), periostin, and protein S, are found in the bone matrix. Most of these NCPs including their origin and potential contribution to bone biology, which is largely based on results from transgenic mouse models, have been described in detail by Boskey and Robey (2013). To date, relatively little information is available for most of the NCPs on how they change in distribution in osteoporosis or other bone diseases, or in response to anabolic or antiresorptive therapies. However, a number of NCPs can interact with collagen fibrils. Osteopontin (OPN) may function as "glue" that provides fiber matrix bonding, thereby enhancing bone's resistance to fracture, as well as crack bridging entity in the case of microcrack formation where it inhibits crack propagation (Sroga and Vashishth 2012). Also, recent genewide association studies suggest that osteocalcin (OC) and OPN are important for fracture resistance. Both OPN and OC have an important role in bone mineralization (Mandair and Morris 2015), as demonstrated by the reduction in cortical hardness and elastic modulus in $OPN^{-/-}$ mice (Kavukcuoglu et al. 2007) and the finding that OC appears to regulate the growth of apatite crystals in $OC^{-/-}$ mice, even though genotype mineral/matrix ratios were not different between $OC^{-/-}$ and $OC^{+/+}$ mice (Kavukcuoglu et al. 2009). OPN also binds to osteoclasts and promotes their adherence to the mineral during the process of bone resorption.

A minor but potentially interesting fraction of NCPs in the mineralized matrix of bone is the enzymes, mainly phosphatases (alkaline phosphatase (ALP), tartrate-resistant acid phosphatase (TRAP)), FAM210A, and also matrix metalloproteases (MMP2, MMP9, MMP13, and ADAMTS18) and other signaling factors. While their

biological role has been under intense investigation and considerable knowledge of their function is available, only very limited published evidence is available regarding changes in the expression of enzymes and signaling factors in the matrix of patients with metabolic bone disease or under drug treatment (Boskey 2013).

The glycoprotein ALP is used as a biomarker of bone formation, since it hydrolyzes pyrophosphates, which inhibit mineral deposition by binding to mineral crystals. Since ALP is produced by many different organs like the liver and kidney, it is not a specific marker for bone formation. In contrast, the bone-specific isoform of alkaline phosphatase (BSAP) which is found on the surface of osteoblasts has been shown to be a sensitive and reliable indicator of bone metabolism.

Lipids, which make up ~3% of the total bone matrix, are known to be important for cell function regulating the flux of ions and signaling molecules into and out of the cells. The distribution of lipids in the matrix can be observed from histology, based on sudanophilia, from FTIR and Raman analysis, or by nuclear magnetic resonance (NMR) (Reid et al. 2012). However, lipid composition and its association with mechanical properties have not been studied in the context of fragility fractures or other bone diseases in humans and animal models of human disease.

2.1.4 Osteoblasts

Osteoblasts are engaged in bone formation. The extracellular matrix synthesized by osteoblasts is known as osteoid when first deposited and not yet mineralized, but it is subsequently mineralized through the accumulation of calcium phosphate in the form of hydroxyapatite (Fig. 2.5). This process results in the hard but lightweight composite material (with both organic and inorganic components) that is the major constituent of bone. After active bone formation, osteoblasts have three alternative fates: they either undergo apoptosis, or become buried in the mineralizing bone matrix where they undergo terminal differentiation to become osteocytes, or become "inactive" lining cells that continue to exist on quiescent bone surfaces. Bone lining cells show a flattened shape containing only a few cell organelles, indicative of their low metabolic activity. However, these apparently dormant cells are in close contact with matrix-embedded osteocytes through gap junctions and participate in the calcium exchange between the mineralized matrix and the bone marrow compartment, and they can be reactivated within a few hours in response to PTH to contribute to local bone formation processes (Dobnig and Turner 1995; Kim et al. 2012).

Cytologically, actively bone-forming osteoblasts have a strongly basophilic cytoplasm and abundant mitochondria and show typical secretory characteristics, possessing well-developed rough endoplasmic reticulum with dilated cisterna. All these features are consistent with their capacity to produce a large amount of extracellular proteins. Osteoblasts are polarized, in the sense that the part of the cell membrane which is in direct contact with the bone surface possesses many cytoplasmic processes that extend into the newly deposited osteoid.

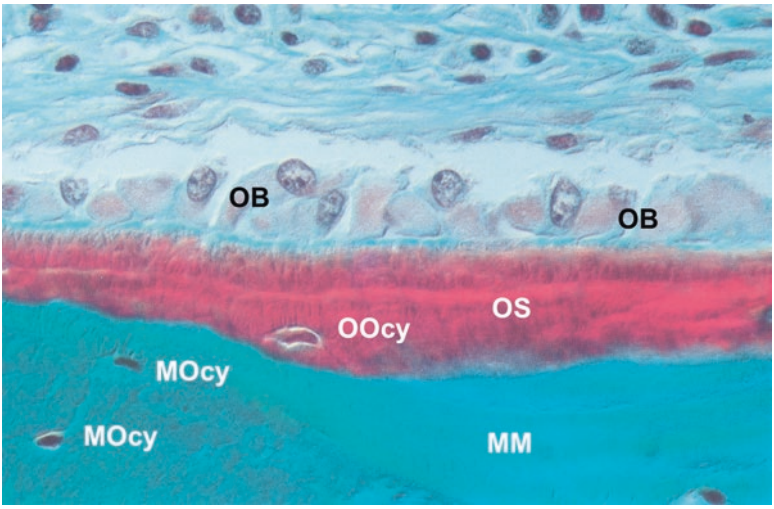

Fig. 2.5 Osteoblasts: matrix synthesizing osteoblasts (OB) are lined up on the endocortical bone-forming surface covered by osteoid (OS, *red*) in rat bone (Goldner Trichrome stain). An osteoblast undergoing differentiation into an osteocyte (OOcy, osteoid osteocyte) has remained completely embedded in the osteoid. Mature osteocytes (MOcy) are visible in the mineralized matrix (MM)

Osteoblasts originate from mesenchymal stem cells (MSCs) which are capable of differentiating into chondrocytes, osteoblasts, myoblasts, and adipocytes (Caplan and Bruder 2001; Jiang et al. 2002). Their differentiation is regulated by specific transcription factors. Sox-5, Sox-6, and Sox-9 regulate chondrocytic differentiation, while their differentiation to adipocytes and myoblasts is determined by PPARγ and Myo D, respectively.

The osteoblast-lineage cells form a group that includes their mesenchymal progenitors, preosteoblasts, osteoblasts, bone lining cells, and osteocytes (Fig. 2.6). Among the cytokines involved in osteoblast differentiation are the Hedgehogs, BMPs, TGF-β, PTH, and WNTs (see reviews by de Gorter and ten Dijke 2013; Nakamura 2007; Long 2012). Runx2/Cbfa (Komori et al. 1997; Ducy et al. 1997) and Osterix/Sp7 (Nakashima et al. 2002) are essential regulators, and they are indispensable for both endochondral and intramembranous ossification. Runx2-deficient mice completely lack osteoblasts, fail to form hypertrophic chondrocytes, and produce a cartilaginous skeleton that is completely devoid of a mineralized matrix (Otto et al. 1997). Runx2 interacts with transcriptional activators and repressors and other coregulatory proteins, to either positively or negatively regulate expression of osteoblast-specific genes including Col1, ALP, OPN, osteonectin (ON), and OC (Harada et al. 1999; Kern et al. 2001). Runx2 appears to directly regulate the expression of the zinc finger-containing transcription factor Osterix (Osx) (Nishio et al. 2006). Similar to mice deficient in Runx2, $Osx^{-/-}$ mice lack osteoblasts, showing the critical role of this transcription factor in bone formation. Osx can interact with the nuclear factor for activated T cells 2 (NFAT2), which cooperates with Osx in

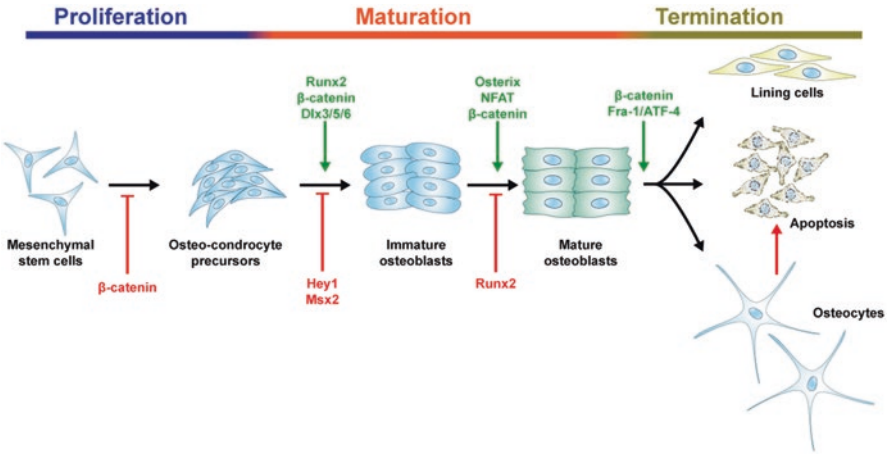

Fig. 2.6 Osteoblastogensis and fate: scheme illustrating osteoblastogenesis and the main transcription factors governing proliferation and differentiation of osteoblast precursors. Upon termination of bone formation, mature osteoblasts can flatten to cover the quiescent bone surface as lining cells, die by apoptosis, or surround themselves by bone matrix while differentiating to become osteocytes. *ATF-4* activating transcription factor-4, *Dlx* distalless homeobox, *Fra* Fos-related antigen, *Osx* Osterix, *Runx2* runt-related transcription factor 2

controlling the transcription of target genes such as OC, OPN, ON, and collagen1 (Nakashima et al. 2002; Koga et al. 2005).

In cell culture, osteoblasts are morphologically nearly indistinguishable from fibroblasts. However, in contrast to fibroblasts, they express Runx2 (Komori et al. 1997; Ducy et al. 1997) and osteocalcin (Ducy et al. 1996), a secreted molecule that inhibits osteoblast function.

Active matrix synthesizing osteoblasts produce a unique combination of extracellular proteins, including osteocalcin, osteopontin, osteonectin, bone sialoprotein, alkaline phosphatase, and a large amount of type I collagen (de Gorter and ten Dijke 2013). They also synthesize and secrete proteoglycans such as decorin and biglycan, and due to their ability to bind calcium, these glycoproteins and proteoglycans are considered to be involved in two functions: the storage of calcium ions for calcification and the regulation of hydroxyapatite growth by preventing excess calcification. Osteoblasts also produce cytokines including insulin-like growth factor I and II, transforming growth factor β (TGF-β), and bone morphogenetic proteins (BMPs) (de Gorter and ten Dijke 2013). These growth factors are stored in calcified bone matrix and play an important role in differentiation and function of osteoblasts. Thus, bone matrix acts as a storage site of growth factors in addition to calcium and phosphates. IGF-1 secreted by osteoblasts is considered an auto- or paracrine regulator of osteoblastic cell function (Canalis 2009). IGF-1 signals via the IGF1 receptor, which in line with other tyrosine kinase receptors activates the phosphatidylinositol 3-kinase (PI3K)-Akt and Ras-ERK MAP kinase pathways.

BMPs belong to the TGF-β superfamily and were originally identified as the active components in bone extracts capable of inducing bone formation at ectopic sites (Urist 1965) and as osteo-inductive factors in decalcified bone and dentin (Urist et al. 1979). They are expressed and stored in skeletal tissue, and are required for skeletal development and maintenance of adult bone homeostasis, and they play an important role in fracture healing (Chen et al. 2004; Gazzerro and Canalis 2006). BMP-2, BMP-4, and BMP-7 trigger endochondral ossification by inducing mesenchymal cells to differentiate into osteogenic cells (Yamaguchi et al. 1991). BMPs bind as dimers to type I and type II serine/threonine receptor kinases, thereby forming an oligomeric complex. Binding of BMPs to their specific receptor complex leads to phosphorylation of Smads (R-Smads) that form heterodimer with Smad4 and regulate gene expression (de Gorter and ten Dijke 2013). BMP activity is also regulated by inhibitory Smads (I-Smads) and antagonists including noggin, chordin, and sclerostin. Although BMPs promote differentiation of osteoblasts by preventing MyoD expression and inducing Runx2 expression, the precise transcriptional mechanism has not been clarified yet.

TGF-β is one of the most abundant cytokines in bone matrix and plays a major role in development and maintenance of the skeleton, where depending on the context and concentration, it can exert both positive and negative effects on bone formation (Janssens et al. 2005; Maeda et al. 2004). TGF-β signals via a similar mechanism as the related BMPs. However, upon binding to its specific receptors, TGF-β induces activation of Smad2 and Smad3 (Feng and Derynck 2005; Massague et al. 2005). Smad3 overexpression in mouse osteoblastic MC3T3-E1 cells enhanced the levels of bone matrix proteins, ALP activity, and mineralization (Sowa et al. 2002). For more details on TGF-b and BMP signaling in osteoblasts, the reader is referred to the article published by de Sánchez-Duffhues et al. (2015).

Numerous markers for osteoblasts have been identified such as cbfa1, Osx, alkaline phosphatase (ALP), and collagen type I. Recent research of tissue nonspecific alkaline phosphatase (TNAP)-deficient mice revealed that TNAP acts as pyrophosphatase hydrolyzing pyrophosphate, an inhibitor of calcification, and increases the concentration of inorganic phosphates required for calcification (Hessle et al. 2002). Although ALP activity is intense in the basolateral plasma membrane of osteoblasts, their membrane facing toward osteoid and the plasma membrane of osteocytes hardly show ALP activity. Histochemical evidence indicates that the distribution of ALP does not always correlate with calcification sites and calcification is not completely disturbed in TNAP-deficient mice. Thus, the exact function of ALP in osteoblasts remains controversial.

2.1.5 Osteocytes

Osteocytes are derived from osteoblast progenitors which become entombed during the process of matrix deposition in small spaces called lacunae (Fig. 2.7). Osteocytes contribute to over 90% of the bone cells as compared to 4–6% osteoblasts and

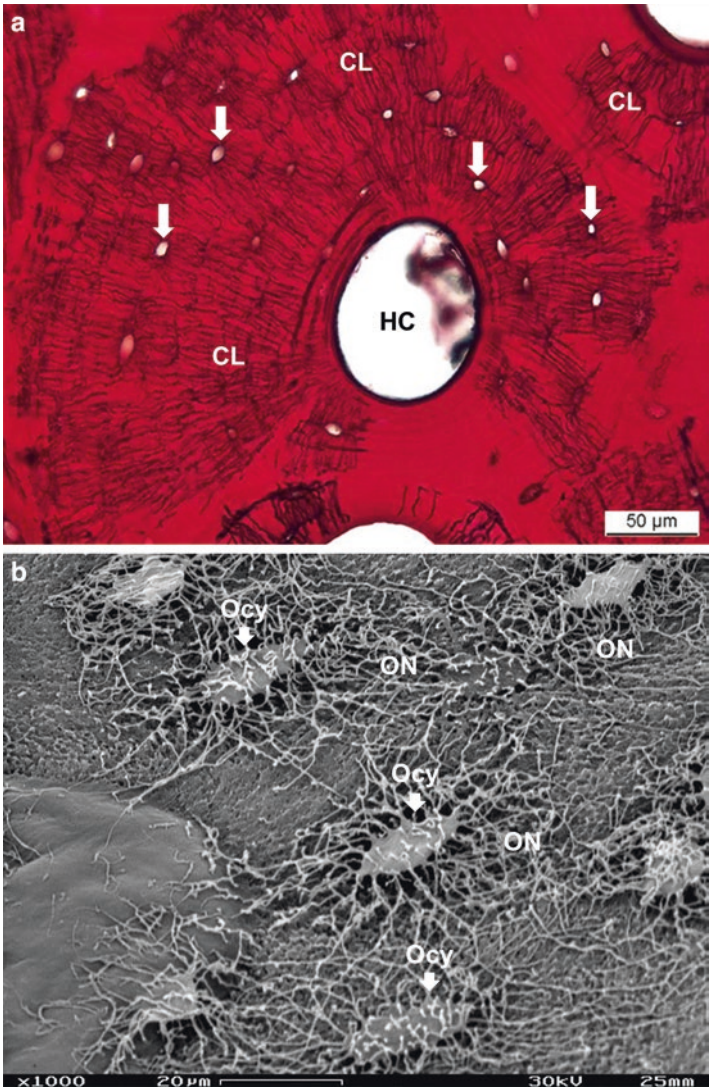

Fig. 2.7 Osteocyte. (**a**) decalcified human femur showing spatial distribution of osteocyte lacunae (*arrows*) and canaliculi (CL) surrounding a Haversian canal (HC). Silver impregnation according to Tripp (Tripp and MacKay 1972) with picrosfuchsin counterstaining. (**b**) SEM image of osteocytes (Ocy, *arrows*) on an acid edged human trabecular bone surface showing the extensive osteocyte network (ON) connecting with each other (SEM Image courtesy of Prof. Alan Boyde, Queen Mary University of London, UK)

1–2% osteoclasts, making them by far the most abundant cell in the bone matrix and on bone surfaces (Bonewald 2013). Osteocytes are regularly distributed throughout the mineralized matrix and connected with each other and the cells on the bone surface and even to cells within the bone marrow through dendrite-like

processes contained in fluid-filled micro-canals (canaliculi), which radiate toward the surface and the blood supply (Knothe Tate et al. 2004; Bonewald 2013). Recently developed methods (Schneider et al. 2010; Pacureanu et al. 2012) have allowed to understand the complexity and better define the magnitude of this network, which in terms of size appears to match the neural network of the brain (Buenzli and Sims 2015). The total number of osteocytes within the average adult human skeleton is ~42 billion and that the total number of osteocyte dendritic projections from these cells is ~3.7 trillion.

Their unique location in the bone matrix permits osteocytes to detect local changes in mechanical signals, either through strain or fluid flow; to respond to changes in levels of circulating factors like hormones and ions; and to amplify these signals leading to a coordinated adaptive response of the skeleton to environmental changes (Schaffler et al. 2014). These changes include adaptations in bone shape as well as the microarchitecture through a process called modeling (resorption and/or formation). Observational studies indicate that osteocytes might also detect fatigue-induced microdamage and send signals to the osteoclast progenitor cells on the nearby surface to initiate the complex remodeling process leading to the replacement of the damaged bone (Verborgt et al. 2002). Similarly, apoptotic osteocytes can send out stress signals which will result in their replacement via the process of bone remodeling. Osteocytes thus perform an essential task in the adaptation of bones to changes in mechanical loading as well as the maintenance of "healthy" bone tissue.

Relatively recent evidence suggests that the osteocyte network not only contributes to calcium homeostasis but also that FGF23 is released to regulate phosphate homeostasis in the kidney (Fukumoto and Martin 2009). The role of osteocytes in phosphate metabolism begins with their embedding in osteoid, when molecules known to be involved in phosphate metabolism such as dentin matrix protein 1 (DMP1) (Feng et al. 2006), phosphate-regulating neutral endopeptidase (Phex or PEX) (The HYP Consortium 1995), and matrix extracellular phosphoglycoprotein (MEPE) (Rowe et al. 2004) are elevated.

During the process of bone formation, between 5% and 20% of the osteoblasts become osteocytes. During this transformation the osteoblast cell body is reduced by roughly 30% at the early stage where cytoplasmic processes are formed and by about 70% when osteocyte maturation is complete. It is only recently that osteocyte markers such as E11/gp38, PEX, DMP1, sclerostin, FGF23, and ORP150 have been identified (Guo et al. 2010; Bonewald 2013). Some of these markers overlap in expression with osteoblasts, but others have been identified for specific stages of differentiation. Membrane expression of the membrane-associated proteins E11/PDPN/GP38 and MMP-14 is required for the formation of dendritic processes and canaliculi. The osteocyte-selective promoter, the 8 kb DMP1 driving GFP, showed selective expression in early and late osteocytes (Kalajzic et al. 2004).

A marker for the mature, embedded osteocyte is sclerostin, which is encoded for by the *SOST* (Balemans et al. 2001; Poole et al. 2005). This secreted protein is a negative key regulator of bone mass. It acts in the osteoblastic lineage as an antago-

nist of canonical WNT signaling, which is critical to bone homeostasis (Baron and Kneissel 2013). It impacts directly bone formation and indirectly bone resorption, and its absence or inhibition results in increased bone mass in several species including humans. Neutralizing antibodies or small molecules are being tested clinically with the aim to increase bone mass. Similar to sclerostin, albeit less selectively, WNT antagonist Dickkopf 1 (Dkk-1) is also robustly expressed by osteocytes. Finally ORP150 which may have a role in the protection of osteocytes from hypoxia is also highly expressed in mature osteocytes (Guo et al. 2010).

Osteocytes are able to modify their microenvironment. The term "osteocytic osteolysis" was introduced over 100 years ago to describe the enlargement of the osteocyte lacunae observed in patients with severe hyperparathyroidism and in immobilized rats (Recklinghausen 1910; Belanger 1969). In addition to the enlargement of the lacunae, changes can take place in the perilacunar matrix (Qin and Bonewald 2009). Perilacunar demineralization (osteocyte halos) was observed in rickets (Heuck 1970) as well as X-linked hypophosphatemic rickets (Marie and Glorieux 1983). Glucocorticoids not only cause enlargement of the osteocyte lacunae but might also be able to reduce mineral in the perilacunar space, thereby generating a zone of hypomineralized bone (Lane et al. 2006). Glucocorticoids may thus not only induce osteocyte death through their proapoptotic effect but in addition compromise the metabolism and function of the osteocyte. Interestingly, tetracycline label uptake, which occurs at sites of active bone mineralization, was observed in the osteocyte lacunae suggesting some ability of osteocytes to impact matrix mineralization. Taken together, this suggests that osteocytes may be capable of adding and removing mineral from their surroundings, which in turn may affect metabolic functions and mechanical properties of bone. Enlargement of the lacunae and canaliculi would reduce bone fluid flow shear stress, thereby reducing mechanical loading on the osteocyte which may trigger an adaptive response. Since the osteocyte lacuno-canalicular system is several orders of magnitudes greater than the bone surface area, the removal of only a few angstroms of mineral could have significant effects on circulating, systemic ion levels.

Osteocytes are long-lived cells, but like osteoblasts and osteoclasts, they die by apoptosis (programmed cell death). Decreased osteocyte viability is associated with bone fragility induced by estrogen and androgen deficiency or withdrawal, glucocorticoid excess, and mechanical disuse or overuse. Apoptosis is also triggered in response to microdamage, and it is proposed that dying osteocytes are targeted for removal by osteoclasts and replaced with new tissue in the process called remodeling. In this context, the expression of antiapoptotic and proapoptotic molecules in osteocytes surrounding microcracks was mapped, and it was found that proapoptotic molecules are elevated in osteocytes immediately at the microcrack locus, whereas antiapoptotic molecules are expressed 1–2 mm from the microcrack (Verborgt et al. 2002).

Given the crucial metabolic, mechanosensory, and tissue maintenance functions, it is clear that osteocyte viability is of crucial for skeletal health. The role of the osteocyte in skeletal growth, in mechanosensation needed for adaptation to

mechanical usage (modeling) in the postnatal skeleton, as well as bone tissue renewal and repair of microdamage (remodeling) will be discussed in a separate section of this chapter.

2.1.6 Osteoclasts

Osteoclasts are multinucleated giant cells responsible for bone resorption. Ultrastructurally, the multiple nuclei are surrounded by many mitochondria, endoplasmic reticulum, and a well-developed Golgi apparatus (Ross 2013). The presence of vesicles, lysosomes, and vacuoles indicates that these cells are actively involved in energy production and protein synthesis, particularly of lysosomal enzymes.

Osteoclasts are a member of the monocyte-macrophage family derived from the bone marrow macrophage, and they can be generated in vitro from mononuclear phagocyte precursors (Suda et al. 1999) (Fig. 2.8). Osteoclastogenesis critically depends on two cytokines, namely, macrophage-colony stimulating factor (M-CSF or CSF-1) (Pixley and Stanley 2004) and receptor activator of nuclear factor-κB ligand (RANKL) (Suda et al. 1999; Boyle et al. 2003). Both proteins exist as membrane bound and soluble form and are produced by marrow stromal cells and osteoblasts. Thus, recruitment of osteoclasts from their mononuclear precursor is

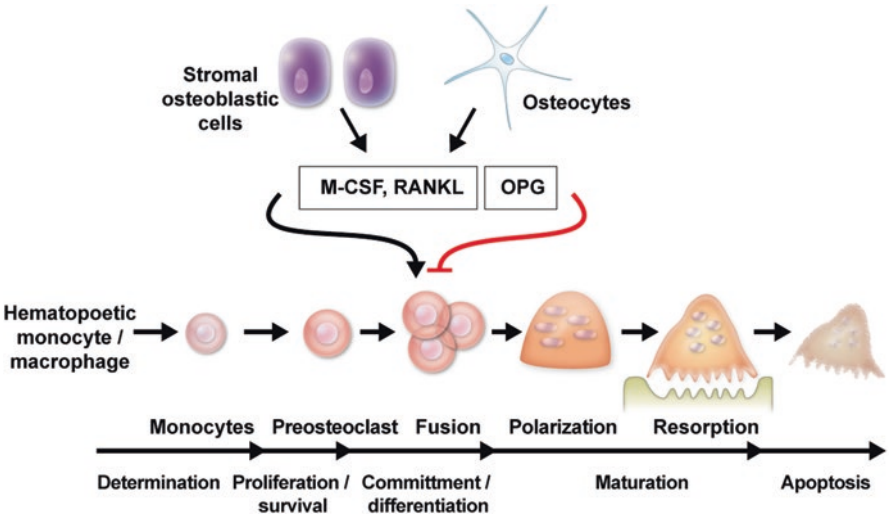

Fig. 2.8 Osteoclastogenesis and apoptosis: Osteoclast differentiation is governed by RANKL and M-CSF, as well as other cytokines secreted by osteoblasts and osteocytes that control various steps of osteoclastogenesis, including precursor proliferation, commitment, differentiation, and maturation. OPG, which is also secreted by osteoblasts and osteocytes, acts as a decoy receptor for RANKL and reduces osteoclast differentiation

critically dependent on the presence of nonhematopoietic cells residing in the bone marrow. RANKL, a member of the tumor necrosis factor (TNF) family, which was discovered originally as a secreted protein of activated T cells (Weitzmann et al. 2000), is the key osteoclastogenic cytokine required for the priming of precursor cells. This has been confirmed by mouse genetic studies showing that mice deficient in either RANK or RANKL show osteopetrosis which is attributable to a defect in osteoclastogenesis. In bone, RANKL produced by osteoblast-lineage cells including osteocytes binds to the RANK receptor, which is expressed in osteoclast progenitors and mature osteoclasts. Stimulators of osteoclastogenesis like PTH, PTH-related protein (PTHrP), prostaglandin E_2 (PGE_2), interleukin 1 (IL-1), and 1,25-$(OH)_2D_3$ act on osteoblast-lineage cells to upregulate RANKL expression. Conversely, osteoprotegerin (OPG), a soluble form of the TNF receptor, which is also expressed by osteoblasts and osteocytes, is acting as a decoy receptor for RANKL to inhibit osteoclastogenesis (Kostenuik and Shalhoub 2001). OPG is upregulated by estrogen, BMP, and TGF-β and suppressed by pro-inflammatory cytokines (Ross 2013). The balance between RANKL and OPG in osteoblast-lineage cells controls differentiation and activation of osteoclasts (Hofbauer et al. 2000; Boyle et al. 2003; Ross 2013). M-CSF appears to contribute to the proliferation, differentiation, and survival of osteoclast precursors, as well as the cytoskeletal rearrangement required for efficient bone resorption.

Active bone-resorbing osteoclasts show cellular polarization with the apical membrane consisting of the clear zone (or sealing zone) and the ruffled border and a basolateral plasma membrane (Nakamura 2007) (Figs. 2.9 and 2.10). The sealing zone (SZ) is the site of bone attachment which delineates the bone-resorbing space where the ruffled border is formed. The capacity of the osteoclast to form a sealed microenvironment between itself and the underlying bone matrix is a prerequisite to the resorptive event. The sealing zone appears as a ring of filamentous actin (F-actin also called actin ring or podosome belt), with the podosomes acting as focal adhesion points. It serves to isolate the bone-resorbing compartment from the extracellular fluid. The attachment of the osteoclast to the bone matrix is mediated primarily by the $\alpha_v\beta_3$ integrin transmembrane protein (vitronectin receptor), which engages in the sealing zone with the recognized amino acid motif Arg-Gly-Asp (RGD)-containing matrix proteins osteopontin and sialoprotein (Ross and Teitelbaum 2005; Teitelbaum 2005). Competitive RGD ligands are able to block osteoclast attachment and bone resorption. Cell matrix interaction stimulates the non-receptor-type tyrosine kinase c-Src, which is crucially involved in the maintenance of cell polarity and activity of osteoclasts.

The actual process of bone resorption is a two-step process, initiating with the dissolution of the mineralized matrix, followed by the enzymatic degradation of the organic matrix. The process takes place under the tightly sealed clear zone where the ruffled border, a surface extension, is formed. The acidification of the enclosed Howship's lacuna is achieved by carbonic anhydrase, which converts CO_2 and H_2O into H^+ and HCO^{3-} (Anderson et al. 1982; Gay and Mueller 1974), and by a vacuolar-type H^+-ATPase (Blair et al. 1989; Teitelbaum and Ross 2003). The pH of

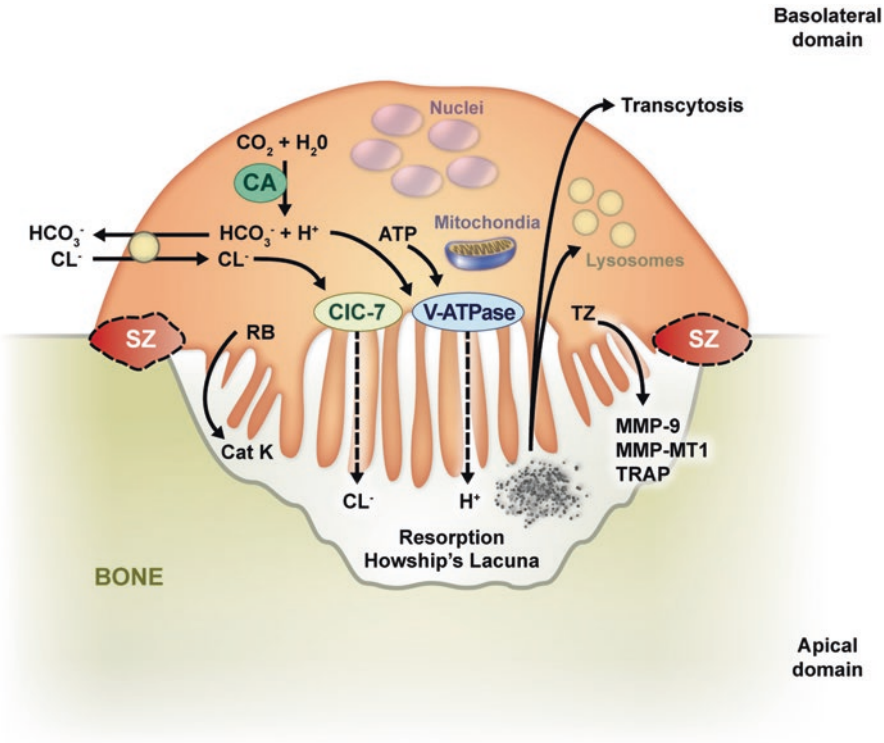

Fig. 2.9 Osteoclast ultrastructure/resorption: schematic representation of a resorbing osteoclast showing the sealing zone (SZ), ruffled border (RB), transition zone (TZ), nuclei, and resorption lacuna. Mature osteoclasts are polarized cells, with the apical domain facing the bone surface. In the process of bone resorption, H^+-protons and chloride ions (Cl^-) generated by carbonic anhydrase (CA) are transported via the V-ATPase and CIC-7 respectively to the RB membrane where they are secreted to acidify the resorption lacuna. Electroneutrality is maintained by a coupled basolateral bicarbonate/chloride exchanger, thus avoiding changes in pH and/or membrane polarization of the cell. Mitochondria generate the necessary ATP. Degradation of the demineralized bone matrix occurs through action of secreted cathepsin K (Cat K), matrix metalloproteinases (MMPs), and tartrate-resistant acid phosphatase (TRAP). Bone degradation products are released into the bone microenvironment, internalized into the cell to be degraded by lysosomes, or secreted at the basolateral membrane via transcytosis

4.5 leads to focal decalcification of hydroxyapatite leading to the exposure of the organic matrix, consisting largely of type I collagen. To prevent intracellular polarization, proton secretion is balanced by parallel extrusion of chloride ions through the ruffled border via a CIC-7-type chloride channel. The degradation of the demineralized extracellular organic components is accomplished by lysosomal enzymes such as cathepsin K (Gelb et al. 1996; Inaoka et al. 1995), MMP-9, and MMP-13 (Reponen et al. 1994; Ross 2013). Cathepsin K belongs to a cysteine protease family, and the acidic conditions in the Howship's lacuna provide an ideal milieu for the

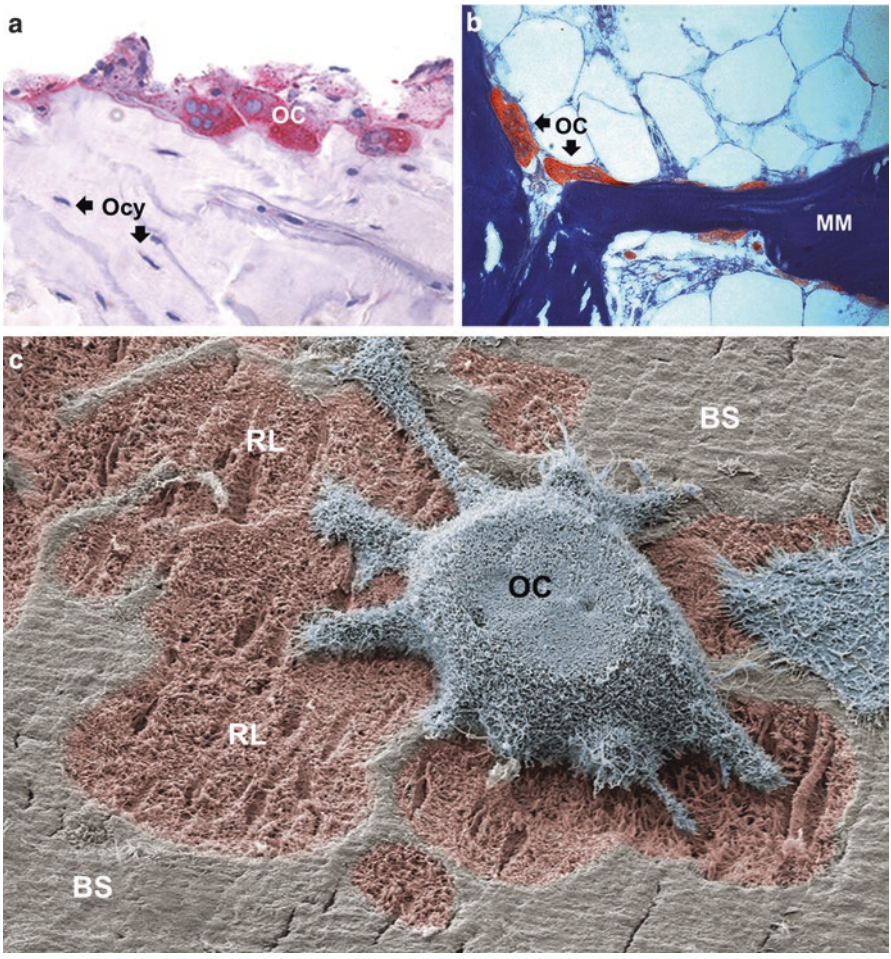

Fig. 2.10 Osteoclast morphology. (**a**) multinucleated osteoclasts (OC) on a subperiosteal bone surface in the rat. TRAP-stain with toluidine blue, (*Ocy* osteocytes). (**b**) TRAP-stained multinucleated rat osteoclasts (OC) on a trabecular surface (*MM* mineralized matrix). (**c**) colored SEM image of an osteoclast (OC). Resorption pit (RL) and 'intact' bone surface (BS) (SEM image courtesy Prof Timothy Arnett, University College London, UK)

degradation of collagen fibers. MMP-9 acts as a gelatinase for further digestion of segmented collagen fibrils. Degraded protein fragments are endocytosed and transported in vesicles to lysosomes where they are either degraded or transported to the basolateral surface where they appear to discharge their content into the surrounding extracellular milieu (Salo et al. 1997; Stenbeck and Horton 2004). The importance of this transcytosis of growth factors released from the mineralized matrix during the step of matrix demineralization and its perceived importance for bone

formation (coupling of bone resorption to bone formation) will be discussed in more detail in the section on bone remodeling further below.

Tartrate-resistant acid phosphatase (TRAP) is widely used as a marker enzyme of osteoclasts and secreted in Howship's lacunae. This enzyme appears to be involved in the dephosphorylation of osteopontin and bone sialoprotein, a prerequisite for integrin binding, and for the generation of reactive oxygen species involved in matrix degradation.

The Rho family of small GTPases is central to remodeling of the actin cytoskeleton in many cell types, including osteoclasts. Following attachment to bone, signals from $\alpha_v\beta_3$ and/or receptor tyrosine kinases activate small GTPases Rho and Rac, which bind GTP and translocate to the cytoskeleton to exert their specific effects. Rho signaling appears to affect predominantly cell adhesion mediated by the formation of the actin ring and a constitutively active form of the GTPase which stimulates podosome formation, osteoclast motility, and bone resorption (Jaffe and Hall 2005). In contrast, Rac stimulation in osteoclast precursors prompts appearance of lamellipodia, thus forming the migratory front of the cell to which $\alpha_v\beta_3$ moves when activated (Chellaiah 2005). Bisphosphonates, the potent antiresorptive drugs, inhibit the enzyme farnesyl pyrophosphate synthase in the mevalonate pathway, thereby blocking the addition of hydrophobic moieties onto the GTPases (inhibition of protein prenylation). This in turn prevents their membrane targeting and activation. Since active GTPases also regulate cell viability, bisphosphonates also trigger osteoclast apoptosis.

After completion of bone resorption, osteoclasts undergo programmed cell death or apoptosis. The signals that trigger osteoclast apoptosis are not well understood. High concentrations of extracellular calcium, Fas-ligand secreted by osteoblasts, the process of osteoclast detachment, and a decrease in the production of pro-survival cytokines (M-CSF, and RANKL), all these events have been suggested as potential mechanisms. ERK-activation is crucial for osteoclast survival, and TNF-α and IL-1 delay osteoclast apoptosis via ERK-activation. Finally, M-CSF, RANKL, and TNF-α also activate NF-kB in osteoclasts, a transcription factor which is known to inhibit apoptosis in many cell types. Several steroid hormones are known to regulate osteoclast formation, their activity, and survival. Estrogens and androgens inhibit the production of osteoclastogenic cytokines IL-1 and IL-6, and estrogens also induce osteoclast apoptosis. In mice, glucocorticoids reduce the number of osteoclast progenitors, but they also increase the life span of the mature osteoclast, so that their number does not decrease immediately. This may explain the transient increase in bone resorption in patients exposed to pharmacological doses of glucocorticoids. The inhibitory effect of glucocorticoids on osteoclast progenitors appears to be indirect, and it is likely mediated by the direct inhibitory effect of the steroid hormone on osteoblast numbers. The known effects of glucocorticoids are able to explain the transient increase in bone resorption followed by the low remodeling rate and suppression of bone formation which is typically seen during prolonged exposure in patients.

2.2 Skeletal Growth, Adaptation, and Maintenance

Fetal limb buds removed in utero and grown in vitro develop the shape of the proximal femur implying that bone shape is "imprinted" in the genetic material (Murray and Huxley 1925). This indicates that mechanical strain is required for postnatal, but not for prenatal skeletal development and maintenance. Studies in families and twins support this view (Seeman et al. 1989; Seeman et al. 1996). Both the postnatal and adult skeleton are able to continually adapt their structure where bone is added in response to an increase in loading, or being removed in response to unloading or disuse. The ability of bone to bear these loads is dependent on the type and magnitude of the applied load and the structural properties of the bone that is loaded (Wallace 2014). When loads exceed the structural strength of the bone, damage will occur and the bone may eventually fracture. Bone remodeling is essential for the maintenance of healthy bone tissue. This facilitates the replacement of apoptotic osteocytes, the repair of microdamage in the mineralized matrix, and the remodeling of the fracture callus into normal lamellar bone during the secondary stage of fracture healing.

Cortical bone undergoes both modeling (resorption and formation occurring independently of each other at different locations) and remodeling (coupled and sequential resorption and formation occurring at the same site). The goal in modeling is to either shape bone or change bone mass, whereas the purpose of remodeling is foremost to renew bone. Modeling and remodeling occur on both the endocortical and subperiosteal surfaces of the cortex, whereas within the cortex only remodeling – referred to as Haversian remodeling – takes place. Modeling occurs predominantly during skeletal growth but to a lesser extent also in adults, primarily in response to changes in mechanical loading. Recently, newer drugs such as PTH and anti-sclerostin antibodies used to treat osteoporosis have been shown to be either permissive to modeling or to stimulate it. This has considerably raised the interest in the topic of modeling in the adult skeleton and in its potential for therapeutic manipulation.

2.2.1 Skeletal Growth and Bone Modeling

Bone modeling is the process by which bone is either formed on an existing bone surface by osteoblasts without prior resorption (formation modeling) or being removed by osteoclasts (resorption modeling), with the aim to alter the shape of bone or adapt it to a change in mechanical loading (Fig. 2.11). Modeling occurs on subperiosteal, endocortical, and trabecular bone surfaces, and it is the dominant process during skeletal growth and before attainment of peak bone mass, even though it does continue throughout life at low levels. Bone modeling is thus essential for the proper functioning of three major processes, namely, longitudinal growth, radial growth, and cortical and cancellous bone drifts.

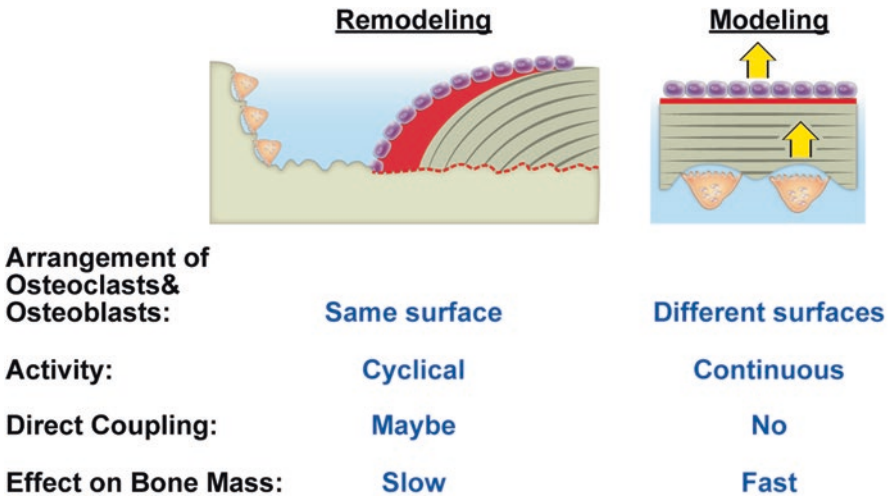

Fig. 2.11 Modeling vs remodeling: Bone remodeling involves sequential osteoclast-mediated bone resorption and bone formation at the same location. Its principal purpose is to repair microdamage and to renew the skeleton. Remodeling occurs on trabecular, endocortical, intracortical, and periosteal envelopes. In contrast, bone modeling occurs predominantly during skeletal growth. Formation modeling and resorption modeling occur on different surfaces. The two processes are either independent of each other (maintenance of local tissue strain) or happen in a coordinated fashion (cortical modeling drift during growth). Modeling can occur on periosteal, endocortical, or trabecular bone surfaces

In humans, skeletal development begins during the first trimester of gestation involving two distinct processes, namely, intramembranous or endochondral ossification. Most parts of the skull, the scapula and clavicula, are formed through intramembranous ossification, whereas the remainder of the bones of the skeleton is formed by endochondral ossification.

Intramembranous ossification is initiated by the formation of the blastema, a consolidation of mesenchymal cells which differentiate into osteoblasts and initiate matrix production, thereby establishing an ossification center (Allen and Burr 2014; Yang 2013). The transcription factor RUNX2 plays a crucial role in driving the cells of the blastema into the osteoblast lineage. The initial collagen matrix produced is disorganized and known as woven bone. Some of the osteoblasts become encapsulated in the mineralizing matrix and differentiate into osteocytes. The primary ossification center forms a small island serving as a template, to which lamellar or woven bone is added on the surface. During growth of these islands, several islands will merge to create a larger structure. When blood supply to the osteocytes becomes insufficient, blood vessels will invade the structure in some bones of the skull and even form a bone marrow space, a process not seen in the clavicula or scapula. Although intramembranous ossification is associated mainly with embryonic development, the process is recapitulated postnatally during bone healing.

In contrast, during *endochondral ossification*, bone is formed on a hyaline cartilage template produced by chondrocytes, which is replaced by mineralized bone tissue

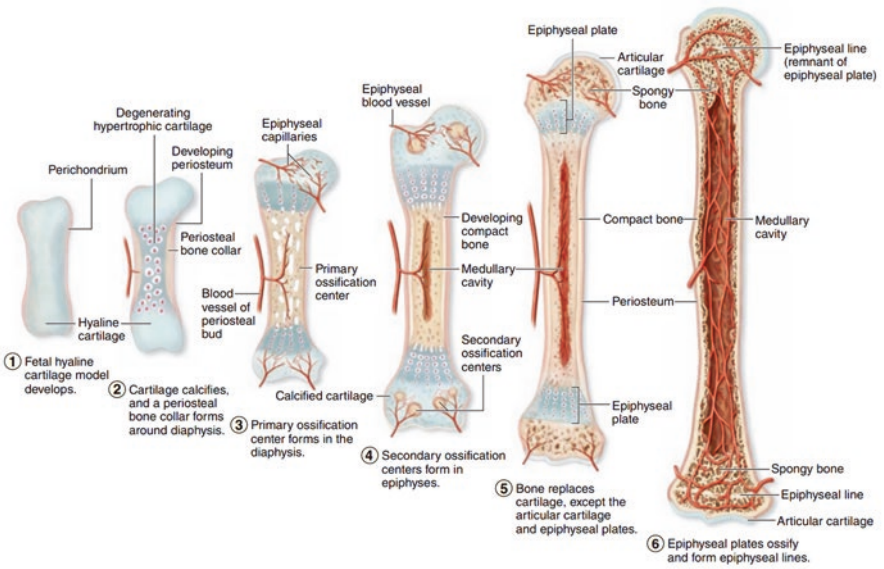

Fig. 2.12 Endochondral ossification forms most bones of the skeleton and occurs in the fetus in models made of hyaline cartilage (1). The process takes many weeks, and major developmental stages include formation of a bone collar around the middle of the cartilage model and degeneration of the underlying cartilage (2), followed by invasion of the resulting ossification center by capillaries and osteoprogenitor cells from the periosteum (3), and osteoid deposition by the new osteoblasts, calcification of woven bone, and its remodeling as compact bone (4). This primary ossification center develops in the diaphysis, along the middle of each developing bone. Secondary ossification centers develop somewhat later by a similar process in the epiphyses. The primary and secondary ossification centers are separated by the epiphyseal plate (5) which provides for continued bone elongation. The two ossification centers do not merge until the epiphyseal plate disappears (6) when full stature is achieved (Reproduced with permission from Junqueira's Basic Histology, 14th Edition)

(Fig. 2.12). In analogy to intramembranous ossification, endochondral ossification begins with a condensation of mesenchymal cells (Allen and Burr 2014; Yang 2013). However, these cells do not develop into osteoblasts, but are differentiated into chondroblasts by the transcription factor SOX-9. Chondroblasts initiate cartilage matrix synthesis with some of the cells becoming engulfed in the matrix where they differentiate into chondrocytes. The hyaline cartilage which is formed in this process is surrounded by a membrane called perichondrium, from where under the control of RUNX2, some of the cells differentiate into osteoblasts and begin forming bone matrix on the cartilage template. This process initiates at the circumference of the diaphysis of long bones (primary or diaphyseal ossification center), thereby creating a lamellar structure referred to as bone collar. The perichondrium is replaced by the periosteum, which provides the source for osteoblasts required for the subperiosteal expansion of the bone collar. The formation and expansion of the bone collar increasingly limit the provision of nutrients to the initial cartilage structure resulting in its calcification and eventually the death of the chondrocytes,

followed by the removal of these cartilage remnants by osteoclasts. It is the process of vascular invasion which results in the formation of the bone marrow space.

Over time, through a similar process, secondary ossification centers are being formed at both ends of the long bone in the epiphyses. The central diaphyseal region which contains a marrow cavity remains separated from the two secondary ossification centers by a cartilage layer called the epiphysis. The epiphysis or growth plate which forms at the interface of the two ossification centers is responsible for longitudinal bone growth. In the growth plate, morphologically distinct zones can be identified, namely, the resting zone, the proliferative zone, the prehypertrophic and hypertrophic zone, the calcified cartilage zone, and the ossification zone (Fig. 2.13). The resting zone (or reserve zone) which is comprised of hyaline cartilage matrix with embedded chondrocytes is the most distant region from the primary ossification center. This zone is rich in type II collagen produced by the chondroblasts located near the perichondrium that embed themselves in the matrix and differentiate into chondrocytes. The proliferation zone is readily identifiable by its stacked coin appearance, resulting from chondrocyte mitosis along the longitudinal axis of the bone. Growth hormone (GH), insulin-like growth factors (IGFs), bone morphogenetic proteins (BMPs), Indian hedgehog protein (IHH), and the Wnt-β-catenin signaling pathway all play important roles in stimulation of chondrocyte mitosis, while fibroblast growth factor (FGF) inhibits chondrocyte proliferation in the growth plate (Allen and Burr 2014; Yang 2013).

Longitudinal growth is predominantly driven by the cells located in the prehypertrophic zone. In the hypertrophic zone, chondrocytes begin to enlarge under the control of thyroxine and components of the WNT-β-catenin pathway, followed by their death through apoptosis. In the hypertrophic zone, type II collagen production is switched to type X collagen. This switch provides more stiffness to the region, but it also limits the diffusion of nutrients, and it may act as a trigger for the vascular invasion which is seen further below in the ossification zone. Also, cartilage calcification can be observed around the dying hypertrophic chondrocytes, an active process driven by the release of ALP containing vesicles by chondrocytes into the surrounding matrix, hence the term calcified cartilage zone. Chondroclasts, cells specialized in the removal of mineralized cartilage, are recruited to the site to resorb the calcified cartilage. In the ossification zone, osteoblasts produce woven bone on top of the mineralized cartilage. This woven bone is later removed by osteoclasts and replaced by lamellar bone, thereby forming the trabecular structures. Essentially, the complex process of endochondral ossification results in the production of a large number of parallel-oriented, narrowly spaced, trabecular elements that grow at a 90°

Fig. 2.13 (continued) the matrix is undergoing calcification, and 5. ossification zone, a zone in which blood vessels and osteoblasts have invaded the lacunae of the old cartilage, producing marrow cavities and osteoid for new bone. (**b**) growth plate of a young adult rat. Toluidine blue stain of the epiphysis. (**c**) and (**d**) Movat Pentachrome stain of the growth plate of a skeletally mature, 8-month-old rat. The proliferative zone is "less active," and the epiphysis shows signs of calcification as well as disruption of the pillar-like arrangements

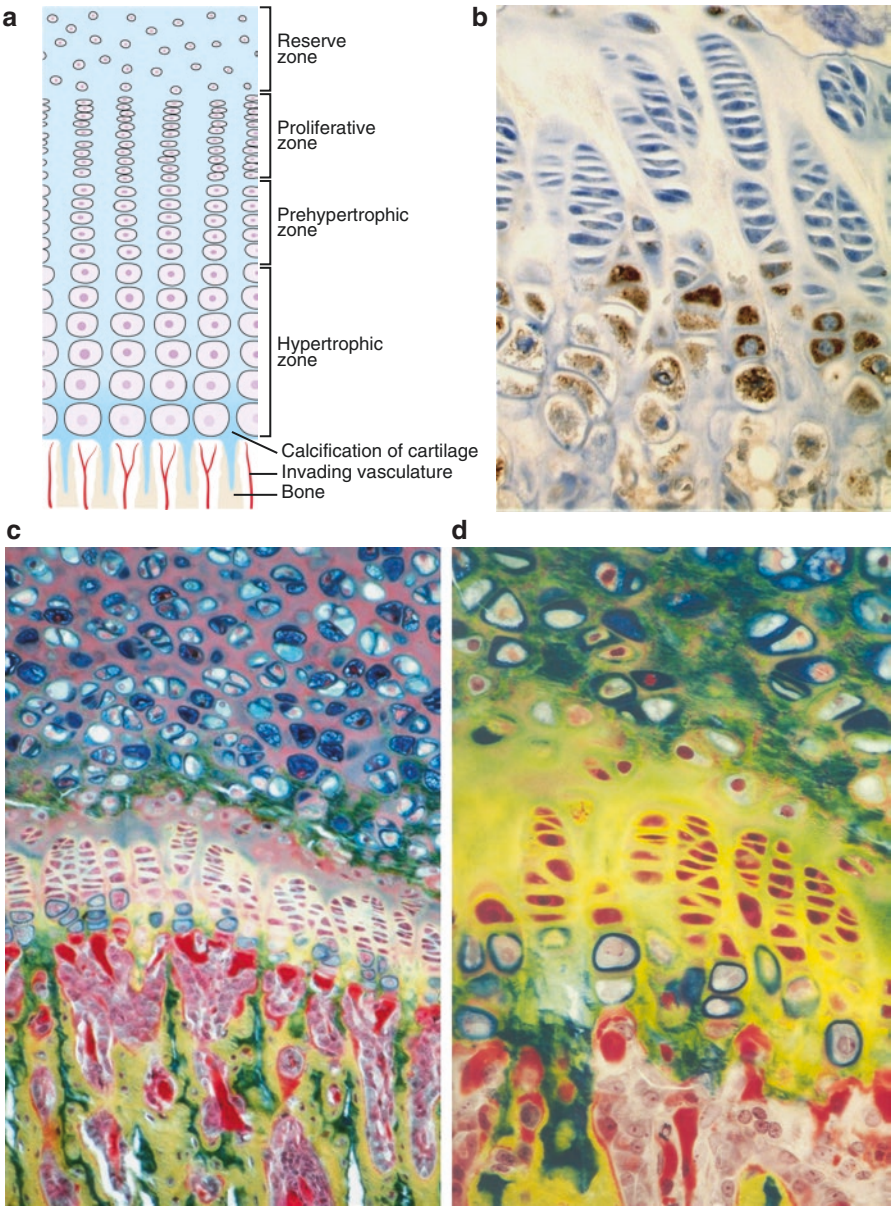

Fig. 2.13 Growth plate: Cells in epiphyseal growth plates are responsible for continued elongation of bones until the body's full size is reached. Based on the histologic appearance of the cells and surrounding matrix, the epiphyseal growth plate is classified into different zones (**a**) 1. resting or reserve zone (hyaline cartilage), 2. proliferative zone consisting of cartilage with proliferating chondroblasts aligned in lacunae as axial aggregates, 3. prehypertrophic- and hypertrophic zone consisting of degenerating cartilage in which the aligned cells are hypertrophic and the matrix condensed, 4. zone of calcified cartilage, an area in which the chondrocytes have disappeared and

angle from the growth plate and form the primary spongiosa. In a second step, these primary trabecular elements are thickened, connected to each other via lateral supports, reduced in number, and reoriented to align them with the principal direction of the local strain through remodeling and modeling activities, to finally form the secondary spongiosa.

In humans, longitudinal growth through endochondral ossification occurs until the epiphyseal plate becomes ossified in the late teens and early twenties. Epiphyseal closure is accelerated by the onset of estrogen production in puberty, since estrogen causes more rapid senescence of chondrocytes. In females, this process is driven by ovarian estrogen production picking up during late puberty, while in the male, different forms of estrogen are synthesized from androgens, specifically testosterone and androstenedione, by the enzyme aromatase.

During endochondral ossification associated with longitudinal bone growth, both formation modeling and resorption modeling play an essential role to maintain the shape in the metaphyseal region (Fig. 2.14). Resorption modeling removes

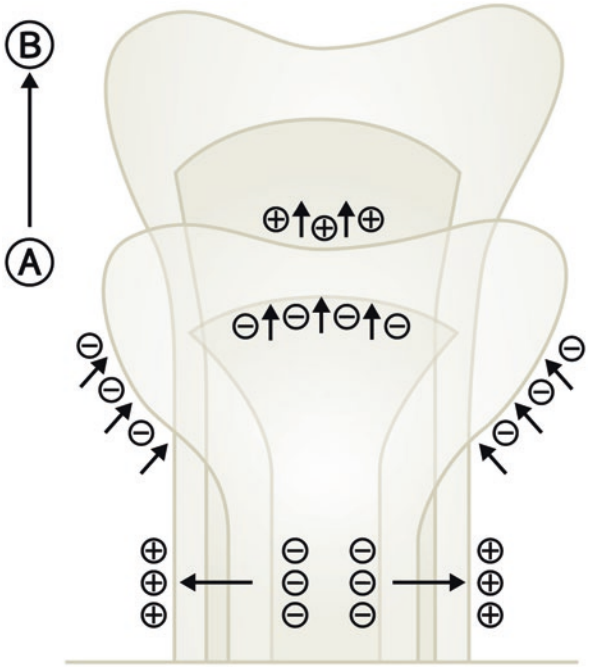

Fig. 2.14 Skeletal growth. Example of classical modeling of ends of long bone: shaping of long bone by modeling drifts during growth. Formation (+) and resorption (−) activities during bone growth from A to B. Resorption drifts (−) in the diaphysis enlarge the marrow cavity, while formation drifts (+) add bone periosteally to maintain the mechanical competence during bone elongation. In the lower metaphysis, an inward drift of cortical bone narrows the cross-sectional diameter of the metaphysis down to the smaller diameter of cortical bone to create the diaphysis and maintain the overall shape of the bone as it grows

bone from the periosteal surface in the metaphysis, while formation modeling adds bone on the endocortical surface which essentially leads to an inward drift of the cortex at this site. This inward drift of cortical bone narrows the cross-sectional diameter of the metaphysis down to the smaller diameter of cortical bone in the diaphysis, thus maintaining the overall shape during bone elongation. In contrast, radial growth is observed at the level of the diaphysis, where bone is added to the periosteal surface (formation modeling) and at the same time being removed at the endocortical surface (resorption modeling) to keep cortical thickness relatively constant, at least during skeletal growth (Fig. 2.14). Subperiosteal expansion is highest during skeletal growth but continues at a much slower pace throughout life. Skeletal growth is sexually dimorphic, and estrogen acts to inhibit periosteal expansion through modeling in the female, while increasing testosterone levels in the male accelerate this process (Garn 1970; Seeman 2008). Gender-specific hormonal differences thus determine the difference with males having larger-sized bones and higher bone mass relative to females at the age where peak bone mass is reached.

During aging, periosteal apposition is believed to increase as an adaptive response to compensate for the loss of strength produced by endocortical bone loss. In a 7-year prospective study of over 600 premenopausal women, Szulc and colleagues report that endocortical bone loss occurred with concurrent periosteal apposition (Szulc et al. 2006). As periosteal apposition was less than endocortical resorption, the cortices were thinned, but there was no net bone loss because the thinner cortex was now distributed around a larger perimeter. As a result of improved spatial distribution, resistance to bending increased despite bone loss and cortical thinning.

Bone modeling is not only important for longitudinal and radial growth during bone elongation, it is also the crucial process driving bone drifts (Fig. 2.15). Bone drifts are related to radial growth, but they can occur in the adult skeleton, although the limited capability for periosteal expansion with increasing age reduces the speed and magnitude at which adaptations can occur. During aging, both increasing endocortical bone resorption and reduced periosteal apposition cause net bone loss, alterations in the distribution of the remaining bone, and the emergence of the bone fragility. In addition, modeling drifts allow changing the position of the cortex relative to its central axis. Bone drifts are essential to allow adaptation of the skeleton to changes in the direction of the principal loading axis. Typical examples are orthodontic tooth movements, the spatial redistribution of bone mass of the humerus in the playing arm of tennis players (Haapasalo et al. 2000; Bass et al. 2002), or the change in the orientation of the hip joint axis during aging. The trabecular network can also undergo modeling drifts for the same reason. A typical example is the conversion of primary trabecular bone growing out of the growth plate at a 90° angle (e.g., independent of the direction of loads), into secondary trabecular bone, which is optimally aligned with the local direction of loads, thus allowing optimal transmission of mechanical forces from the joint to the cortical bone compartment.

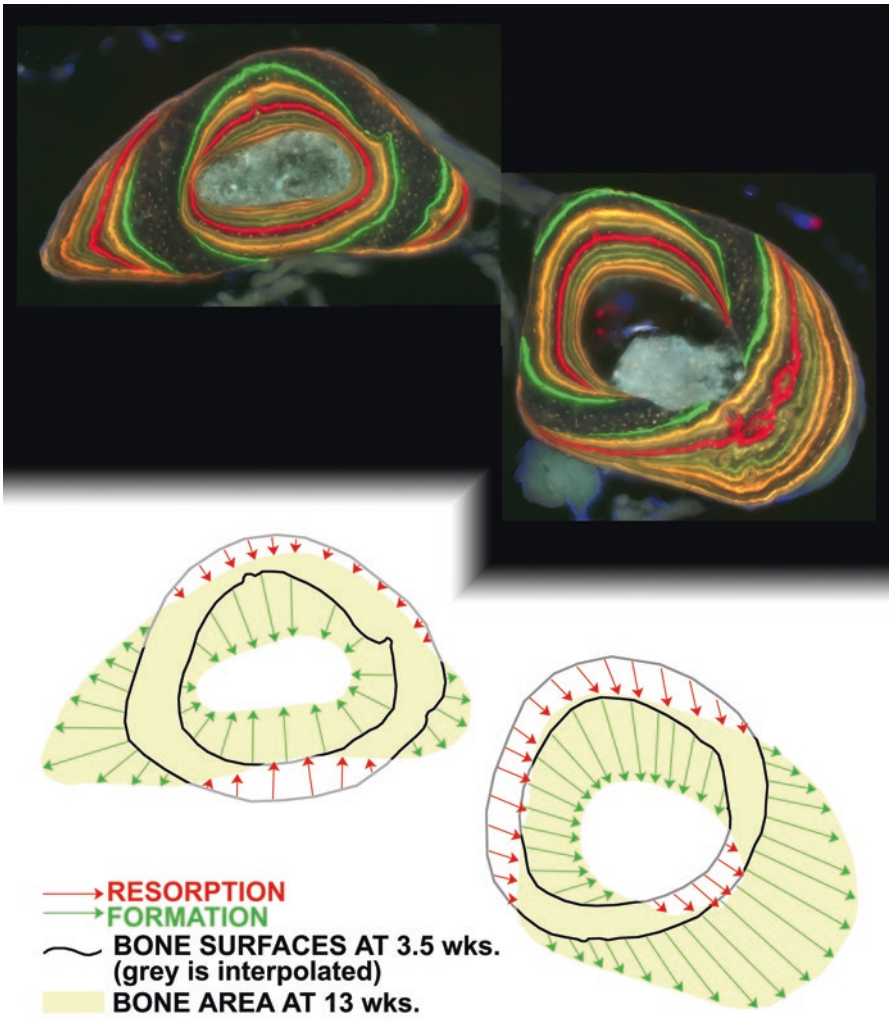

Fig. 2.15 Modeling drifts: Using multiple fluorochrome labels, bone drift can be visualized in a growing mouse. Different fluorochromes were administered roughly 1 week apart to a growing mouse between age 3.5 weeks and 13 weeks. At necropsy, the radius and ulna were sectioned for histological analysis. Radial growth occurred in the ulna (*left bone*) as the periosteal surfaces expanded outward, while there was also some formation modeling on the endocortical surface (modeling drift). The radius (*right bone*) underwent significant drift (*down* and to the *right* in the picture) by formation modeling on one periosteal surface and the opposite endocortical surface, along with resorption modeling on the other two surfaces. The schematic below the photomicrograph conceptualizes what the bone probably looked like at 3.5 weeks of age and how it was transformed through modeling to the eventual geometry (Reproduced with permission from Allen and Burr 2014 (Original image provide by Prof. Matthew Allen, Indiana University School of Medicine, USA))

2.2.2 *Bone Remodeling*

Bone remodeling involves sequential osteoclast-mediated bone resorption and osteoblast-mediated bone formation at the same location, and it is performed by the so-called basic multicellular unit (BMU) (Frost 1964; Crockett et al. 2011). The process can occur at any of the four envelopes, namely, periosteal, endocortical, intracortical, and trabecular. The final product of bone remodeling in cortical bone is an osteonal structure characterized by concentric layers of bone surrounding a Haversian canal and enclosed by a cement line (Fig. 2.16). In contrast, when remodeling occurs on a cancellous, endocortical, or very rarely the subperiosteal surface, no blood vessel is incorporated, and the resulting structure is called a hemiosteon.

It is commonly believed that two types of remodeling exist, namely, targeted and non-targeted (stochastic) remodeling (Parfitt 2002a). In targeted remodeling, a specific, local signaling event such as osteocyte apoptosis or microdamage would trigger a repair response to restore "healthy" viable bone to the affected site. In contrast, stochastic remodeling is thought to be a random process, which is believed to play a role in calcium homeostasis. The concept of microdamage serving as a signal for initiation of targeted remodeling was first theorized by Harold Frost in the 1960s. Since then, experimental evidence suggests that supraphysiologic mechanical loads can indeed induce microdamage (Mori and Burr 1993). Histological analysis demonstrated that the increased number of resorption cavities found in the overloaded limb was spatially related to the site of microdamage (Burr et al. 1985). Rodent studies showed that microdamage resulted in localized disruption of the osteocyte network via physical breakage of the cytoplasmic connections, which in turn induced osteocyte apoptosis (Verborgt et al. 2000). While the apoptotic osteocytes actively produce RANKL, the key factor in osteoclast development, the nearby healthy osteocytes produce antiapoptotic signals like OPG which may serve to target the remodeling response to the site of damage (Kennedy et al. 2012). A role for osteocyte apoptosis is further suggested by the fact that mechanical disuse, estrogen deficiency, and glucocorticoid excess induce this process and are associated with increased remodeling.

The remodeling cycle is divided into five distinct stages: activation, resorption, reversal, formation, and quiescence (Figs. 2.17 and 2.18) (Allen and Burr 2014). Bone remodeling takes place at various places throughout the skeleton, and these cycles are not coordinated with each other. As will be discussed later in this chapter, the length of the remodeling cycles varies between species, and it can be highly altered by disease. Hauge (Hauge et al. 2001) suggested that cancellous bone remodeling takes place in a special bone remodeling compartment (BRC, Fig. 2.17) (Crockett et al. 2011). Histological evidence suggests that the compartment is lined on its marrow side by flattened cells and on its osseous side by the remodeling bone surface, resembling a roof of flattened cells covering the bone surface (canopy cells). The flat marrow lining cells are in continuity with the bone lining cells at the margins of the BRC. The BRC model has gained support as it may help to explain how coupling of bone resorption and bone formation, two processes in the remodeling

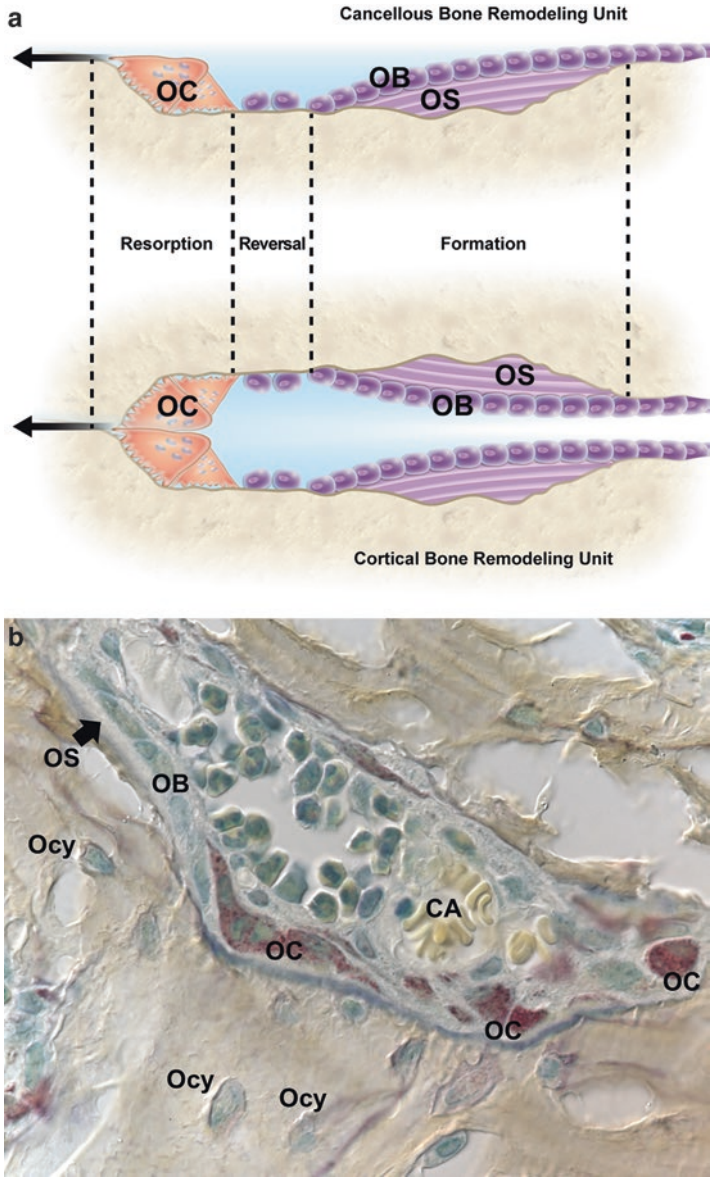

Fig. 2.16 (**a**) Diagram showing schematic of hemi-osteonal and osteonal remodeling carried out by a team of cells referred to as the basic multicellular unit (BMU). In cortical bone, osteonal remodeling in the BMU comprises a cutting cone of osteoclasts (OC) in front, a closing cone lined by osteoblasts (OB) following behind, and connective tissue, blood vessels, and nerves filling the cavity. The BMU maintains its size, shape, and internal organization for many months as it travels through bone in a controlled direction. Individual osteoclast nuclei are short-lived, turning over about 8% per day, and replaced by new pre-osteoclasts that originated in the bone marrow and travel in the circulation to the site of resorption. Refilling of bone at each successive cross-sectional location is accomplished by a team of osteoblasts, probably originating from precursors that reside

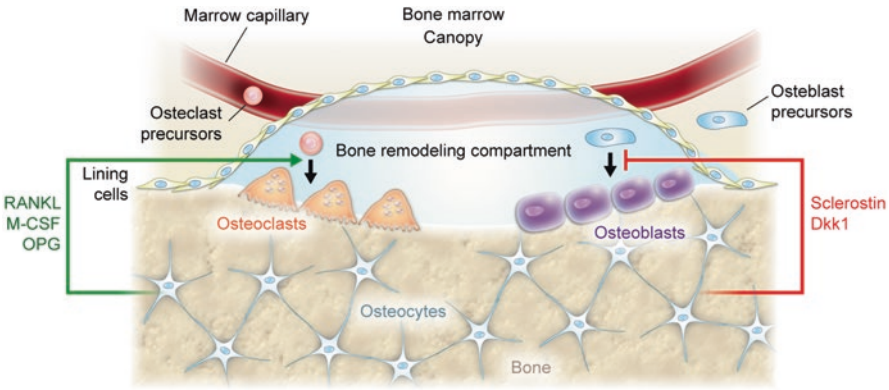

Fig. 2.17 Bone remodeling compartment: When bone remodeling is needed, osteocytes send signals through the canalicular network to the nearby bone lining cells, which retract from the bone surface to form a structure named bone remodeling compartment (BRC). Osteoclast precursors are attracted to the BRC by marrow capillaries where, under the influence of osteocyte-derived pro-osteoclastogenic cytokines RANKL and M-CSF, they differentiate to become mature osteoclasts, leading to the initiation of the bone remodeling cycle. Presumably in response to osteocyte-derived signals (including sclerostin and Dkk-1), and/or bone-derived factors which are released during bone resorption, osteoblast precursors from the bone marrow or the circulation are attracted to the BRC, where they differentiate into mature bone-forming osteoblasts resulting in the refilling of the resorption lacuna

cycle, may be linked, even though they take place at different time windows during the cycle (Sims and Martin 2015).

The activation phase initiates with the lining cells producing collagenase which digests the layer of unmineralized matrix, thereby exposing the bone surface to osteoclastic bone resorption (Chambers and Fuller 1985). Osteoclast precursors are recruited to the bone surface where they differentiate and fuse to become fully functioning osteoclasts. It has been suggested that the signal for the formation of these osteoclasts is provided by the canopy cells of the BRC, which have been shown to express a range of regulators of osteoclastogenesis, including RANKL (Crockett et al. 2011). In humans, the length of the activation phase is estimated to evolve over approximately 10 days (Fig. 2.18). With the presence of mature osteoclasts,

Fig. 2.16 (continued) within the local connective tissue, all assembled within a narrow window of time, at the right location, and in the right orientation to the surface. Hemi-osteonal remodeling, a term reserved for the remodeling of trabecular bone, conforms to the same sequence of surface activation, resorption, and formation as osteonal remodeling. Essentially, the trabecular BMU travels across the surface digging a trench rather than a tunnel, but maintaining its size, shape, and individual identity by the continuous recruitment of new cells. (**b**) Colored SEM of a cutting Cone. A longitudinal section through a cortical BMU, showing the osteoclasts (OC) at the front, followed by osteoblasts (OB) depositing osteoid (OS) at the tunnel wall. The BMU is supported by a capillary (CA). In the bone, osteocytes are visible (Colored SEM image courtesy of Prof. Robert S. Weinstein, University of Arkansas for Medical Sciences, USA)

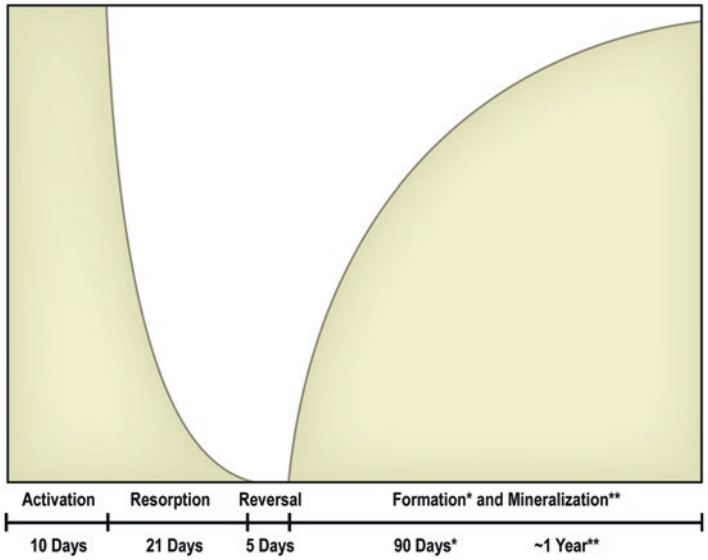

Fig. 2.18 Remodeling cycle: The four stages of bone remodeling, namely, activation, resorption, reversal, and formation, occur over different time frames, with the formation time taking four to five times longer than the resorption phase. Final mineralization of newly formed bone may take up to 1 year. The remodeling period (Rm.P), the time over which these processes occur at a given site, vary greatly between various species, and it may be influenced by disease states or pharmacological interventions. Approximate values reported in the literature for the Rm.P in healthy and estrogen-deficient humans, nonhuman primates, and rats are reported in Table 2.1 later in this chapter. The remodeling cycle is followed by a phase of quiescence of unknown duration. In healthy human bone, the amount of bone formed relative to the amount of bone resorbed by an individual bone remodeling unit (BMU-balance) is slightly negative. In postmenopausal osteoporosis, the BMU balance becomes more negative which together with the observed increase in the number of BMUs (increased activation frequency) results in significant bone loss

the bone lining cells on the targeted surface retract to expose the mineralized matrix to the osteoclasts allowing them to attach. The process of bone resorption, which in humans lasts on average 21 days, has been described earlier in this chapter. In cancellous bone, the size of resorption sites (Howships lacunae) varies considerably, and new osteoclasts can be recruited to the surface undergoing remodeling to extend it or to replace those osteoclasts that die of apoptosis. In contrast, in cortical bone, the size of the cutting cone in osteonal remodeling appears to be relatively constant.

The resorption phase is followed by the reversal phase, which is characterized by the cessation of resorption and initiation of bone formation. During this 5-day phase, remaining collagen fragments which were exposed during the resorption phase are being removed, by little-defined specialized form of cell. This process is essential for the progression of the BMU into the formation phase. These cells also appear to deposit a thin layer of collagen, thus forming the cement or reversal line, a visible delineation of the new hemiosteon or osteon respectively from the sur-

rounding, older matrix. The cement line which is rich in osteopontin (OPN) makes an important contribution to the mechanical properties, with OPN providing fiber matrix bonding which enhances bone's resistance to fracture, as well as crack bridging in the case of microcrack formation and inhibition of crack propagation (Sroga and Vashishth 2012). During the formation phase, osteoblasts deposit the osteoid, which consists primarily of type I collagen fibers and serves as a template for the mineralization. In humans, the bone formation stage (osteoid synthesis), lasts approximately 90 days (see * in Fig 2.18). Mineralization is divided into two phases: primary mineralization accounts for roughly 70% of the mineral deposition and in humans takes place between 2 and 3 weeks. In contrast, secondary mineralization which involves the maturation of mineral crystals to reach the final mineral content may take up to 1 year or more (see ** in Fig 2.18). The difference in time required for resorption (3–6 weeks) and the time needed for bone formation (4–6 months) explain why in histomorphometric analysis of healthy bone, the ratio of bone formation to bone resorption sites is roughly 4:1. The two-step process of bone mineralization has important consequences for the tissue-level mineralization. In general, when bone turnover is high, average tissue mineralization drops and the degree of heterogeneity increases, whereas a low rate of bone remodeling leads to higher average tissue mineralization and greater degree of homogeneity in tissue mineralization. Similarly, nonenzymatic but not enzymatic cross-linking is affected by the rate of bone remodeling. High levels of bone turnover reduce levels of nonenzymatic cross-linking, while low remodeling rates result in increased levels. Changes in tissue-level mineral density and the degree of heterogeneity affect mechanical properties of bones (material stiffness) and as a consequence the way microcracks propagate through the material. On the tissue level, the bone mineral density distribution (BMDD) can be assessed on bone biopsies by quantitative backscattered electron imaging (qBEI) or synchrotron radiation micro computed tomography (SRμCT) (Boyde and Jones 1983; Roschger et al. 2008). For example, transiliacal bone biopsies of postmenopausal osteoporotic women were found to have mostly lower mineralization densities than normal, which were partly associated by an increase of bone turnover, but also caused by calcium and Vit-D deficiency (Roschger et al. 2008). Pharmacological interventions changing bone remodeling and modeling have been shown to influence the BMDD. Antiresorptive treatment for 2–3 years results in a characteristic change in the BMDD profile indicative of an increased degree of homogeneity and a slight shift of the peak position toward higher mineral content. This was observed in postmenopausal osteoporotic women treated with alendronate (Roschger et al. 2001) and in the VertNA-study after 3 years of risedronate (Zoehrer et al. 2006).

Intermittent treatment with PTH is now approved for anabolic treatment worldwide. Given the substantial formation of new bone on trabecular and endocortical envelopes, and the increase in bone turnover under PTH treatment, it is not surprising that the BMDD was shown to shift slightly to lower mineralization densities with an increased peak width (higher degree of heterogeneity in mineral density) (Misof et al. 2003). In an estrogen-depleted rat animal model, comparable effects on BMDD had been observed (Kneissel et al. 2001). It can be assumed that this effect

is only transient and if PTH therapy would be followed by an antiresorptive treatment, the matrix would have time for a longer period of secondary mineralization and the BMDD would normalize eventually. In general, antiresorptive therapy causes an increase of degree and homogeneity of mineralization within 3 years of treatment, while normal mineralization levels are not exceeded. In contrast, anabolic therapy like PTH decreases the degree and homogeneity of matrix mineralization, at least transiently (Roschger et al. 2008). Furthermore, BMDD measurements combined with other scanning techniques like nano-indentation, Fourier transform infrared spectroscopy, and small angle X-ray scattering can provide important insights into the structure-function relation of the bone matrix and may ultimately allow for better prediction of fracture risk in diseases and after treatment.

Bone resorption and bone formation in the remodeling cycle are timed in a sequential manner, and under normal conditions, the bone balance after completion of the BMU should be neutral. This stimulation of osteoblast activity in response to resorption is termed "coupling," and it has long been of interest to understand how these two distinct cell types, on the same bone surface but at different times, could be linked so their activities are equal (Sims and Martin 2015; Crockett et al. 2011). There are four main classes of osteoclast-derived signals that are thought to contribute to the process coupling of bone resorption to bone formation in the context of the BMU. They include (1) matrix-derived signals released during bone resorption, (2) factors synthesized and secreted by the mature osteoclast, (3) factors expressed on the osteoclast cell membrane, and (4) topographical changes effected by the osteoclast on the bone surface which are sensed by osteocytes.

During bone formation, osteoblasts deposit a number of growth factors in the mineralizing matrix including TGF-β, platelet-derived growth factor (PDGF), insulin-like growth factors (IGFs), and bone morphogenetic protein 2 (BMP-2), which can be released as a result of the bone resorptive activity of the osteoclast. However, their contribution to the coupling of bone resorption to bone formation appears questionable since it is unlikely that, once released from the matrix, they remain within the BRC during the entire reversal phase to influence mature osteoblasts during the reversal phase and the 90-day formation process. Their principal role may be in the stimulation, recruitment, migration, and differentiation of osteoblast progenitors (Sims and Martin 2015). Similarly, the second class of osteoclast-derived signals, namely, the factors synthesized and secreted by the mature osteoclast, cannot be expected to exist throughout the reversal and bone formation phase of the bone remodeling cycle. Osteoclast-secreted factors, some of which were validated by studies in genetically altered mice, include cardiotrophin-1, sphingosine-1-phosphate, Wnt10b, BMP-6, CTHRC1, and complementfactor3a (C3a) (Sims et al. 2015; Crockett et al. 2011). It is important to note that none of these factors are produced exclusively by osteoclasts making it likely that nearby cells in the vicinity of the BMU are the main sources for the production of these factors which contribute to the coupling. More recently it has been suggested that EphrinB2 (Zhao et al. 2006) and semaphorin (Negishi-Koga et al. 2011), two cell surface regulatory proteins expressed by the osteoclast, may act via direct cell to cell contact with osteoblasts. However, direct cell-cell contact between osteoclasts

and osteoblasts at a remodeling site is rarely observed, making it unlikely that they act as coupling factor of bone resorption to bone formation. Direct cell-cell contact between osteoclasts with osteoblast progenitors may exist in the bone marrow or within the constraints of the bone remodeling compartment (Hauge et al. 2001; Kristensen et al. 2014).

Taken together, the question how coupling signals between the osteoclast and osteoblast could be transmitted directly remains elusive, given the fact that bone resorption and bone formation in the BMU are separated in time. The bone remodeling compartment may serve as a way to keep local coupling factors secreted by osteoclasts, osteoblasts, or their progenitors at concentrations sufficiently high to contribute to the coupling. On the other hand, osteocytes located in the vicinity of the Howship lacuna would be in an optimal position to detect the physical changes brought about by the osteoclast-mediated bone resorption (Schaffler et al. 2014). In this model, it is proposed that the increase in mechanical strain caused by the bone resorption process may be detected by the osteocytic network, which may provide the paracrine and endocrine signals required for the initiation as well as completion of the correct amount of matrix production by mature osteoblasts on the bone surface via the extensive canalicular network (McNamara et al. 2006).

It seems hence plausible to propose that the osteocytes could provide the coupling factors between bone resorption and formation and that they provide the final refining control to ensure that sufficient bone is formed by osteoblasts, generated in response to messages from osteoclasts either directly or via other cells residing within the BMC.

In humans, the length of the remodeling cycle, e.g., the time from the initiation of bone resorption until completion of the matrix formation by the osteoblast in the BMU, is roughly 4–6 months. In most laboratory animals, the remodeling cycle is much shorter (see comparative bone biology below). Under pathologic conditions, the length of the remodeling cycle can be altered and the rate of remodeling changed. The rate of bone remodeling is very high during early growth, but continues to slow down until peak bone mass is attained. In adult life, the rate of remodeling is controlled by age and genetics, but also modifiable factors such as nutrition, hormonal status, the level of physical activity, and medications. At menopause, the loss of ovarian estrogen production, which normally acts to suppress osteoclast production and promotes osteoclast apoptosis, results in accelerated bone turnover and bone loss. Men experience a less dramatic increase in bone remodeling and bone loss, and this occurs about a decade later than in women.

In healthy individuals, the bone balance in the remodeling cycle is mildly negative, meaning that the process of bone formation in the BMU does not fully replace the amount of bone that has previously been removed by the osteoclast. As part of the aging process, the mean wall thickness, which is a histomorphometric measure of the bone balance, becomes more negative (Lips et al. 1978). This negative bone balance has serious consequences on the mechanical competence of the skeleton, especially in situations where bone turnover is increased through a disease process (e.g., immobilization, estrogen deficiency, and secondary hyperparathyroidism), leading

to accelerated bone loss. Bone remodeling rates double at menopause, triple 13 years later, and remain elevated in osteoporosis (Recker et al. 2004; Seeman 2008).

Over time, the increase in bone turnover will change the material properties by shifting the mineral density profile to a lower level, thereby changing its elastic properties (Roschger et al. 2008). More densely mineralized bone is removed and replaced with younger, less densely mineralized bone, reducing stiffness (Boivin and Meunier 2002; Seeman 2008). Perhaps more importantly, high bone turnover contributes to trabecular thinning and perforation by increasing the likelihood of resorption lacunae coinciding on opposite sides of a trabecular structure (Allen and Burr 2014). But even in the absence of a perforation, an increase in activation frequency will lead to trabecular fragility by causing stress concentrators, which focus stresses to a single point (Hernandez et al. 2006). The negative effects of cavities on bone mechanical performance relative to bone volume are greater when cavities are targeted to regions of high strain and cannot be predicted using standard microarchitecture measures. In computer simulation models in trabecular bone specimens which were run to analyze how apparent level strains are resolved into local tissue-level strains, the importance of trabecular remodeling acting as local stress concentrator was highlighted by the observation that a 10% reduction in relative volume fraction by resorption cavities reduced relative stiffness by approximately 27%, whereas the same loss occurring through trabecular thinning reduced it "only" by approximately 18% (Van der Linden et al. 2001) (Fig. 2.19).

Increased remodeling on the cortical envelope (Haversian canals) resulting from estrogen deficiency, secondary hyperparathyroidism, other pathologies, or aging lead to increased cortical porosity (Martin 1984; Brockstedt et al. 1993; Yeni et al. 1997). Compromised osteoblast function with aging appears to add to this effect by

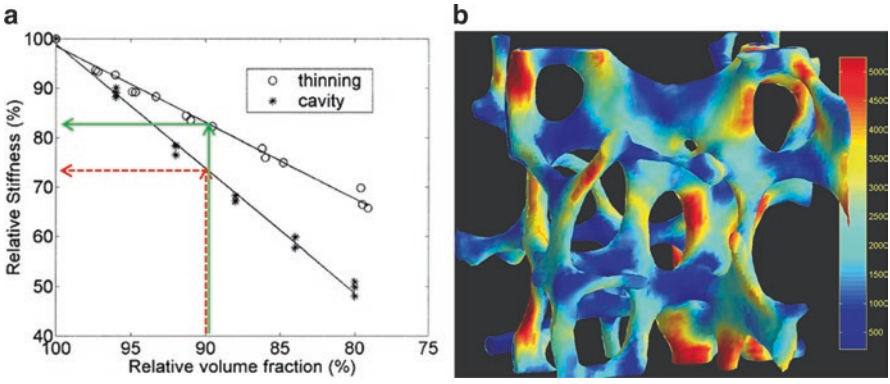

Fig. 2.19 (**a**) Simulation model calculating the change in maximum of apparent Young's modulus resulting from bone loss by resorption cavities (*) and by thinning of trabeculae (o). The reduction in relative stiffness as a consequence of a 10% reduction in relative volume fraction is greater when this deficit is produced by a resorption cavity than by trabecular thinning (Adapted from Van der Linden et al. (2001). With permission from the publisher. (**b**) Original colored SEM image provided by Prof. Harrie Weinans, UMC Utrecht, The Netherlands)

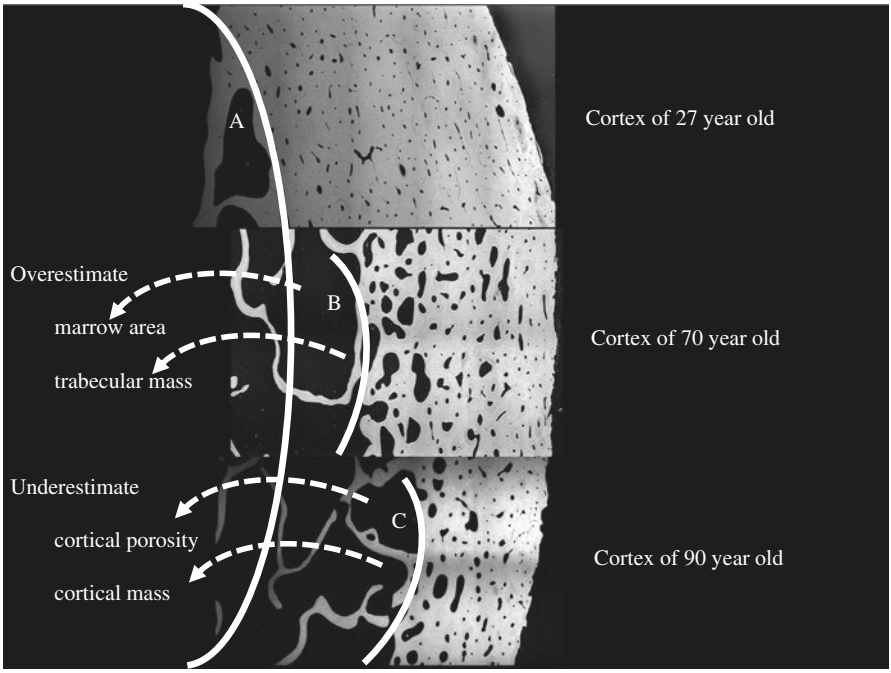

Fig. 2.20 Endocortical trabecularization with aging: Intracortical and endocortical remodeling erode the cortex. The endocortical surface (*white line* A of a specimen from a 27 years old) denotes the true medullary cavity/cortical interface achieved at completion of growth. If the surface of the thinned but still compact-appearing cortex (white line B in a 70 years old or C in a 90 years old) is erroneously described as the endocortical surface, several errors occur by incorrectly apportioning in the cortical fragments and porosity that created them to the seemingly expanded medullary canal (Reproduced with permission from Zebaze and Seeman 2015. Original image provide by Prof. E Seeman, University of Melbourne, Australia)

leading to an increased size of the central canal (larger pores). This effect can be observed particularly in the inner third of the cortical structure leading to the fusion of pores to generate large-sized defects referred to as superosteons and eventually to trabecularization of the endocortical surface (Fig. 2.20) (Bell et al. 2000; Zebaze and Seeman 2015). Clinical evidence suggests that superosteons contribute substantially to cortical porosity and that the elastic modulus of bone decreases approximately as the square root of porosity, suggesting it constitutes an important risk factor for hip fractures (Bell et al. 1999). In addition, from the mechanical point of view, cortical porosity reduces the ability of bone to limit crack propagation so that bone cannot absorb the energy experienced by a fall (Martin 1984; Yeni et al. 1997).

Given the negative effect of increased remodeling on cancellous (trabecular thickness and connectivity, stress raisers, material properties) and cortical bone (cortical thinning and porosity, material properties, endocortical trabecularization), it is not surprising that strategies to reduce the remodeling rate to a more "nor-

mal" level have been pursued clinically. For this purpose, various treatment options targeting osteoclast assembly or reducing their function like bisphosphonates and the RANKL-inhibitor denosumab have become available clinically (Kanis et al. 2013; Ferrari et al. 2012; Lekamwasam et al. 2012). Antiresorptive treatments are efficacious in slowing down or arresting cancellous and cortical bone loss, thereby reducing loss of trabecular connectivity, endocortical trabecularization, and trabecular surface-based and intracortical remodeling. Normalization of bone turnover has been shown to lead to a normalization of the mineral density profile. On the other hand, antiresorptive treatment is unable to restore trabecular bone connectivity or normal cortical bone thickness by adding lost bone back at the endocortical envelope.

2.3 Comparative Bone Biology

Animal models provide a more uniform experimental setup and allow for appropriate testing of potential therapies in preclinical settings. Animal models can be divided into three main categories, namely, homologous, isomorphic, and partial, based on how closely they recapitulate human disease processes. Ideally, an animal model would belong to the category of homologous models meaning that it shares the same causes, symptoms, and treatment options. In contrast, isomorphic animal models share the same symptoms but not etiologies, while all other models would be classified as partial models. Due to sometimes limited understanding of disease pathologies and obvious species differences, homologous models are rarely available, and isomorphic models remain the principle research tool for most studies. Animal models can also be divided into spontaneous (naturally occurring) and induced (surgical, genetic, or pharmacological intervention).

Like in other fields of study, genetically modified mice have become the main tool for mechanistic studies of bone metabolism, which have contributed greatly to improve our understanding of the molecular and cellular processes involved in normal bone physiology and disease pathology.

In animal models, bone loss can be induced by a range of interventions: creation of postmenopausal-like state of estrogen deficiency in female animals by surgical bilateral ovariectomy, orchidectomy in male animals, immobilization, or chemically through the administration of high-dose glucocorticoids or of estrogen antagonists such as ICI 182,780 or of aromatase inhibitors (Iwaniec and Turner 2008; Jee and Yao 2001). None of the animal models available to study osteoporosis show the full spectrum of human disease and can be considered a homologous model. Especially the lack of spontaneous fractures, which is perhaps the most important negative consequence of bone loss in humans, is typically only found in few genetically modified mouse strains. However, in animal models, the negative effect of bone loss on bone strength can be evaluated through a number of mechanical testing procedures ex vivo (Turner 2006; Sharir et al. 2008; Wallace 2014). This is relevant since it was realized that in humans, changes in bone mass do not always predict

fracture risk. Three-point bending, 4-point bending, and torsion testing are used frequently to assess bone mechanical strength in the diaphysis of the femur, a site where osteoporotic fractures rarely happen in humans. Perhaps more predictive – at least when performed in nonhuman primates – are the vertebral compression tests and femoral head (cantilever testing), sites where fractures are common in humans (Sogaard et al. 1994). Mechanical testing procedures will be discussed in more detail in a separate chapter (see Bone Biomechanics, Chapter 7). In land-dwelling animals, most of the diversity in bone shape and strength is the result of structural diversity, which is obvious at the macroscopic level. This structural diversity is largely due to individual differences in the genetic makeup rather than differences in lifestyle (Pocock et al. 1987; Christian et al. 1989). Also, although variations in material composition of bone exist, the differences are relatively small in land-dwelling animals that are commonly used to study osteoporosis (Keaveney 1998). This chapter will only discuss the most frequently used animals used to study metabolic bone disease, namely, the mouse, rat, and nonhuman primate, and highlight differences and commonalities with humans.

2.3.1 Nonhuman Primates

2.3.1.1 Strengths of the Nonhuman Primate Model

Nonhuman primates (old world monkeys) can be used to study changes in bone remodeling as they occur in human postmenopausal osteoporosis. They are genetically very close to humans and have menstrual cycles and even a natural menopause similar to human females, although their menopause occurs much later chronologically. Some nonhuman primates maintain an upright body posture with a bone biomechanical loading pattern similar to that of humans. At advanced age, they lose bone mass (Jayo et al. 1994; Lees and Ramsay 1999; Colman et al. 1999a, b) and their immune system is similar to humans. In consideration of all these aspects, the nonhuman primate is the most widely used large animal model to evaluate the effects on bone of new drugs designed to treat postmenopausal osteoporosis. Especially with the increase in the need for testing of new biologic agents (Brommage 2001; Smith et al. 2009; Vahle et al. 2015), primates often remain the sole alternative to test therapeutic monoclonal antibodies. Most investigations of bone metabolism have examined rhesus, cynomolgus, or pigtailed macaques, baboons, or African green (vervet) monkeys.

Nonhuman primates have a menstrual cycle very similar to that of women. Ovulatory cycles have been extensively characterized in baboons (Koyama et al. 1977) and in rhesus (Kerber and Reese 1969; Bosu et al. 1973) and cynomolgus macaques (Goodman et al. 1977; Shaikh et al. 1978; Sopelak et al. 1983; Mehta et al. 1986) and involve a follicular phase, ovulation, a luteal phase, and menstruation over 4 weeks. This is different from rats which have a 4- to 5-day estrous cycle that does not involve a true luteal phase unless mating (or pseudopregnancy) occurs.

Also in contrast to rats and similar to humans, a natural menopause occurs in baboons (Chen et al. 1998) and rhesus monkeys (Hodgen et al. 1977; Walker 1995; Gilardi et al. 1997; Colman et al. 1999a; Black et al. 2001) during their third decade of life, which is later than it occurs in humans when taking relative life spans into consideration.

Despite the occurrence of a natural menopause, nonhuman primates must be ovariectomized to induce ovarian hormone deficiency and bone loss of the postmenopausal type. A complete discussion of this model can be found in reviews by Smith et al. (2009) and Brommage (2001). Careful attention to surgical technique is essential, as cynomolgus monkeys continue to cycle normally with as little as 5% of their ovarian tissue present (Danforth et al. 1989). As alternative to surgical induction of the menopause, inhibition of menstrual cyclicity with the use of GnRH agonists and antagonists is also possible (chemical ovariectomy), with the advantage that the loss of ovarian function is reversible (Kenigsberg and Hodgen 1986; Mann et al. 1990; Gordon et al. 1991; Butterstein et al. 1997). Relatively large groups of 15–20 animals are required to provide adequate statistical power to reach valid conclusions which may raise ethical issues (Jerome and Peterson 2001). Special facilities are required resulting in relatively high cost. Following ovariectomy in skeletally mature nonhuman primates, bones exhibit increases in remodeling activity resulting in bone loss reaching a new steady-state bone mass within 8–9 months (Jerome et al. 1997, Smith et al. 2009). Since similar bone changes occur after menopause in women, ovariectomized monkeys provide an excellent model of the early skeletal events following menopause (Brommage 2001; Jerome 2004; Smith et al. 2009).

Another good reason to examine skeletal metabolism and the response to pharmacological treatments in monkeys involve the presence of well-organized osteonal structures in cortical bone. Thus like humans, nonhuman primate cortical bone undergoes osteonal (Haversian) remodeling which in rodents is virtually nonexistent under basal conditions. However, adult human cortical bone is largely composed of Haversian systems occupying about 45% of the total cortical area, whereas in adult macaques the corresponding value is only 5–7% (Schaffler and Burr 1984). This difference may be a reflection of both the longevity and the rate at which cortical bone turnover occurs.

Unlike cortical bone, the volume and structure of vertebral cancellous bone in nonhuman primates are very similar to humans (Vahle et al. 2015). Normative values for fractional bone volume range between 13% and 30% in human iliac crest biopsies and bone volume in intact cynomolgus iliac crest and lumbar vertebrae average about 25% and 27%, respectively (see Table 2.1 below from Vahle et al. 2015). With the exception of trabecular number, which is about 25% higher in nonhuman primates, estimates for other structural cancellous bone parameters in the lumbar vertebrae are consistent with human values. Bone formation rates in macaque lumbar vertebrae tend to be somewhat higher than those in human iliac crest (Vahle et al. 2015).

The fractional intestinal calcium absorption in adolescent pigtailed monkeys has been determined as 37% (Hoffman et al. 1972) and in adult male cynomolgus macaques as 40% of the dietary calcium intake (Lipkin 1998), values which are

Table 2.1 Comparative trabecular bone parameters in humans, macaques, and rats

	Humans		Macaques[a]		Rats[b]	
Parameter	Healthy subjects[c]	Postmenopausal women[d]	Intact	OVX	Intact	OVX
BV/TV (%)	13–28	14–30	26–28	21–25	19–26	~6
Tb.Th (μm)	100–225	93–105	107–127	97–122	40–60	53
Tb.N (mm^{-1})	1.0–1.8	1.2–2.0	2.1–2.6	2.1–2.5	3.89–5.62	1.10
Tb.Sp (μm)	800–1500	480–850	282–359	306–388	133–286	883
MS/BS (%)	5–20	1.0–13.5	11–14	13–22	4.6–15.4	8.2–29.4
MAR (μm/day)	0.83–0.98	0.5–2.0	0.61–0.66	0.65–0.80	0.62–1.56	0.68
BFR/BS (μm^3/μm^2/day)	7–15	1–25	26–31	31–67	103–232	85
Rm.P (days)	120–180	22–131	153	67	28	~20
Ac.f (cycles/year)	1–2	0.15–0.43	0.57–1.43	1.57–2.74	~0.7	0.9–1.6

BV/TV cancellous bone volume, *Tb.Th* trabecular thickness, *Tb.N* trabecular number, *Tb.Sp* trabecular separation, *MS/BS* mineralizing surface, *MAR* mineral apposition rate, *BFR/BS* bone formation rate, tissue level, *Rm.P* remodeling period, *Ac.f* activation frequency

[a]Based on measurements of lumbar vertebrae from Jerome et al. (1994, 1999), Stroup et al. (2009), Jerome CP, 1999, personal communication, and Cabal et al. (2013). Data either are averaged from several sources or presented as ranges.

[b]Based on measures from both the proximal tibia and lumbar vertebra in 3- to 19-month-old female rats. Mori et al. (1992), Jee and Li (1990), Chen et al. (1995a), and Ma et al. (1995)

[c]Based on iliac crest biopsies from 25 healthy subjects, age 19–46 years (for static data); dynamic data are normal values for 13 white adults (Weinstein 1992)

[d]Based on iliac crest biopsies from Recker et al. (1988) and Hauge et al. (1999)

similar to those reported for human adolescents. Interestingly, serum levels of calcitriol, the active metabolite and hormonal form of vitamin D, are five- to tenfold higher in baboons and macaques (Vieth et al. 1987; Knutson et al. 1995) than humans and are higher than in most other animals. The binding affinity for calcidiol, the circulating vitamin D binding protein in rhesus monkeys, appears to be normal, and the reason for this increase remains to be elucidated (Vieth et al. 1990).

2.3.1.2 Limitations of the Nonhuman Primate Model

Pigtailed, cynomolgus, and rhesus macaques raised in colonies attain peak bone mass at the ages of approximately 7, 9, and 10–11 years, respectively (Ott et al. 1997; Jayo et al. 1994; Champ et al. 1996; Cerroni et al. 2000). However, the availability of colony-raised monkeys is clearly limited, and maintaining monkeys in captivity in advance of starting a study increases its expense and raises putative ethical concerns. As an alternative monkeys imported from the wild can be used. A consistent observation is that spine bone mineral density (BMD) values for adult female monkeys imported from the wild increase several percent during the first several

years of captivity (Jerome et al. 1995), an effect that can only be mitigated by introducing an extended period of housing prior to the initiation of the study (Jerome et al. 1995; Binkley et al. 1998). These spontaneous gains in spine BMD in control, sham-ovariectomized monkeys are a complication in studies on osteoporosis because, although the ovariectomized monkeys lose spine BMD relative to controls, they may show only small declines or even gains in spine BMD during the experiment. Yet another complication is that the individual ages of wild-caught monkeys are unknown, the only method of verifying maturity is radiographic evidence of closed growth plates. However, even the exclusion of adolescent monkeys with open growth plates from studies does not prevent gains in spinal BMD during the initial period of captivity. The factors responsible for increased spine BMD during early years of captivity have not been identified conclusively, but they result likely from multiple causes. They are likely to include improvement of nutritional status (protein and calcium) and changes in other environmental factors and the recovery from a recent episode of reproduction including weaning.

Monkeys are mostly housed in groups allowing for interactions with peers and formation of hierarchical social groups. In addition, the monkeys have sufficient space for adequate physical exercise. However, group housing, though mimicking the settings in the animals' natural environment, exposes the subordinate individuals to continual psychological stress from losing fights and harassment. In studies involving intact, non-ovariectomized monkeys, the subordinate animals experience ovarian dysfunction and develop more severe atherosclerosis (Kaplan et al. 1991; Shively et al. 1997). Although individual housing eliminates these potential complications, the cages often do not allow sufficient room for movement and weight-bearing exercise, with the possible complication that bone loss due to inactivity might be encountered beside ethical concerns. A reasonable compromise might be pair housing, which allows psychosocial enrichment and a more easily established social hierarchy (Brommage 2001).

2.3.1.3 Methods and Study End-Points Available for Nonhuman Primates

Recent reviews (Vahle et al. 2015; Smith et al. 2009) provide a comprehensive source of information regarding the use of nonhuman primates in skeletal biology.

Ovariectomized monkeys consistently exhibit bone loss, as measured by spine BMD, when compared to sham ovariectomized controls (Jerome 2004). Like in humans, methods used to monitor bone changes associated with disease progression or pharmacological interventions noninvasively include determinations of BMD by dual-energy X-ray absorptiometry (DEXA) and peripheral quantitative computed tomography (QCT) (Jerome et al. 1997; Hotchkiss 1999; Cabal et al. 2013). Bone mineral density is monitored using DEXA bone scanners (e.g., Hologic QDR 2000 or Discovery A densitometers, Bedford, MA) at clinically relevant sites, i.e., the spine, hip, and radius (Smith et al. 2009). PQCT (XCT Research SA, Stratec Medizintechnik, Pforzheim, Germany) is a useful tool in preclinical studies providing complementary bone densitometry data, in conjunction with the DEXA data,

and has been previously reported to be a valuable tool for use in nonhuman primates (Dickerson and Hotchkiss 2008; Hotchkiss 1999). In contrast to DEXA, pQCT is not influenced by changes in body composition. It allows separate analysis of trabecular and cortical bone regions to detect BMD changes with greater sensitivity and provides information on geometric parameters such as periosteal circumference, endosteal circumference, and cortical thickness.

In addition, the same serum and urine biomarkers indicative of bone formation or bone resorption that exist in humans are available for nonhuman primates. These include the serum markers of bone formation, serum bone-specific alkaline phosphatase (BAP), osteocalcin and procollagen I intact N-terminal (PINP), and markers of bone resorption N-telopeptides (urinary NTx), serum C-terminal cross-linked peptide of type I collagen (serum CTx), and tartrate-resistant acid phosphatase 5b (TRAP5b).

Ovariectomy-induced bone loss is associated with an elevation of bone remodeling, and markers of bone turnover have been successfully employed including serum activities of TRAP5b and both total and bone-specific alkaline phosphatase, serum levels of osteocalcin, and assays measuring the urinary excretion of various degradation products of bone collagen fragments. Recent experience indicates that bone resorption can be reliably estimated by analyzing serum levels of CTx, thereby avoiding the need to collect urine (Jerome et al. 1994; Register and Jerome 1996; Brommage et al. 1999).

Bone biopsies for chemical and histomorphometric analyses can be taken from monkeys at the start of a study to obtain baseline values or during a study to obtain intermediate data. As is the case in humans, the iliac crest is the easiest and most reliable site to obtain a biopsy with minimal complications, and several technical procedures to obtain such biopsies have been published (Goodwin and Jerome 1987; Nogues and Milhaud 1988; Klein et al. 1991; Inskip et al. 1992). Limited experience is also available for other sites indicating that the rib (Ott et al. 1999; Binkley et al. 1999), vertebral body (Hermann and Smith 1985), and humerus (Ott et al. 1999) are possible. Rib biopsies provide the opportunity to examine osteonal bone metabolism, which is limited in iliac crest biopsies. Histological processing of plastic embedded sections of undecalcified bone (Brommage and Vafai 2000), to conduct static and dynamic histomorphometric measurements of bone structure and activity (Jerome et al. 1994), and bone immunohistochemistry (Carlson et al. 1993; Johnson et al. 2000) are well-established procedures. Other sites which are typically evaluated become available only after sacrifice of the animals including the lumbar vertebral body, femoral neck, tibial shaft, and rib (Smith et al. 2009).

Additional tests to assess bone quality include collagen cross-link analyses, mineral density fractionation to measure the degree of mineralization, and spectrophotometric tests such as FTIR. The use of specimens from nonhuman primate studies to perform these specialized tests provides excellent opportunities to further elucidate the underlying causes of bone fragility and to better understand the effect of pharmacological interventions.

Serum hormone analysis (Hotchkiss et al. 1998) can be performed, and oftentimes, reagents designed for use in human samples can be used successfully in non-

human primates if no specific test kit is available. Nonetheless, caution is always advised, and all human assays should be adequately validated before being "transferred" for use in monkey samples.

Just like other animal species, nonhuman primates do not develop spontaneous fractures as a consequence of bone loss after ovariectomy. For this reason, bone biomechanical measurements on excised bones (Jerome et al. 1997) have to be performed as a surrogate instead. Measures of biomechanical competency are important end-points in the assessment of bone quality. Strength testing on a materials testing machine is typically performed on a long bone, usually the femur (in 3-point bending), at the femoral neck (shear test) and at the lumbar spine (vertebral compression test) (Smith et al. 2009). Importantly, these basic tests allow evaluation of disease or a treatment at clinically relevant sites. Bone strength in the spine and femoral neck is decreased by ovariectomy (Jerome et al. 1997).

For more complete information on the use of nonhuman primates in bone research including special considerations on experimental design, the reader is referred to Chapter 1.

2.3.2 Rats

Among all animal species, the rat has become the preferred animal for many researchers to study bone disorders (Jee and Yao 2001; Iwaniec and Turner 2008). Its skeleton has been studied extensively, and although there are distinct differences compared to human physiology, these can be mostly overcome through appropriate study design, or at least taken appropriately into account in the interpretation of data generated experimentally. In contrast to humans, rats do not experience natural menopause. Under laboratory conditions, rats will maintain regular estrous cycles of 4–5 days duration. Unlike seasonal breeders (sheep, dogs), the rat skeleton is exposed to regular fluctuations in gonadal steroids and, like the human skeleton, more sensitive to the loss of ovarian hormones. Rats cycle through four distinct stages of the estrous cycle, the pro-estrous (12–18 h), estrous (10–20 h), met-estrous (12 h), and di-estrous (48 h). Not surprisingly, the most common approach for inducing bone loss in the rat is via surgical intervention on the gonadal axis, namely, ovariectomy (Bagi et al. 1993; Jee and Yao 2001; Lelovas et al. 2008) and orchidectomy (Erben et al. 2000; Blouin et al. 2007). Alternative models to surgical ovarie-/orchidectomy are targeting the endocrine system leading to osteoporosis that is reversible after withdrawal. These reversible methods include the administration of gonadotropin-releasing hormone agonists (Goulding and Gold 1989), estrogen receptor antagonists (Gallagher et al. 1993), and aromatase inhibitors (Gasser et al. 2006). The administration of gonadotropin-releasing hormone agonists creates a hypogonadotrophic-hypogonadal model, whereas estrogen receptor antagonists and aromatase inhibitors produce a hypergonadotrophic-hypogonadal model of osteoporosis.

Bone loss can also be achieved through surgical intervention at a higher level of the hypothalamic-pituitary-gonadal axis by performing a hypophysectomy (Chen et al. 1995b; Yeh et al. 1995), a surgical procedure that is more traumatic and complicated, and affects broader and unintended target tissues than needed. More popular are various procedures that cause immobilization/disuse induced and thus regional bone loss (Blouin et al. 2007; Jee and Ma 1999; Bagi et al. 1993). Immobilization models in rats include hind-limb immobilization, limb taping, nerve resection, tenotomy, limb casting, and reversible immobilization through injections of botulinus toxin (Jee and Yao 2001; Lelovas et al. 2008).

2.3.2.1 Strengths and Limitations of the Rat Model

In the past, many scientists were convinced that in the rat skeleton, the prevailing activity is modeling, and consequently the rat was not an appropriate model for human osteoporosis. However, this perception was based largely on data derived from the use of skeletally immature, growing animals, which were inappropriately compared to human adult bones. Although rats reach sexual maturity at the age of 2.5 months, their skeleton is considered fully mature only after the age of 10 months. In female rats, bone growth in the proximal tibia and distal tibia epiphysis stops at the age of 15 and 3 months, respectively, whereas in lumbar vertebrae, it continues for up to 21 months (Jee and Yao 2001). However, in analogy to the human skeleton, the rat skeleton shows a gradual transition from modeling to remodeling that is related to age progression and cessation of longitudinal bone growth in both cancellous and cortical bone. In the cancellous bone of the lumbar vertebrae, this transition is evident from the age of 3 months onward, whereas in the proximal tibia metaphysis, this transition takes place from 6 to 9 months of age (Iwaniec and Turner 2008). After the age of 10 months, the bone growth rate for the proximal tibia epiphysis is less than 3 μm/day, and it stops altogether after the age of 15 months. If experimentation in female rats starts around 10 months, e.g., the time when peak bone mass is achieved, the total longitudinal bone growth adjacent to the epiphyseal plate of the tibia until cessation of growth will be less than 0.5 mm. In contrast in male rats, the closure of the epiphyses of many long bones is delayed with many of them remaining open past 30 months. At the endocortical envelope in vertebral bodies, this gradual transition from modeling to remodeling evolves at the age of 3–6 months and at the endocortex of the proximal tibia metaphysis at 9–12 months (Jee and Yao 2001).

A potential drawback to the use of rat models for osteoporosis is the lack of Haversian remodeling in the rat skeleton. In humans, increased Haversian remodeling is the main cause of cortical porosity, but rats lack a well-developed Haversian remodeling system. In the rat skeleton, cortical bone gain occurs in the periosteum, and cortical bone is lost at the endosteum (Turner 2001). Larger animal models such as rabbits, dogs, and especially primates are considered more appropriate for the study of Haversian remodeling. Despite this drawback, ovariectomy of skeletally mature rats leads to a condition similar to the menopause in humans. Like in humans,

cancellous and endocortical bone loss is mediated by an increase in the overall rate of bone remodeling and by altering the balance between bone formation and bone resorption (Jee and Yao 2001).

The ovariectomized skeletally mature rat is the most commonly used animal model to study postmenopausal osteoporosis. After the ovariectomy, accelerated bone remodeling leads to rapid loss of cancellous bone, eventually reaching a steady state, where resorption and formation are balanced (Boyd et al. 2006). Statistically significant bone loss is seen in the proximal tibia metaphysis after 14 days and near steady state is reached from around 90 days onward post-ovariectomy (Wronski et al. 1988; Wronski et al. 1989; Brouwers et al. 2008; Gasser et al. 2006). In lumbar vertebral bodies, significant bone loss is observed after 60 days (Wronski et al. 1990) and in the femoral neck after 30 days (Li et al. 1997), steady state is reached for both sites after 270 days. It should be noted that ovariectomy does not induce bone loss in the epiphyses of long bones, the distal tibia metaphysis, or the caudal vertebrae (Li et al. 1996; Miyakoshi et al. 1999).

Losses of endocortical as well as cancellous bone are the primary causes of postmenopausal osteoporosis in humans, whereas intracortical remodeling-induced bone loss in the Haversian system seems to play a less important role (Iwaniec and Turner 2008). Given the ethical considerations and the high cost of acquisition and maintenance, reduced availability in experimental centers associated with large animal models of osteoporosis, the lack of the Haversian remodeling in the rat skeleton is a shortcoming that can often be accommodated (Turner 2001).

2.3.2.2 Methods and Study End-Points Available for Rats

In general, the methods used in the evaluation of bone mass, architecture, and metabolism in the rat skeleton are the same as those used for humans. Measurements of calcium, phosphorus, and magnesium in blood and urine can be obtained from the rat model. In analogy to humans, the most commonly used biochemical markers representative of "global" bone turnover can be measured in rats including peptides originating from osteoblasts indicative of bone formation (BAP, osteocalcin) or osteoclastic resorption (TRAP5b). In addition, organic compounds released during the synthesis (P1NP) and resorption of bone matrix (urinary or serum CTX-1) (Loeb 1999) can easily be measured.

Like in clinical studies, DEXA and pQCT with small animal software can be used to measure both total and regional bone density and get limited cortical structural parameters in rats and mice (Turner et al. 2001; Gasser and Willnecker 2012; Breen et al. 1998). The recent arrival of high-resolution in vivo microCT provides the ability to noninvasively monitor microarchitectural changes in cancellous bone in individual animals over time (Boyd et al. 2006; Gasser et al. 2006; Bouxsein et al. 2010; van't Hof 2012). Comparison of two-dimensional histomorphometry and three-dimensional microCT demonstrates the superiority of microCT in revealing early changes in bone architecture (Jiang et al. 2005).

Because spontaneous fractures do not occur in aged or ovariectomized rats, data regarding mechanical competence of bones have to be obtained ex vivo on excised bones with mechanical testing procedures. In rats, the most common test procedures are the 3- or 4-point bending of the femur diaphysis, the vertebral compression, and the femoral head test (cantilever testing) (Sogaard et al. 1994). The nature and clinical relevance of the mechanical testing procedures available in rats, which do not reproduce the situation under which spontaneous fractures occur in humans, will be discussed in more detail in a separate chapter (see Bone Biomechanics, Chapter 7). Last but not least, histomorphometric analysis provides a two-dimensional study of bone volume and architecture at a very high resolution unmatched by any of the noninvasive devices. Histomorphometry accurately evaluates bone architecture and indices of bone fragility independently of bone mass. Parameters measured by histomorphometry include the numbers of osteoblasts, osteoclasts, osteocytes, and active osteoblasts relative to bone perimeter; trabecular thickness, number, and separation; and many others (Meunier 1988). The use of fluorochrome labeling is especially valuable in the evaluation of dynamic bone changes (Frost 1964). In rats, this invasive assessment can be carried out ex vivo at every site that is relevant for human disease (Erben and Glösmann 2012). This is in contrast to clinical studies, where the tissue sampling is limited to the iliac crest, a site which may not be fully representative of the actual location where the majority of the fractures occur such as the vertebrae, the hip, and the forearm.

Comparative data for histomorphometric parameters in healthy and ovariectomized rats with human and primate data has been published (Vahle et al. 2015). One of the main differences which is readily apparent when comparing histomorphometric parameters between rat, macaques, and humans is the remodeling period (Table 2.1), e.g., the time that is required for completion of one whole remodeling event. In healthy rats, the remodeling period is on average 28 days, compared to approximately 153 days in macaques and 120–180 days in healthy human subjects. The length of the remodeling cycle is influenced by age, disease, or drug treatment, and some evidence suggests that differences exist between locations where it is measured. Estrogen deficiency, which is known to lead to increased activation of remodeling, also results in shortening of the remodeling period to 20 days in ovariectomized rats, 67 days in ovariectomized macaques, and 22–131 days in postmenopausal women.

Compared to healthy human subjects, the remodeling period in the rat is roughly four to six times shorter which explains the fact that skeletal changes as a consequence of perturbances by disease or pharmacological interventions evolve more rapidly in the rodent. This is convenient since it allows reducing the duration of rat studies under most experimental conditions by a factor of 6.

In summary, after the age of 12 months, remodeling becomes the predominant activity in cancellous and cortical bone in the lumbar vertebral body and proximal tibial metaphysis in the rat skeleton (Jee and Yao 2001; Erben 1996). The modeling-to-remodeling transition is associated with reduction of longitudinal bone growth to very low rates. To conduct research on new potential modalities for the treatment of postmenopausal osteoporosis in rats, the bone site and age of the animal must be

such that remodeling is the predominant activity. Despite the limitations discussed above, the skeletally mature rat (>10 months in female rats) is generally considered an appropriate animal model for the research of postmenopausal and immobilization osteoporosis (Turner et al. 2001; Iwaniec and Turner 2008; Jee and Yao 2001).

The broad availability of noninvasive methods to study changes in bone mass, cancellous and cortical bone architecture, and biochemical markers longitudinally, combined with invasive end-points including histomorphometry and bone mechanical testing, makes the rat a very versatile tool for the evaluation of preventive or therapeutic strategies for the treatment of osteoporosis.

2.3.3 Mice

Mice are often employed in bone studies because of their availability, ease of handling, high reproductive rates, and low cost of use (Jilka 2013). Owing to technical feasibility, the mouse is to date the predominant mammalian species for targeted genetic modification, and it has assumed a crucially important role toward dissecting the molecular pathways, which are critical to bone homeostasis. In addition the study of mouse strains has contributed to a better understanding of genetic contributions to peak bone mass and age-related bone loss (Beamer et al. 1996). Mice also successfully replicate the skeletal phenotypes related to several genetic disorders in humans. In fact, the ability to manipulate gene expression in mice in a cell-specific fashion has allowed scientists to address fundamental questions underlying the regulation of bone cells based on observations in the culture dish and to move them into the in vivo situation. The most commonly used technique in mice has been to date genetic modification such as transgenesis, knock-outs and knock-ins, large-scale mutagenesis, and conditional gene modifications (Lyons 2013; Kan 2013). In contrast, the surgical induction of a postmenopausal bone loss by bilateral ovariectomy, as well as immobilization- or glucocorticoid-induced bone loss, is technically more challenging in mice and is thus predominantly performed in rats and primates. This section will focus on mouse biology and the challenges faced when the mouse is used as a preclinical model for postmenopausal- or age-related osteoporosis (Jilka 2013). For a more in-depth discussion of genetically manipulated mice, the reader is referred to the recent reviews written by Lyons (2013) and Kan (2013).

The ovulatory or estrus cycle of female mice has a length of 4–6 days. The estrus cycle can become synchronized in female mice housed together continuously and can be suspended in the absence of exposure to male pheromones. Due to their short 3-week gestation period, high reproductive capacity (five to six animals per litter), and ease of genetic manipulation, standardized outbred and inbred strains of laboratory mice have become very popular in almost every aspect of research, including skeletal biology.

Starting in the early twentieth century, over 34 well-defined outbred strains have been established with the aim to preserve genetic heterogeneity, analogous to the genetic variation in human populations (Chia et al. 2005). They are thus particularly

suited for genetic studies and as the starting point for developing models of human disease. As a disadvantage, the genetic variability of outbred strains contributes to differences in phenotype and response to treatment among individuals, just as is observed when studying human populations. As a consequence, larger numbers of animals per treatment group are required to achieve appropriate statistical power.

In contrast, inbred strains of mice were derived from outbred strains by intensive brother-sister mating to produce mice with practically identical genomes. There were 450 known inbred strains in 2000 (Beck et al. 2000). By convention (Committee on Standardized Genetic Nomenclature for Mice 1952), the standard definition of an inbred strain assumes two basic requirements: (i) 20 or more consecutive generations of full-sib mating (or its genetic equivalent in terms of other relationships) and (ii) all members of the strain derived from a single breeding pair of individuals in the 20th or a later generation. These criteria theoretically assure a minimum level of inbreeding of 98.6% or, alternatively, 2% of the genetic variance existing in the base generation. Inbred mice are thus remarkably isogenic, guaranteeing the reproducibility of research experiments in many cases. The mouse phenome database from Jackson Lab contains body weight, body composition, and bone mineral density data assessed by DEXA for 32 strains for ages 6, 12, and 20 months (Ackert-Bicknell et al. 2008). In addition, Beamer and colleagues (1996) applied pQCT, to analyze the femur from 11 inbred strains of female mice to determine the extent of heritable differences at 12 months. In their analysis, C3H/HeJ mice ranked highest in femur density compared to C57BL/6J mice which displayed the lowest density value of the 11 inbred strains analyzed. In addition, bone mineral density in the femur was determined longitudinally in a subset of four strains (C3H/HeJ, DBA/2J, BALB/cByJ, C57BL/6J) at 2, 4, and 8 months. These four strains are representative of high, middle, and low total femur densities. The greatest difference in femur density was found between C57BL/6J and C3H/HeJ females. DBA/2J and BALB/cByJ also had densities significantly lower than C3H/HeJ, although the relative differences were not as great as for C57BL/6J. The difference in femur BMD between strains was visible at 2 weeks and was maintained pretty much at a constant level after peak bone mass was achieved at 4 months of age. With the exception of DBA/2J mice which stopped growing at 8 months, femur length continued to grow after 4 months up to the study end-point at 12 months, but at a much slower rate. Taken together the results indicate that one of the most commonly used mouse strains in skeletal biology, the C57BL/6J strain, exhibits the lowest bone mineral density which may represent a technical challenge when conducting experiments with this mouse strain (see section on limitations below).

In the axial skeleton, mouse strain-related differences in vertebral biomechanics and histomorphometry were assessed in inbred mouse strains C3H/HeJ, C57BL/6J, and DBA/2J (Akhter et al. 2004). Despite the greatest BMC and areal BMD in C3H/HeJ mice, the lack of strain-related differences in vertebral body strength data suggests that the biomechanical properties may be affected by the bone distribution and/or complex combination of cortical and cancellous bone at this site.

With the exception of 2 strains that die before 1 year of age from lymphoma or sarcoma, the median life span among 30 inbred mice ranges from 476 to 964 days

(Yuan et al. 2009). The median life span of C57BL/6 mice is 866 days for females and 901 days for males, similar to the 880-day median life span of UM-HET3 mice (Yuan et al. 2009). Due to the development of age-related pathologies which includes susceptibility to carcinogenesis, metabolic, immunologic, or other abnormalities, short-lived mice are not useful for studies of normal aging. Thus, the relatively long life span of C57BL/6 mice makes them attractive for aging studies.

2.3.3.1 Strengths and Limitations of Mouse Models

Unlike the human skeleton, the murine skeleton continues to grow slowly after puberty (Beamer et al. 1996), osteonal remodeling is absent in younger mice, but cortical porosity increases with age. Cancellous bone loss initiates at approximately 4 months of age soon after peak bone mass is reached and proceeds throughout adult life into senescence (Glatt et al. 2007).

Cancellous bone turnover in the distal femur in mice is approximately 0.7% per day, and each remodeling cycle takes about 2 weeks to complete (Weinstein et al. 1998). In humans, turnover is about 0.1% per day as measured in the iliac crest (Parfitt 2002b), and each remodeling cycle takes 6–9 months to complete (Parfitt et al. 1997). The more rapid pace of events in the murine skeleton is in keeping with the higher metabolic rate of small animals. Metabolic rate among animals varies in proportion to the ¾ power of body mass (Gillooly et al. 2001). This difference may explain at least in part the need to administer higher concentrations of biological agents to mice than to humans to achieve an equivalent physiologic effect.

Size is probably the most limiting factor in the mouse model affecting almost all standard end-points that are routinely measured in larger mammals and humans. As in humans, age-related bone loss in long bones of mice begins shortly after peak bone mass is achieved which in mice is at around 4 months of age (Lazner et al. 1999; Glatt et al. 2007). The cancellous bone volume in long bones in one of the most commonly used mouse strains for genetic manipulations, the C57BL/6, is as low as 3% in 7-month-old females which achieve peak bone mass at roughly 4 months of age (Iwaniec et al. 2006; Glatt et al. 2007). A μCT study on the distal femur of female and male C57BL/6 mice at various ages between 2 and 20 months of age revealed a 94% (female) and 56% drop (male) in trabecular bone volume from their initial value of 17.7% and 24.1%, respectively. This age-related drop of 56% in cancellous bone volume in male C57BL/6 mice is well in line with the paper published by Halloran, reporting a 60% decrease between 6 weeks and 24 months of age (Halloran et al. 2002). Cancellous bone loss appears to result predominantly from a reduction in trabecular numbers and connectivity, but not a change in their thickness (Glatt et al. 2007; Halloran et al. 2002). This is different from humans, where age-related changes in cancellous architecture are characterized by decreased trabecular number, thickness, and connectivity (Seeman 2002). Murine trabecular structures are thinner than human trabeculae (40–50 μm vs. 120–150 μm, respectively), and it has been hypothesized that it is thus more likely that they get disconnected during unbalanced bone remodeling, with a consequent decrease in number

and connectivity. A decline in wall thickness contributes to age-related cancellous bone loss in both mice and humans.

In mice of both genders, the majority of the age-related drop in cancellous bone volume had already occurred at 6 months, but cancellous bone loss continued to decline thereafter, albeit at a lower rate. The small amount of cancellous bone present at 4 months when mice are considered adult (especially in female mice), and the rapid age-related decline to 6 months makes a robust detection of changes in cancellous bone with noninvasive X-ray-based technologies (pQCT and microCT) challenging. The same applies to the measurement of cellular and dynamic histomorphometric parameters (osteoclast and osteoblast perimeter and number, mineralizing surface, and mineral apposition rate) that require a minimal cancellous bone perimeter for accurate detection, which makes it difficult in mice to generate a robust readout with a trabecular bone volume of 5% or less.

In male C57BL/6J mice, cortical bone thickness increased between 6 weeks and 6 months of age and then decreased continuously to 24 months (−12%), while cortical bone area remained constant between 6 and 24 months (Halloran et al. 2002).

Like in humans, OVX in the mouse does result in accelerated bone turnover (Beamer et al. 1996), but the magnitude is highly strain dependent and less consistent than in rats (Lazner et al. 1999). Detection of OVX-induced cancellous bone loss can be very challenging, since the trabecular bone volume in the metaphysis of the appendicular skeleton at 4 months, when OVX is carried out, is typically below 10% and the decline in trabecular bone has to be "detected" against the background of the rapid age-related decline.

The limitations discussed above can be partially addressed by investigating lumbar vertebral bodies which have a higher cancellous bone volume, even though the axial skeleton in mice cannot be measured in vivo with noninvasive techniques, thus limiting the readout to a single time-point after necropsy. Trabecular bone volume has been shown to decline by 52% in aging female C57BL/6 mice between 2 and 20 months starting from 28.6% (Glatt et al. 2007). In male mice, the trabecular bone volume at 2 months is 29.1%, declining by 26% at 20 months due to aging (Glatt et al. 2007). Following OVX in skeletally mature C57BL/6 mice, vertebral cancellous bone volume dropped from 12% to 9% in 3 months, representing a 27% change (Iwaniec et al. 2006).

2.3.3.2 Methods and Study End-Points Available for Mice

Several noninvasive methods are available for use in mice. This includes radiological techniques such as plain X-ray (e.g., Faxitron) (Bassett et al. 2012) and DEXA. Although plain x-rays are adequate to detect gross morphological changes in the skeleton of mice, they do not have sufficient resolution and sensitivity to detect subtle changes in bone architecture or to pick up compartment-specific changes in bone density. Since most of the changes occur in cancellous bone, pQCT which allows separate monitoring of cancellous and cortical bone offers greater sensitivity over DEXA (Gasser and Willnecker 2012). In recent years, microCT scanners like

the vivaCT40 (Scanco) and the SkyScan 1176 have become the method of choice for skeletal phenotyping and to study skeletal growth and aging in mice (Van't Hof 2012; Bouxsein et al. 2010). In addition to the in vivo microCT scanners, a number of highly versatile desktop systems such as the Skyscan 1275 are available, and nanoCT systems, like the μCT50 from SCANCO, the MicroXCT-200 from Xradia, or the GE Nanotom S nanoCT system, allow nondestructive ex vivo analysis of canalicular structures or osteocyte lacunae in cortical bone at submicron pixel size.

In recent years, optical imaging has evolved as a valuable technique for visualizing and quantifying biological processes in anesthetized mice. Both bioluminescence imaging and fluorescence imaging can be used to study cell- and tissue-specific promoters and to follow trafficking, differentiation, and the fate of reporter gene-expressing cells or biological processes such as apoptosis, protein-protein interactions, angiogenesis, proteolysis, and gene transfer in mice (Snoeks et al. 2012).

Bone histomorphometry is an indispensable tool for assessing the mechanism by which bone diseases occur, studying the effect of pharmacologic interventions, and especially determining the bone phenotype of transgenic mice. The article written by Erben and Glösman provides guidance on the tissue processing and histomorphometric evaluation for rodent bones (Erben and Glösmann 2012). Similarly, Kramer and colleagues described in detail how temporal and spatial patterns of gene expression can be studied in mouse bones by in situ hybridization (Kramer et al. 2012).

Assessment of mouse bones by mechanical testing is a critical step when evaluating the functional effects of an experimental perturbation (Jämsä et al. 1998; Schriefer et al. 2005). Recently, Jepsen and colleagues published detailed practical guidelines for systematically evaluating phenotypic changes in the diaphyses of long bones in mice (Jepsen et al. 2015). Importantly, the recommendation of minimum reportable standards for testing conditions and outcome variables, if adopted, will improve the comparison of data across studies. Typical in vivo loads experienced by mice include bending and torsion. For this reason, whole-bone mechanical tests of mouse long bones are most often performed in bending (Schriefer et al. 2005; Jämsä et al. 1998), but can also be performed in tension, compression (Akhter et al. 2004), and torsion. Descriptions of biomechanical methods, including for vertebral compression testing, that can be used in mice to determine whether a genetic or environmental perturbation affects bone strength have been published recently (Smith et al. 2013). The synthesis of morphological, tissue-level and whole-bone mechanical properties of long bones is a crucial step in the characterization of transgenic mouse strains (Jepsen et al. 2015; Jämsä et al. 1998; Schriefer et al. 2005).

In conclusion, mice will continue to play an important role toward a better understanding of the molecular mechanisms underlying skeletal biology. Their availability, ease of handling, high reproductive rates, and low cost provide additional arguments for their use (Jilka 2013). Full appreciation of the differences in the physiology of the human and murine skeletons is required to distinguish clinically relevant findings from mouse-specific findings. In addition, differences among mouse strains and genders must be considered. Like rats, mice lack osteonal cortical remodeling, but they clearly exhibit an accelerated increase in cortical porosity that

may be informative for the situation in humans. As in humans, cancellous bone loss initiates shortly after peak bone mass is achieved; it results from accelerated bone turnover, but in contrast to humans, the predominant feature is a decrease in trabecular number and connectivity with little effect on trabecular thickness. Some mouse strains may continue to show very low rates of longitudinal bone growth even at old age, but the rate is so slow that bone loss due to aging can be detected in the presence of an open but largely inactive growth plate. Despite some species differences, studies using mice will undoubtedly continue to contribute significantly to our understanding of skeletal biology in humans.

Acknowledgements We wish to thank Alan Abrams, Novartis Institutes for BioMedical Research (Cambridge, USA) for contributing the scientific artwork for Figs. 2.1, 2.2, 2.6, 2.8, 2.9, 2.11, 2.14, 2.16a, 2.17, and 2.18. Our sincere thanks go to Nathalie Gris-Accard, Novartis Institutes for BioMedical Research (Basel, Switzerland) for providing histologic images for Figs. 2.3 and 2.7a.

References

Ackert-Bicknell C, Beamer WG, Rosen CJ, Sundberg JP. Aging study: bone mineral density and body composition of 32 inbred strains of mice.MPD;Ackert1. Mouse Phenome Database Web Site. Bar Harbor: The Jackson Laboratory. 2008. http://phenome.jax.org/db/q?rtn=projects/details&id=250.

Akhter MP, Otero JK, Iwaniec UT, et al. Differences in vertebral structure and strength of inbred female mouse strains. J Musculoskelet Neuronal Interact. 2004;4(1):33–40.

Allen MR, Burr DB. Bone modeling and remodeling. In: Burr DB, Allen MR, editors. Basic and applied bone biology. San Diego: Academic; 2014. p. 75–90.

Anderson RE, Schraer H, Gay CV. Ultrastructural immunocytochemical localization of carbonic anhydrase in normal and calcitonin-treated chick osteoclasts. Anat Rec. 1982;204(1):9–20.

Bagi CM, Mecham M, Weis J, et al. Comparative morphometric changes in rat cortical bone following ovariectomy and/or immobilization. Bone. 1993;14:877–83.

Balemans W, Ebeling M, Patel N, et al. Increased bone density in sclerosteosis is due to the deficiency of a novel secreted protein (SOST). Hum Mol Genet. 2001;10(5):537–43.

Baron R, Kneissel M. WNT signaling in bone homeostasis and disease: from human mutations to treatments. Nat Med. 2013;19(2):179–92.

Bass SL, Saxon L, Daly R, et al. The effect of mechanical loading on the size and shape of bone in pre-, peri- and postpubertal girls: a study in tennis players. J Bone Miner Res. 2002;17(12):2274–80.

Bassett JHD, Van der Spek A, Gogakos A et al. Quantitative X-ray imaging of the rodent bone by Faxitron. In: Helfrich, MH and Ralston, SH, editors. Methods in molecular medicine, Vol. 816: bone research protocols. 2nd ed. Totowa: Humana Press; 2012. p. 499–506. 978-1-61779-414-8.

Beamer WG, Donahue LR, Rosen CJ, et al. Genetic variability in adult bone density among inbred strains of mice. Bone. 1996;18(5):397–403.

Beck JA, Lloyd S, Hafezparast M, et al. Genealogies of mouse inbred strains. Nat Genet. 2000;24:23–5.

Belanger LF. Osteocytic osteolysis. Calcif Tissue Res. 1969;4(1):1–12.

Bell KL, Loveridge N, Power J, et al. Regional differences in cortical porosity in the fractured femoral neck. Bone. 1999;24:57–64.

Bell KL, Loveridge N, Jordan GR, et al. A novel mechanism for induction of increased cortical porosity in cases of intracapsular hip fracture. Bone. 2000;27:297–304.

Binkley N, Kimmel D, Bruner J, et al. Zoledronate prevents the development of absolute osteopenia following ovariectomy in adult rhesus monkeys. J Bone Miner Res. 1998;13:1775–82.
Binkley N, Ellison G, O'Rourke C, Hall D, Johnston G, Kimmel D, Keller ET. Rib biopsy technique for cortical bone evaluation in rhesus monkeys (*Macaca mulatta*). Lab Anim Sci. 1999;49:87–9.
Black A, Tilmont EM, Handy AM, et al. A nonhuman primate model of age-related Bone loss: a longitudinal study in male and premenopausal female rhesus monkeys. Bone. 2001;28:295–302.
Blair HC, Teitelbaum SL, Ghiselli R, et al. Osteoclastic bone resorption by a polarized vacuolar proton pump. Science. 1989;245(4920):855–7.
Blouin S, Gallois Y, Moreau MF, et al. Disuse and orchidectomy have additional effects on bone loss in the aged male rat. Osteoporos Int. 2007;18(1):85–92.
Boivin G, Meunier PJ. Changes in bone remodeling rate influence the degree of mineralization of bone. Connect Tissue Res. 2002;43:535–7.
Bonewald LF. Osteocytes. In: Rosen CJ, editor. Primer on the metabolic bone dis-eases and disorders of mineral metabolism. 8th ed. New York: Wiley; 2013. p. 34–41.
Boskey AL. Organic and inorganic matrices. In: Wnek G, Bowlin GL, editors. Encyclopedia of biomaterials and biomedical engineering. London: Dekker Encyclopedias, Taylor & Francis Books; 2006a. p. 1–15.
Boskey AL. Assessment of bone mineral and matrix using backscatter electron imaging and FTIR imaging. Curr Osteoporos Rep. 2006b;4:71–5.
Boskey A. Mineralization of bones and teeth. Elements Mag. 2007;3:385–92.
Boskey AL. Bone composition: relationship to bone fragility and antiosteoporotic drug effects. BoneKEy Reports 2, Article number: 447. 2013. doi:10.1038/bonekey.2013.181.
Boskey AL, Coleman R. Aging and bone. J Dent Res. 2010;89:1333–48.
Boskey AL, Robey PG. The regulatory role of matrix proteins in mineralization of bone. In: Marcus R, Feldman D, Dempster DW, Luckey M, editors. Osteoporosis. New York: Elsevier; 2013. p. 235–58.
Bosu WT, Johansson ED, Gemzell C. Peripheral plasma levels of oestrone, oestradiol-17ß and progesterone during ovulatory menstrual cycles in the rhesus monkey with special reference to the onset of menstruation. Acta Endocrinol. 1973;74:732–42.
Bouxsein ML, Boyd SK, Christiansen BA, et al. Guidelines for assessment of bone microstructure in rodents using micro-computed tomography. J Bone Miner Res. 2010;25:1468–86.
Boyd SK, Davison P, Müller R, et al. Monitoring individual morphological changes over time in ovariectomized rats by in vivo micro-computed tomography. Bone. 2006;39(4):854–62.
Boyde A, Jones SJ. Backscattered electron imaging of skeletal tissues. Metab Bone Dis Rel Res. 1983;5:145–50.
Boyle WJ, Simonet WS, Lacey DL. Osteoclast differentiation and activation. Nature. 2003;423:337–42.
Brandi ML, Collin-Osdoby P. Vascular biology and the skeleton. J Bone Miner Res. 2006;21:183–92.
Breen SA, Loveday BE, Millest AJ, et al. Stimulation and inhibition of bone formation: use of peripheral quantitative computed tomography in the mouse in vivo. Lab Anim. 1998;32:467–76.
Brockstedt H, Kassem M, Eriksen EF, et al. Age- and sex-related changes in iliac cortical bone mass and remodeling. Bone. 1993;14(4):681–91.
Brommage R. Perspectives on using nonhuman primates to understand the etiology and treatment of postmenopausal osteoporosis. J Musculoskelet Neuronal Interact. 2001;1(4):307–25.
Brommage R, Vafai H. Rapid embedding protocol for visualizing bone mineral and matrix. Calcif Tissue Int. 2000;67:479–80.
Brommage R, Allison C, Stavisky R, et al. Measurement of serum bone-specific alkaline phosphatase activity in cynomolgus macaques. J Med Primatol. 1999;28:329–33.
Brouwers JEM, Lambers FM, Gasser JA, et al. Bone degeneration and recovery after early and late bisphosphonate treatment of Ovariectomized Wistar rats assessed by in vivo micro-computed tomography. Calcif Tissue Int. 2008;82(3):202–11.
Buenzli PR, Sims NA. Quantifying the osteocyte network in the human skeleton. Bone. 2015;75:144–50.

Burr DB, Akkus O. Bone morphology and organization. In: Burr DB, Allen MR, editors. Basic and applied bone biology. San Diego: Academic; 2014. p. 3–25.
Burr DB, Martin RB, Schaffler MB, et al. Bone remodeling in response to in vivo fatigue microdamage. J Biomech. 1985;18:189–200.
Burr DB, Turner CH, Naick P, et al. Does microdamage accumulation affect the mechanical properties of bone? J Biomech. 1998;31:337–45.
Butterstein GM, Mann DR, Gould K, et al. Prolonged inhibition of normal ovarian cycles in the rat and cynomolgus monkeys following a single s.c. injection of danazol. Hum Reprod. 1997;12:1409–15.
Cabal A, Jayakar RY, Sardesai S, et al. High-resolution peripheral quantitative computed tomography and finite element analysis of bone strength at the distal radius in ovariectomized adult rhesus monkey demonstrate efficacy of odanacatib and differentiation from alendronate. Bone. 2013;56:497–505.
Canalis E. Growth factor control of bone mass. J Cell Biochem. 2009;108(4):769–77.
Caplan AI, Bruder SP. Mesenchymal stem cells: building blocks for molecular medicine in the 21st century. Trends Mol Med. 2001;7(6):259–64.
Carlson C, Tulli H, Jayo M, et al. Immunolocalization of noncolla-genous bone matrix proteins in lumbar vertebrae from intact and surgically menopausal cynomolgus monkeys. J Bone Miner Res. 1993;8:71–83.
Cerroni AM, Tomilinson GA, Turnquist JE, et al. Bone mineral density, osteopenia, and osteoporosis in the rhesus macaques of Cayo Santiago. Am J Phys Anthropol. 2000;113:389–410.
Chambers TJ, Fuller K. Bone cells predispose bone surfaces to resorption by exposure of mineral to osteoclastic contact. J Cell Sci. 1985;76:155–65.
Champ JE, Binkley N, Havighurst T, et al. The effect of advancing age on bone mineral content of female rhesus monkeys. Bone. 1996;19:485–92.
Chellaiah MA. Regulation of actin ring formation by rho GTPases in osteoclasts. J Biol Chem. 2005;280:32930–43.
Chen HK, Ke HZ, Jee WS, et al. Droloxifene prevents ovariectomy-induced bone loss in tibiae and femora of aged female rats: a dual-energy X-ray absorptiometric and histomorphometric study. J Bone Miner Res. 1995a;10:1256–62.
Chen MM, Yeh JK, Aloia JF. Effect of ovariectomy on cancellous bone in the hypophysectomized rat. J Bone Miner Res. 1995b;10(9):1334–42.
Chen LD, Kushwaha RS, McGill HC Jr, et al. Effect of naturally reduced ovarian function on plasma lipoprotein and 27-hydroxycholesterol levels in baboons (Papio sp.). Atherosclerosis. 1998;136:89–98.
Chen D, Zhao M, Mundy GR. Bone morphogenetic proteins. Growth Factors. 2004;22(4):233–41.
Chia R, Achilli F, Festing MF, et al. The origins and uses of mouse outbred stocks. Nat Genet. 2005;37:1181–6.
Christian JC, Yu PL, Slemenda CW, et al. Heritability of bone mass: a longitudinal study in aging male twins. Am J Hum Genet. 1989;44(3):429–33.
Colman RJ, Kenmitz JW, Lane MA, et al. Skeletal effects of aging and menopausal status in female rhesus monkeys. J Clin Endocrinol Metab. 1999a;84:4144–8.
Colman RJ, Lane MA, Binkley N, et al. Skeletal effects of aging in male rhesus monkeys. Bone. 1999b;24:17–23.
Committee on Standardized Genetic Nomenclature for Mice. 1952. http://www.informatics.jax.org/mgihome/nomen/strains.shtml
Crockett JC, Rogers MJ, Coxon FP, et al. Bone remodelling at a glance. J Cell Sci. 2011;124:991–8.
Currey JD. Bones. Structure and mechanics. New Jersey: Princeton University Press; 2002. p. 1–380.
Danforth DR, Chillik CF, Hertz R, et al. Effects of ovarian tissue reduction on the menstrual cycle: persistent normalcy after near-total oophorectomy. Biol Reprod. 1989;41:355–60.
De Gorter DJJ, Ten Dijke P. Signal transduction cascades controlling osteoblast differentiation. In: Rosen CJ, editor. Primer on the metabolic Bone diseases and disorders of mineral metabolism. 8th ed. New York: Wiley; 2013. p. 15–24.

Dickerson SS, Hotchkiss CE. Relationships between densitometric and morphological parameters as measured by peripheral computed tomography and the compressive behavior of lumbar vertebral bodies from macaques (*Macaca fascicularis*). Spine. 2008;33:366–72.
Dobnig H, Turner RT. Evidence that intermittent treatment with parathyroid hormone increases bone formation in adult rats by activation of bone lining cells. Endocrinology. 1995;136(8):3632–8.
Donnelly E, Meredith DS, Nguyen JT, et al. Bone tissue composition varies across anatomic sites in the proximal femur and the iliac crest. J Orthop Res. 2012;30:700–6.
Ducy P, Desbois C, Boyce B, et al. Increased bone formation in osteocalcin-deficient mice. Nature. 1996;382(6590):448–52.
Ducy P, Zhang R, Geoffroy V, et al. Osf2/Cbfa1: a transcriptional activator of osteoblast differentiation. Cell. 1997;89(5):747–54.
Erben RG. Trabecular and endocortical bone surfaces in the rat: modeling or remodeling? Anat Rec. 1996;246:39–46.
Erben RG and Glösmann. Histomorphometry in rodents. Helfrich, MH and Ralston, SH, editors. Methods in molecular medicine, Vol. 816: bone research protocols. 2nd ed. Totowa: Humana Press; 2012. p. 279–303. 978-1-61779-414-8.
Erben RG, Eberle J, Stahr K, et al. Androgen deficiency induces high turnover osteopenia in aged male rats: a sequential histomorphometric study. J Bone Miner Res. 2000;15(6):1085–98.
Feng XH, Derynck R. Specificity and versatility in TGF-β signaling through Smads. Annu Rev Cell Dev Biol. 2005;21:659–93.
Feng JQ, Ward LM, Liu S, et al. Loss of DMP1 causes rickets and osteomalacia and identifies a role for osteocytes in mineral metabolism. Nat Genet. 2006;38(11):1310–5.
Ferrari S, Bianchi ML, Eisman JA, et al. IOF Committee of Scientific Advisors Working Group on osteoporosis pathophysiology. Osteoporosis in young adults: pathophysiology, diagnosis, and management. Osteoporos Int. 2012;23(12):2735–48.
Frost HM. Dynamics of bone remodeling. In: Frost HM, editor. BoneBiodynamics. Boston: Little Brown & Co; 1964. p. 315–33.
Fukumoto S, Martin TJ. Bone as an endocrine organ. Trends Endocrinol Metab. 2009;20:230–6.
Gallagher A, Chambers TJ, Tobias JH. The estrogen antagonist ICI 182,780 reduces cancellous bone volume in female rats. Endocrinology. 1993;133:2787–91.
Garn S. The earlier gain and later loss of cortical bone. In: Nutritional perspectives. Springfield: Charles C. Thomas; 1970. p. 3–120.
Gasser JA and Willnecker J. Bone measurements by peripheral quantitative computed tomography in rodents. In: Helfrich, MH and Ralston, SH, editors. Methods in molecular medicine, Vol. 816: bone research protocols. 2nd ed. Totowa: Humana Press Inc.; 2012. 477–98. 978-1-61779-414-8.
Gasser JA, Green JR, Shen V, et al. A single intravenous administration of zoledronic acid prevents the bone loss and mechanical compromise induced by aromatase inhibition in rats. Bone. 2006;39(4):787–95.
Gay CV, Mueller WJ. Carbonic anhydrase and osteoclasts: localization by labeled inhibitor autoradiography. Science. 1974;183(123):432–4.
Gazzerro E, Canalis E. Bone morphogenetic proteins and their antagonists. Rev Endocr Metab Disord. 2006;7(1–2):51–65.
Gelb BD, Shi GP, Chapman HA, et al. Pycnodysostosis, a lysosomal disease caused by cathepsin K deficiency. Science. 1996;273(5279):1236–8.
Gilardi KVK, Shideler SE, Valverde CR, et al. Characterization of the onset of menopause in the rhesus macaque. Biol Reprod. 1997;57:335–40.
Gillooly JF, Brown JH, West GB, et al. Effects of size and temperature on metabolic rate. Science. 2001;293:2248–51.
Glatt V, Canalis E, Stadmeyer L, et al. Age-related changes in trabecular architecture differ in female and male C57BL/6J mice. J Bone Miner Res. 2007;22:1197–207.
Goldring MB, Goldring SR. Articular cartilage and subchondral bone in the pathogenesis of osteoarthritis. Ann N Y Acad Sci. 2010;1192:230–7.

Goodman AL, Descalzi CD, Johnson DK, et al. Composite pattern of circulating LH, FSH, estradiol, and progesterone during the menstrual cycle in cynomolgus monkeys. Proc Soc Exp Biol Med. 1977;155:479–81.
Goodwin BT, Jerome CP. Iliac biopsy for histomorphometric analysis of trabecular bone in cynomolgus monkeys and baboons. Lab Anim Sci. 1987;37:213–6.
Gordon K, Williams RF, Danforth DR, et al. Suppression of ovarian estradiol secretion by a single injection of antide in cynomolgus monkeys during the early follicular phase: immediate, sustained, and reversible actions. J Clin Endocrinol Metab. 1991;73:1262–8.
Goulding A, Gold E. A new way to induce oestrogen-deficiency osteopenia in the rat: comparison of the effect of surgical ovariectomy and administration of the LHRH agonist buserelin on bone resorption and composition. J Endocrinol. 1989;121:293–8.
Guo D, Keightley A, Guthrie J, et al. Identification of osteocyte-selective proteins. Proteomics. 2010;10(20):3688–98.
Haapasalo H, Kontulainen S, Sievanen H, et al. Exercise-induced bone gain is due to enlargement in bone size without a change in volumetric bone density: a peripheral quantitative computed tomography study of the upper arms of male tennis players. Bone. 2000;27(3):351–7.
Halloran BP, Ferguson VL, Simske SJ, et al. Changes in bone structure and mass with advancing age in the male C57BL/6J mouse. J Bone Miner Res. 2002;17:1044–50.
Harada H, Tagashira S, Fujiwara M, et al. Cbfa1 isoforms exert functional differences in osteoblast differentiation. J Biol Chem. 1999;274(11):6972–8.
Hauge E, Mosekilde L, Melsen F. Missing observations in bone histomorphometry on osteoporosis: implications and suggestions for an approach. Bone. 1999;25:389–95.
Hauge EM, Qvesel D, Eriksen EF, et al. Cancellous bone remodeling occurs in specialized compartments lined by cells expressing osteoblastic markers. J Bone Miner Res. 2001;16:1575–82.
Hermann LM, Smith KC. Percutaneous trephine biopsy of the vertebral body in the rhesus monkey (*Macaca mulatta*). Am J Vet Res. 1985;46:1403–7.
Hernandez CJ, Gupt A, Keaveny TM. A biomechanical analysis of the effects of resorption cavities on cancellous bone strength. J Bone Miner Res. 2006;21:1248–55.
Hessle L, Johnson KA, Anderson HC, et al. Tissue-nonspecific alkaline phosphatase and plasma cell membrane glycoprotein-1 are central antagonistic regulators of bone mineralization. Proc Natl Acad Sci U S A. 2002;99(14):9445–9.
Heuck F. Comparative investigations of the function of osteocytes in bone resorption. Calcif Tissue Res Suppl. 1970:148–9.
Hodgen GD, Goodman AL, O'Connor A, et al. Menopause in rhesus monkeys: model for study of disorders in the human climacteric. Am J Obstet Gynecol. 1977;127:581–4.
Hofbauer LC, Khosla S, Dunstan CR, et al. The roles of osteoprotegerin and osteoprotegerin ligand in the paracrine regulation of bone resorption. J Bone Miner Res. 2000;15(1):2–12.
Hoffman RA, Mack PB, Hood WN. Comparison of calcium and phosphorus excretion with bone density changes during restraint in immature *Macaca nemestrina* primates. Aerospace Med. 1972;43:376–83.
Hotchkiss CE. Use of peripheral quantitative computed tomography for densitometry of the femoral neck and spine in cynomolgus monkeys (*Macaca fascicularis*). Bone. 1999;24:101–7.
Hotchkiss CE, Brommage R, Du M, et al. The anesthetic isoflurane decreases ionized calcium and increases parathyroid hormone and osteocalcin in cynomolgus monkeys. Bone. 1998;23:479–84.
Inaoka T, Bilbe G, Ishibashi O, et al. Molecular cloning of human cDNA for cathepsin K: novel cysteine proteinase predominantly expressed in bone. Biochem Biophys Res Commun. 1995;206(1):89–96.
Inskip MJ, Franklin CA, Subramanian KS, et al. Sampling of cortical and trabecular bone for lead analysis: method development in a study of lead mobilization during pregnancy. Neurotoxicology. 1992;13:825–34.
Iwaniec UT, Turner RT. Animal models of osteoporosis. In: Marcus R, Feldman D, Nelson DA, Rosen CJ, editors. Osteoporosis. 3rd ed. Amsterdam: Elsevier; 2008. p. 985–1110.

Iwaniec UT, Yuan D, Power RA, et al. Strain-dependent variations in the response of cancellous bone to ovariectomy in mice. J Bone Miner Res. 2006;21:1068–74.
Jaffe AB, Hall A. Rho GTPases: biochemistry and biology. Annu Rev Cell Dev Biol. 2005;21:247–69.
Jämsä T, Jalovaara P, Peng Z, et al. Comparison of three-point bending test and peripheral quantitative computed tomography analysis in the evaluation of the strength of mouse femur and tibia. Bone. 1998;23:155–61.
Janssens K, ten Dijke P, Janssens S, et al. Transforming growth factor-β1 to the bone. Endocr Rev. 2005;26(6):743–74.
Jayo MJ, Jerome CP, Lees CJ, et al. Bone mass in female cynomolgus macaques: a crosssectional and longitudinal study by age. Calcif Tissue Int. 1994;54:231–6.
Jee WS, Li XJ. Adaptation of cancellous bone to overloading in the adult rat: a single photon absorptiometry and histomorphometry study. Anat Rec. 1990;227:418–26.
Jee WS, Ma Y. Animal models of immobilization osteopenia. Morphologie. 1999;83(261):25–34.
Jee WSS, Yao W. Overview: animal models of osteopenia and osteoporosis. J Musculoskelet Neuronal Interact. 2001;1:193–207.
Jepsen KJ. Functional interactions among morphologic and tissue quality traits define bone quality. Clin Orthop Relat Res. 2011;469:2150–9.
Jepsen KJ, Silva MJ, Vashishth D, et al. Establishing biomechanical mechanisms in mouse models: practical guidelines for systematically evaluating phenotypic changes in the Diaphyses of long bones. J Bone Miner Res. 2015;30(6):951–66.
Jerome C. Hormonal therapies and osteoporosis. ILAR J. 2004;45:170–8.
Jerome CP, Peterson PE. Nonhuman primate models in skeletal research. Bone. 2001;29:1–6.
Jerome CP, Carlson CS, Register TC, et al. Bone functional changes in intact, ovariectomized, hormone-supplemented adult cynomolgus monkeys (*Macaca fascicularis*) evaluated by serum markers and dynamic histomorphometry. J Bone Miner Res. 1994;9:527–40.
Jerome CP, Lees CJ, Weaver DS. Development of osteopenia in ovariectomized cynomolgus monkeys (*Macaca fascicularis*). Bone. 1995;17:403S–8S.
Jerome CP, Turner CH, Lees CJ. Decreased bone mass and strength in ovariectomized cynomolgus monkeys (*Macaca fascicularis*). Calcif Tissue Int. 1997;60:265–70.
Jerome CP, Johnson CS, Vafai HT, et al. Effect of treatment for 6 months with human parathyroid hormone (1–34) peptide in ovariectomized cynomolgus monkeys (*Macaca fascicularis*). Bone. 1999;25:301–9.
Jerome CP, Burr DB, Van Bibber T, et al. Treatment with human parathyroid hormone (1–34) for 18 months increases cancellous Bone volume and improves trabecular architecture in Ovariectomized Cynomolgus monkeys (*Macaca fascicularis*). Bone. 2001;28(2):150–9.
Jiang Y, Jahagirdar BN, Reinhardt RL, et al. Pluripotency of mesenchymal stem cells derived from adult marrow. Nature. 2002;418(6893):41–9.
Jiang Y, Zhao J, Liao EY, et al. Application of μCT-assessment of 3D bone microstructure in preclinical and clinical studies. J Bone Miner Metab. 2005;23:122–31.
Jilka RL. The relevance of mouse models for investigating age-related Bone loss in humans. J Gerontol A Biol Sci Med Sci. 2013; doi:10.1093/gerona/glt046.
Johnson CS, Jerome CP, Brommage R. Unbiased determination of cytokine localization in bone: colocalization of interleukin-6 with osteoblasts in serial sections from monkey vertebrae. Bone. 2000;26:461–7.
Kalajzic I, Braut A, Guo D, et al. Dentin matrix protein 1 expression during osteoblastic differentiation, generation of an osteocyte GFP-transgene. Bone. 2004;35(1):74–82.
Kan L. Animal models of bone diseases – a. In: Conn PM, editor. Animal models for the study of human disease. San Diego: Academic; 2013. p. 353–90.
Kanis JA, McCloskey EV, Johansson H, et al. European guidance for the diagnosis and management of osteoporosis in postmenopausal women. Osteoporos Int. 2013;24:23–57.
Kaplan JR, Adams MR, Clarkson TB, et al. Social behavior and gender in biomedical investigations using monkeys: studies in atherogenesis. Lab Anim Sci. 1991;41:334–43.

Kavukcuoglu NB, Denhardt DT, Guzelsu N, et al. Osteopontin deficiency and aging on nanomechanics of mouse bone. J Biomed Mater Res A. 2007;83(1):136–44.
Kavukcuoglu NB, Patterson-Buckendahl P, Mann AB. Effect of osteocalcin deficiency on the nanomechanics and chemistry of mouse bones. J Mech Behav Biomed Mater. 2009;2:348–54.
Kazanci M, Roschger P, Paschalis EP, et al. Bone osteonal tissues by Raman spectral mapping: orientation-composition. J Struct Biol. 2006;156:489–96.
Keaveney TM. Cancellous bone. In: Black J, Hastings G, editors. Handbook of biomaterials properties. London: Chapman and Hall; 1998.
Kenigsberg D, Hodgen GD. Ovulation inhibition by administration of weekly gonadotropin-releasing hormone antagonist. J Clin Endocrinol Metab. 1986;62:734–8.
Kennedy OD, Herman BC, Laudier DM, et al. Activation of resorption in fatigue-loaded bone involves both apoptosis and active pro-osteoclastogenic signaling by distinct osteocyte populations. Bone. 2012;50:1115–22.
Kerber WT, Reese WH. Comparison of the menstrual cycle of cynomolgus and rhesus monkeys. Fertil Steril. 1969;20:975–9.
Kern B, Shen J, Starbuck M, et al. Cbfa1 contributes to the osteoblast-specific expression of type I collagen genes. J Biol Chem. 2001;276(10):7101–7.
Kim SW, Divieti-Pajevic P, Selig M, et al. Intermittent PTH administration converts quiescent lining cells to active osteoblasts. J Bone Miner Res. 2012;27(10):2075–84.
Klein HJ, Seedor G, Frankenfeld DL, Thompson DD. Method for transiliac bone biopsy in baboons. J Am Vet Med Assoc. 1991;198:1977–9.
Kneissel M, Boyde A, Gasser JA. Bone tissue and its mineralization in aged estrogen-depleted rats after long-term intermittent treatment with parathyroid hormone (PTH) analog SDZ PTS 893 or human PTH(1-34). Bone. 2001;28:237–50.
Knothe Tate ML, Adamson JR, Tami AE, et al. The osteocyte. Int J Biochem Cell Biol. 2004;36:1–8.
Knutson JC, Hollis BW, LeVan LW, et al. Metabolism of 1-hydroxyvitamin D2 to activated dihydroxyvitamin D2 metabolites decreases endogenous 1,25-dihydroxyvitamin D3 in rats and monkeys. Endocrinology. 1995;136:4749–53.
Koga T, Matsui Y, Asagiri M, et al. NFAT and Osterix cooperatively regulate bone formation. Nat Med. 2005;11(8):880–5.
Komori T, Yagi H, Nomura S. Targeted disruption of Cbfa1 results in a complete lack of bone formation owing to maturational arrest of osteoblasts. Cell. 1997;89(5):755–64.
Kostenuik PJ, Shalhoub V. Osteoprotegerin: a physiological and pharmacological inhibitor of bone resorption. Curr Pharm Des. 2001;7:613–35.
Koyama T, de la Pena A, Hagino N. Plasma estrogen, progestin, and luteinizing hormone during the normal menstrual cycle of the baboon: role of luteinizing hormone. Am J Obstet Gynecol. 1977;127:67–72.
Kramer I, Salie R, Susa M et al. Studying gene expression in bone by in situ hybridization. In: Helfrich, MH and Ralston, SH, editors. Methods in molecular medicine, vol. 816: bone research protocols. 2nd ed. Totowa: Humana Press Inc.; 2012. 305–320. 978-1-61779-414-8.
Kristensen HB, Andersen TL, Marcussen N, et al. Osteoblast recruitment routes in human cancellous bone remodeling. Am J Pathol. 2014;184:778–89.
Lane NE, Yao W, Balooch M, et al. Glucocorticoid-treated mice have localized changes in trabecular bone material properties and osteocyte lacunar size that are not observed in placebo-treated or estrogen-deficient mice. J Bone Miner Res. 2006;21(3):466–76.
Lanyon LE, Baggott DG. Mechanical function as an influence on the structure and form of bone. J Bone Joint Surg. 1976;58-B(4):436–43.
Lazner F, Gowen M, Pavasovic D, et al. Osteopetrosis and osteoporosis: two sides of the same coin. Hum Mol Genet. 1999;8(10):1839–46.
Lees CJ, Ramsay H. Histomorphometry and bone biomarkers in cynomolgus females: a study in young, mature, and old monkeys. Bone. 1999;24:25–8.
Lekamwasam S, Adachi JD, Agnusdei D, et al. Joint IOF-ECTS GIO guidelines working group. A framework for the development of guidelines for the management of glucocorticoid-induced osteoporosis. Osteoporos Int. 2012;23(9):2257–76.

Lelovas PP, Xanthos TT, Thoma SE, et al. The laboratory rat as an animal model for osteoporosis research. Comp Med. 2008;58(5):424–30.
Li M, Shen Y, Qi H, et al. Comparison study of skeletal response to estrogen depletion at red and yellow marrow sites in rats. Anat Rec. 1996;245:472–80.
Li M, Shen Y, Wronski TJ. Time course of femoral neck osteopenia in ovariectomizd rats. Bone. 1997;20:55–61.
Lipkin EW. A longitudinal study of calcium regulation in a nonhuman primate model of parenteral nutrition. Am J Clin Nutr. 1998;67:246–54.
Lips P, Courpron P, Meunier PJ. Mean wall thickness of trabecular bone packets in the human iliac crest: changes with age. Calcif Tissue Res. 1978;10:13–7.
Loeb WF. The rat. In: Loeb WF, Quimby FW, editors. The clinical chemistry of laboratory animals. 2nd ed. Ann Arbor: Edwards Brothers; 1999. p. 33–45.
Long F. Building strong bones: molecular regulation of the osteoblast lineage. Mol Cell Biol. 2012;13:27–38.
Lozupone E, Favia A. The structure of the trabeculae of cancellous bone. 2. Long bones and mastoid. Calcif Tissue Int. 1990;46:367–72.
Lyons KM. Animal models: genetic manipulation. In: Rosen CJ, editor. Primer on the metabolic bone diseases and disorders of mineral metabolism. 8th ed. New York: Wiley; 2013. p. 69–75.
Ma YF, Li XJ, Jee WS, et al. Effects of prostaglandin E2 and F2 alpha on the skeleton of osteopenic ovariectomized rats. Bone. 1995;17:549–54.
Maeda S, Hayashi M, Komiya S, et al. Endogenous TGF-β signaling suppresses maturation of osteoblastic mesenchymal cells. EMBO J. 2004;23(3):552–63.
Mandair GS, Morris MD. Contributions of Raman spectroscopy to the understanding of bone strength. BoneKEy Reports 4, Article number: 620. 2015. doi:10.1038/bonekey.2014.115.
Mann DR, Gold KG, Collins DC. A potential primate model for bone loss resulting from medical oophorectomy or menopause. J Clin Endocrinol Metab. 1990;71:105–10.
Marenzana M, Arnett TR. The key role of blood supply in bone. Bone Res. 2013;3:203–15.
Marie PJ, Glorieux FH. Relation between hypomineralized periosteocytic lesions and bone mineralization in vitamin D-resistant rickets. Calcif Tissue Int. 1983;35(4–5):443–8.
Martin RB. Porosity and specific surface of bone. CRC Critical Rev Biomed Eng. 1984;10:179–221.
Massague J, Seoane J, Wotton D. Smad transcription factors. Genes Dev. 2005;19(23):2783–810.
McCarthy I. The physiology of bone blood flow: a review. J Bone Joint Surg Am. 2006;88(Suppl 3):4–9.
McNamara LM, Van Der Linden JC, Weinans H, et al. Stress-concentrating effect of resorption lacunae in trabecular bone. J Biomech. 2006;39:734–41.
Mehta RR, Jenco JM, Gaynor LV, et al. Relationships between ovarian morphology, vaginal cytology, serum progesterone, and urinary immunoreactive pregnanediol during the menstrual cycle of the cynomolgus monkey. Biol Reprod. 1986;35:981–6.
Meunier PJ. Assessment of bone turnover by histomorphometry in osteoporosis. In: Riggs BL, Melton LJ, editors. Osteoporosis: etiology, diagnosis, and management. New York: Raven Press; 1988. p. 317–32.
Misof BM, Roschger P, Cosman F, et al. Effects of intermittent parathyroid hormone administration on bone mineralization density in iliac crest biopsies from patients with osteoporosis: a paired study before and after treatment. J Clin Endocrinol Metab. 2003;8(3):1150–6.
Miyakoshi N, Sato K, Tsuchida T, et al. Histomorphometric evaluation of the effects of ovariectomy on bone turnover in rat caudal vertebrae. Calcif Tissue Int. 1999;64:318–24.
Mori S, Burr DB. Increased intracortical remodeling following fatigue damage. Bone. 1993;14:103–9.
Mori S, Jee WS, Li XJ. Production of new trabecular bone in osteopenic ovariectomized rats by prostaglandin E2. Calcif Tissue Int. 1992;50:80–7.
Morris MD, Mandair GS. Raman assessment of bone quality. Clin Orthop Relat Res. 2011;469:2160–9.
Murray PDF, Huxley JS. Self-differentiation in the grafted limb bud of the chick. J Anat. 1925;59:379–84.

Nakamura H. Morphology, function, and differentiation of bone cells. J Hard Tissue Biol. 2007;16(1):15–22.
Nakashima K, Zhou X, Kunkel G, et al. The novel zinc finger containing transcription factor osterix is required for osteoblast differentiation and bone formation. Cell. 2002;108(1):17–29.
Negishi-Koga T, Shinohara M, Komatsu N, et al. Suppression of bone formation by osteoclastic expression of semaphoring 4D. Nat Med. 2011;17:1473–80.
Nishio Y, Dong Y, Paris M, et al. Runx2-mediated regulation of the zinc finger Osterix/Sp7 gene. Gene. 2006;372:62–70.
Nogues C, Milhaud C. A new technique for iliac crest biopsy in rhesus monkeys for use in weightlessness experiments: some results of ground studies. Aviat Space Environ Med. 1988;59:374–8.
Ott SM, O'Hanlan M, Lipkin EW, et al. Evaluation of vertebral volumetric vs areal bone mineral density during growth. Bone. 1997;20:553–6.
Ott SM, Lipkin EW, Newell-Morris. Bone physiology during pregnancy and lactation in young macaques. J Bone Miner Res. 1999;14:1779–88.
Otto F, Thornell AP, Crompton T, et al. Cbfa1, a candidate gene for cleidocranial dysplasia syndrome, is essential for osteoblast differentiation and bone development. Cell. 1997;89(5):765–71.
Pacureanu A, Langer M, Boller E, et al. Nanoscale imaging of the bone cell network with synchrotron X-ray tomography: optimization of acquisition setup. Med Phys. 2012;39:2229–38.
Parfitt AM. Targeted and nontargeted bone remodeling: relationship to basic multicellular unit origination and progression. Bone. 2002a;30(1):5–7.
Parfitt AM. Misconceptions (2): turnover is always higher in cancellous than in cortical bone. Bone. 2002b;30:807–9.
Parfitt AM, Han ZH, Palnitkar S, et al. Effects of ethnicity and age or menopause on osteoblast function, bone mineralization, and osteoid accumulation in iliac bone. J Bone Miner Res. 1997;12:1864–73.
Patsch JM, Burghardt AJ, Kazakia G, et al. Noninvasive imaging of bone microarchitecture. Ann N Y Acad Sci. 2011;1240:77–87.
Pixley FJ, Stanley ER. CSF-1 regulation of the wandering macrophage: complexity in action. Trends Cell Biol. 2004;14:628–38.
Pocock NA, Eisman JA, Hopper JL, et al. Genetic determinants of bone mass in adults. A twin study. J Clin Invest. 1987;80(3):706–10.
Poole KE, van Bezooijen RL, Loveridge N, et al. Sclerostin is a delayed secreted product of osteocytes that inhibits bone formation. FASEB J. 2005;19(13):1842–4.
Qing H, Bonewald LF. Osteocyte remodeling of the perilacunar and pericanalicular matrix. Int J Oral Sci. 2009;1(2):59–65.
Recker RR, Kimmel DB, Parfitt AM, et al. Static and tetracycline-based bone histomorphometric data from 34 normal postmenopausal females. J Bone Miner Res. 1988;3:133–44.
Recker R, Lappe J, Davies KM, et al. Bone remodeling increases substantially in the years after menopause and remains increased in older osteoporosis patients. J Bone Miner Res. 2004;19:1628–33.
Recklinghausen FV, editor. Untersuchungen über rachitis and osteomalacia. Jena: Fischer Verlag; 1910.
Register TC, Jerome CP. Increased urinary markers of collagen degradation accompany ovariectomy in skeletally mature cynomolgus macaques. J Bone Miner Res. 1996;11:S196.
Reid DG, Shanahan CM, Duer MJ, et al. Lipids in biocalcification: contrasts and similarities between intimal and medial vascular calcification and bone by NMR. J Lipid Res. 2012;53:1569–75.
Reponen P, Sahlberg C, Munaut C, et al. High expression of 92-kD type IV collagenase (gelatinase B) in the osteoclast lineage during mouse development. J Cell Biol. 1994;124(6):1091–102.
Roschger P, Rinnerthaler S, Yates J, et al. Alendronate increases degree and uniformity of mineralization in cancellous bone and decreases the porosity in cortical bone of osteoporotic women. Bone. 2001;29(2):185–91.
Roschger P, Paschalis EP, Fratzl P, et al. Bone mineralization density distribution in health and disease. Bone. 2008;42:456–66.

Ross FP. Osteoclast biology and bone resorption. In: Rosen CJ, editor. Primer on the metabolic bone dis-eases and disorders of mineral metabolism. 8th ed. New York: Wiley; 2013. p. 25–33.
Ross FP, Teitelbaum SL. alphavbeta3 and macrophage colony-stimulating factor: partners in osteoclast biology. Immunol Rev. 2005;208:88–105.
Rossert J, de Crombrugghe B. Type I collagen: structure, synthesis and regulation. In: Bilezikian JP, Raisz LA, Rodan GA, editors. Principles of bone biology, vol. 1. 2nd ed. San Diego: Academic; 2002. p. 189–210.
Rowe PS, Kumagai Y, Gutierrez G, et al. MEPE has the properties of an osteoblastic phosphatonin and inhibin. Bone. 2004;34(2):303–19.
Salo J, Lehenkari P, Mulari M, et al. Removal of osteoclast bone resorption products by transcytosis. Science. 1997;276:270–3.
Sánchez-Duffhues G, Hiepen C, Knaus P, et al. Bone morphogenetic protein signaling in bone homeostasis. Bone. 2015;80:43–59.
Schaffler MB, Burr DB. Primate cortical bone microstructure: relationship to locomotion. Am J Phys Anthropol. 1984;65:191–7.
Schaffler M, Cheung W-Y, Majeska R, et al. Osteocytes: master orchestrators of bone. Calcif Tissue Int. 2014;94:5–24.
Schneider P, Meier M, Wepf R, et al. Towards quantitative 3D imaging of the osteocyte lacunocanalicular network. Bone. 2010;47:848–58.
Schriefer JL, Robling AG, Warden SJ, et al. A comparison of mechanical properties derived from multiple skeletal sites in mice. J Biomech. 2005;38(3):467–75.
Seeman E. Pathogenesis of bone fragility in women and men. Lancet. 2002;359:1841–50.
Seeman E. Modeling and remodeling: the cellular machinery responsible for the gain and loss of Bone's material and structural strength. In: Bilezikian JP, Raisz LA, Martin TJ, editors. Principles of bone biology, vol. 1. 3rd ed. San Diego: Academic; 2008. p. 3–28.
Seeman E, Hopper J, Bach L, et al. Reduced bone mass in the daughters of women with osteoporosis. New Engl J Med. 1989;320:554–8.
Seeman E, Hopper JL, Young NR, et al. Do genetic factors explain associations between muscle strength, lean mass, and bone density? A twin study. Am J Phys. 1996;270(2 Pt 1):E320–7.
Shaikh AA, Naqvi RH, Shaikh SA (1978) Concentrations of oestradiol-17, and progesterone in the peripheral plasma of the cynomolgus monkey (*Macaca fascicularis*) in relation to the length of the menstrual cycle and its component phases. J Endocrinol 79:1–7.
Sharir A, Barak MM, Shahar R. Whole bone mechanics and mechanical testing. Vet J. 2008; 177:8–17.
Shively CA, Laber-Laird K, Anton RF. Behavior and physiology of social stress and depression in female cynomolgus monkeys. Biol Psychol. 1997;41:871–82.
Sims NA and Martin TJ. Coupling signals between the osteoclast and osteoblast: how are messages transmitted between these temporary visitors to the bone surface? Frontiers Endocrinol. 2015. http://dx.doi.org/10.3389/fendo.2015.00041 Vol 6 (Article 41) 1–5.
Sims NA, Quinn JM, Martin TJ. Coupling between immune and bone cells. In: Lorenzo JA, Choi Y, Horowitz MC, Takayanagi H, editors. Osteoim- munology: interactions of the immune and skeletal systems. 2nd ed. London: Academic; 2015.
Smith SY, Jolette J, Turner CH. Skeletal health: primate model of postmenopausal osteoporosis. Am J Primatol. 2009;71:752–65.
Smith L, Bigelow EM, Jepsen KJ. Systematic evaluation of skeletal mechanical function. Curr Protoc Mouse Biol. 2013;3:39–67.
Snoeks TJA, Van Beek E, Que I et al (2012) Bioluminescence imaging of bone metastasis in rodents. Helfrich, Miep H and Ralston, Stuart H, editors. Methods in molecular medicine, vol. 816: bone research protocols 2nd ed. Totowa: Humana Press Inc.; 507–15. 978-1-61779-414-8.
Sogaard CH, Wronski TJ, McOsker JE, et al. The positive effect of parathyroid hormone on femoral neck bone strength in ovariectomized rats is more pronounced than that of estrogen or bisphosphonates. Endocrinology. 1994;134:650–7.
Sopelak VM, Lynch A, Williams RF, et al. Maintenance of ovulatory menstrual cycles in chronically cannulated monkeys: a vest and mobile tether assembly. Biol Reprod. 1983;28:703–6.

Sowa H, Kaji H, Yamaguchi T, et al. Smad3 promotes alkaline phosphatase activity and mineralization of osteoblastic MC3T3-E1 cells. J Bone Miner Res. 2002;17(7):1190–9.
Sroga GE, Vashishth D. Effects of bone matrix proteins on fracture and fragility in osteoporosis. Curr Osteoporos Rep. 2012;10:141–50.
Stenbeck G, Horton MA. Endocytic trafficking in actively resorbing osteoclasts. J Cell Sci. 2004;117:827–36.
Stroup GB, Kumar S, Jerome CP. Treatment with a potent cathepsin K inhibitor preserves cortical and trabecular bone mass in ovariectomized monkeys. Calcif Tissue Int. 2009;85:344–55.
Suda T, Takahashi N, Udagawa N, et al. Modulation of osteoclast differentiation and function by the new members of the tumor necrosis factor receptor and ligand families. Endocr Rev. 1999;20:345–57.
Szulc P, Seeman P, Duboeuf F, et al. Bone fragility: failure of periosteal apposition to compensate for increased endocortical resorption in postmenopausal women. J Bone Miner Res. 2006;21:1856–63.
Teitelbaum SL. Osteoporosis and integrins. J Clin Endocrinol Metab. 2005;90:2466–8.
Teitelbaum SL, Ross FP. Genetic regulation of osteoclast development and function. Nat Rev Genet. 2003;4:638–49.
The HYP Consortium. A gene (PEX) with homologies to endopeptidases is mutated in patients with X-linked hypophosphatemic rickets. Nat Genet. 1995;11(2):130–6.
Tripp EJ, Mac Kay EH. Silver staining of bone prior to decalcification for quantitative determination of osteoid in sections. Stain Technol. 1972;47(3):129–36.
Turner AS. Animal models of osteoporosis – necessity and limitations. Eur Cell Mater. 2001;1:66–81.
Turner CH. Bone strength: current concepts. Ann N Y Acad Sci. 2006;1068:429–46.
Turner RT, Lotinun S, Hefferan T, et al. Animal models for osteoporosis. Rev Endocr Metab Disord. 2001;2:117–27.
Urist MR. Bone: formation by autoinduction. Science. 1965;150(698):893–9.
Urist MR, Mikulski A, Lietze A. Solubilized and insolubilized bone morphogenetic protein. Proc Natl Acad Sci U S A. 1979;76(4):1828–32.
Vahle JL, Ma YL and Burr DB. Skeletal assessments in the nonhuman primate. Chapter 32. In: Bluemel J, Korte S, Schenck E, Weinbauer GF, editors. The nonhuman primate in nonclinical drug development and safety assessment. San Diego: Academic; 2015. 605–25. 978–0–12-417144-2.
Van der Linden JC, Homminga J, Verhaar JAN, et al. Mechanical consequences of bone loss in cancellous bone. J Bone Miner Res. 2001;16:457–65.
Van't Hof, R (2012) Analysis of bone architecture in rodents using microcomputed tomography. In: Helfrich, Miep H and Ralston, Stuart H, editors. Methods in molecular medicine, vol. 816: bone research protocols. 2nd ed, Totowa: Humana Press; 461–76. 978-1-61779-414-8.
Verborgt O, Gibson GJ, Schaffler MB. Loss of osteocyte integrity in association with microdamage and bone remodeling after fatigue damage in vivo. J Bone Miner Res. 2000;15:60–7.
Verborgt O, Tatton NA, Majeska RJ, et al. Spatial distribution of Bax and Bcl-2 in osteocytes after bone fatigue: complementary roles in bone remodeling regulation? J Bone Miner Res. 2002;17(5):907–14.
Vieth R, Kessler MJ, Pritzker KPH. Serum concentrations of vitamin D metabolites in Cayo Santiago Rhesus macaques. J Med Primatol. 1987;16:347–57.
Vieth R, Kessler MJ, Pritzker KP. Species differences in the binding kinetics of 25-hydroxyvitamin D3 to vitamin D binding protein. Can J Physiol Pharmacol. 1990;68:1368–71.
Walker ML. Menopause in female rhesus monkeys. Am J Primatol. 1995;35:59–71.
Wallace JM. Skeletal hard tissue biomechanics. In: Burr DB, Allen MR, editors. Basic and applied bone biology. San Diego: Academic; 2014. p. 115–30.
Weiner S, Wagner HD. The material bone: structure-mechanical function relations. Annu Rev Mater Sci. 1998;28:271–98.
Weinstein RS. Clinical use of bone biopsy. In: Coe FL, Favus MJ, editors. Disorders of bone and mineral metabolism. New York: Raven Press; 1992. p. 455–74.

Weinstein RS, Jilka RL, Parfitt AM, et al. Inhibition of osteoblastogenesis and promotion of apoptosis of osteoblasts and osteocytes by glucocorticoids. Potential mechanisms of their deleterious effects on bone. J Clin Invest. 1998;102:274–82.
Weitzmann MN, Cenci S, Rifas L, et al. Interluekin-7 stimulates osteoclast formation by upregulating the T-cell production of soluble osteoclastogenic cytokincs. Blood. 2000;96:1873–8.
Wronski TJ, Cintron M, Dann LM. Temporal relationship between bone loss and increased bone turnover in ovariectomized rats. Calcif Tissue Int. 1988;43:179–83.
Wronski TJ, Dann LM, Scott KS, et al. Long-term effects of ovariectomy and aging on the rat skeleton. Calcif Tissue Int. 1989;45:360–6.
Wronski TJ, Dann LM, Horner SL. Time course of vertebral osteopenia in ovariectomized rats. Bone. 1990;10:295–301.
Yamaguchi A, Katagiri T, Ikeda T, et al. Recombinant human bone morphogenetic protein-2 stimulates osteoblastic maturation and inhibits myogenic differentiation in vitro. J Cell Biol. 1991;113(3):681–7.
Yang Y. Skeletal morphogenesis and embryonic development. In: Rosen CJ, editor. Primer on the metabolic bone diseases and disorders of mineral metabolism. 8th ed. New York: Wiley; 2013. p. 3–14.
Yeh JK, Chen MM, Aloia JF. Skeletal alterations in hypophysectomized rats: I. A histomorphometric study on tibial cancellous bone. Anat Rec. 1995;241(4):505–12.
Yeni YN, Brown CU, Wang Z, et al. The influence of bone morphology on fracture toughness of the human femur and tibia. Bone. 1997;21:453–9.
Yuan R, Tsaih SW, Petkova SB, et al. Aging in inbred strains of mice: study design and interim report on median lifespans and circulating IGF1 levels. Aging Cell. 2009;8:277–87.
Zebaze R, Seeman E. Cortical bone: a challenging geography. J Bone Miner Res. 2015;30(1):24–9.
Zhao C, Irie N, Takada Y, et al. Bidirectional ephrinB2-EphB4 signaling controls bone homeostasis. Cell Metab. 2006;4:111–21.
Zoehrer R, Roschger P, Durchschlag E, et al. Bone mineralization density distribution in triple biopsies of the iliac crest in post-menopausal women. J Bone Miner Res. 2006;21(7):1106–12.

http://www.springer.com/978-3-319-56190-5

Bone Toxicology
Smith, S.Y.; Varela, A.; Samadfam, R. (Eds.)
2017, XII, 474 p. 72 illus., 63 illus. in color., Hardcover
ISBN: 978-3-319-56190-5